U.S. DEPARTMENT OF COMMERCE
National Technical Information Service

PB-277 075

Fine Particle Collection by a Flux-Force/Condensation Scrubber Pilot Demonstration

Air Pollution Technology, Inc, San Diego, Calif

Prepared for

Industrial Environmental Research Lab, Research Triangle Park, N C

Dec 77

PB 277 075

REPRODUCED BY
NATIONAL TECHNICAL
INFORMATION SERVICE
U. S. DEPARTMENT OF COMMERCE
SPRINGFIELD, VA. 22161

RESEARCH REPORTING SERIES

Research reports of the Office of Research and Development, U.S. Environmental Protection Agency, have been grouped into five series. These five broad categories were established to facilitate further development and application of environmental technology. Elimination of traditional grouping was consciously planned to foster technology transfer and a maximum interface in related fields. The five series are:

1. Environmental Health Effects Research
2. Environmental Protection Technology
3. Ecological Research
4. Environmental Monitoring
5. Socioeconomic Environmental Studies

This report has been assigned to the ENVIRONMENTAL PROTECTION TECHNOLOGY series. This series describes research performed to develop and demonstrate instrumentation, equipment, and methodology to repair or prevent environmental degradation from point and non-point sources of pollution. This work provides the new or improved technology required for the control and treatment of pollution sources to meet environmental quality standards.

EPA REVIEW NOTICE

This report has been reviewed by the U.S. Environmental Protection Agency, and approved for publication. Approval does not signify that the contents necessarily reflect the views and policy of the Agency, nor does mention of trade names or commercial products constitute endorsement or recommendation for use.

This document is available to the public through the National Technical Information Service, Springfield, Virginia 22161.

TECHNICAL REPORT DATA

(Please read Instructions on the reverse before completing)

1. REPORT NO.
EPA-600/2-77-238

2.

3. RECIPIENT'S ACCESSION NO.
PB277075

4. TITLE AND SUBTITLE
Fine Particle Collection by a Flux-Force/Condensation Scrubber: Pilot Demonstration

5. REPORT DATE
December 1977

6. PERFORMING ORGANIZATION CODE

7. AUTHOR(S)
Seymour Calvert and Shamim Gandhi

8. PERFORMING ORGANIZATION REPORT NO.

9. PERFORMING ORGANIZATION NAME AND ADDRESS
Air Pollution Technology, Inc.
4901 Morena Boulevard, Suite 402
San Diego, California 92117

10. PROGRAM ELEMENT NO.
1AB012; ROAP 21ADL-002

11. CONTRACT/GRANT NO.
68-02-1869

12. SPONSORING AGENCY NAME AND ADDRESS
EPA, Office of Research and Development
Industrial Environmental Research Laboratory
Research Triangle Park, NC 27711

13. TYPE OF REPORT AND PERIOD COVERED
Final; 6/74-6/77

14. SPONSORING AGENCY CODE
EPA/600/13

15. SUPPLEMENTARY NOTES IERL-RTP project officer for this report is Dale L. Harmon, Mail Drop 61, 919/541-2925.

16. ABSTRACT The report gives results of a pilot-scale demonstration of flux-force/condensation (FF/C) scrubbing for fine particle control, carried out on a secondary metal recovery furnace. Results were consistent with those of preceding laboratory bench-scale and pilot-plant studies. The system was generally capable of 90-95% efficiency on particles with a mass median aerodynamic diameter of 0.7-0.8 micrometers A, achieved with a 68 cm W.C. gas-phase pressure drop. A conventional high energy scrubber without FF/C effects would require pressure drops of roughly 250 cm W.C. for 90% and 535 cm W.C. for 95% particle collection efficiency. FF/C effects are those which accompany the condensation of water vapor from the gas and are generally caused by contacting hot humid gas with colder liquid and/or by injecting steam into saturated gas. Mathematical models have been developed for predicting FF/C effects and for use in scrubber system design. Agreement between the model predictions and experimental results was good. The report gives FF/C system design details, experimental results, analysis of results, description of mathematical models, design of an optimized system, cost estimates, and recommendations for future research.

17. KEY WORDS AND DOCUMENT ANALYSIS

a. DESCRIPTORS		b. IDENTIFIERS/OPEN ENDED TERMS	c. COSATI Field/Group	
Air Pollution	Mathematical Models	Air Pollution Control	13B	
Scrubbers		Stationary Sources	07A	12A
Condensing		Flux-Force/Condensation Scrubbers	07D	
Dust			11G	
Iron and Steel Industry		Particulate		
Furnaces		Secondary Metal Recovery	11F 13A	

18. DISTRIBUTION STATEMENT
Release to Public

19. SECURITY CLASS *(This Report)*
Unclassified

20. SECURITY CLASS *(This page)*
Unclassified

21. NO. OF PAGES
193

22. PRICE
A09 - A01

EPA Form 2220-1 (9-73)

EPA-600/2-77-238
December 1977

FINE PARTICLE COLLECTION BY A FLUX-FORCE/CONDENSATION SCRUBBER: PILOT DEMONSTRATION

by

Seymour Calvert and Shamim Gandhi

Air Pollution Technology, Inc.
4901 Morena Boulevard, Suite 402
San Diego, California 92117

Contract No. 68-02-1869
ROAP No. 21ADL-002
Program Element No. 1AB012

EPA Project Officer: Dale L. Harmon

Industrial Environmental Research Laboratory
Office of Energy, Minerals, and Industry
Research Triangle Park, N.C. 27711

Prepared for

U.S. ENVIRONMENTAL PROTECTION AGENCY
Office of Research and Development
Washington, D.C. 20460

ia

ABSTRACT

A pilot-scale demonstration of flux force/condensation (F/C) scrubbing for fine particle control was carried out on a secondary metal recovery furnace. Control of the entire source effluent, a maximum flow rate of 200 Am^3/min (7,000 ACFM) at temperatures up to 800°C, required both particle collection and acid gas absorption. Demonstration plant performance was consistent with the preceding laboratory bench-scale and pilot-plant studies.

The nature of the source emissions entering the scrubber depended greatly on the type of scrap wire being incinerated to remove the insulation from the copper wire and other metal scrap and on the operating conditions. A conventional high energy scrubber would be incapable of controlling emissions at a practically feasible pressure drop from anything but the premium grade of scrap. An F/C scrubber system would be feasible for the control of lower (more polluting) grade scrap, the type of scrap which had more commercial importance.

The system was generally capable of about 90% to 95% efficiency on particles with a mass median aerodynamic diameter of 0.7 to 0.8 μmA (about 0.3 μm physical diameter for particles with a density of 4.0 g/cm^3). This efficiency was achieved with a 68 cm (27 in.) W.C. gas phase pressure drop. A conventional high energy scrubber without F/C effects would require pressure drops of roughly 250 cm (98 in.) W.C. for 90% and 535 cm (210 in.) W.C. for 95% particle collection efficiency.

F/C effects are those which accompany the condensation of water vapor from the gas and are generally caused by

Preceding page blank

contacting hot, humid gas with colder liquid and/or by injecting steam into saturated gas. Mathematical models have been developed for predicting the F/C effects and for use in scrubber system design. Agreement between the model predictions and experimental results was good.

This report presents the F/C system design details, experimental results, analysis of results, description of mathematical models, design of an optimized system, cost estimates, and recommendations for future research.

CONTENTS

Abstract iii
Figures vi
Tables xi
Abbreviations and Symbols. xiv
Acknowledgement. xvii

1. Introduction 1
2. Summary, Conclusions and Recommendations 4
3. Demonstration Plant Site Selection 10
4. Engineering Design 23
5. System Performance Testing 41
6. Experimental Results and Discussion. 51
7. F/C Scrubber Performance Prediction Model. 77
8. Engineering Analysis 95
9. Future Research Recommendations. 123

References 133
Appendices 134

A. Process Data 134
B. Particle Size Data 137
C. Particle Size Distribution Plots 144
D. Impinger Data. 156
E. Calculation of Particle Number Concentration From Cascade Impactor Data. 159
F. Example Calculation and Prediction of Fractional and Overall Penetration. 169

FIGURES

Number — Page

3-1 Flowsheet for the 1.4 m^3/min pilot scale F/C scrubber system 16

3-2 Schematic of 1.4 m^3/min pilot scrubber 19

4-1 Flow diagram of F/C scrubbing system 28

4-2 Quencher unit of F/C demonstration system 29

4-3 Scrubber unit of F/C demonstration plant. 30

4-4 Cooling tower of F/C demonstration scrubbing sysgem . . 31

4-5 General elevation, F/C scrubber demonstration system. . 32

4-6 Top view, F/C scrubber demonstration system 33

4-7 Quencher details. 34

4-8 F/C scrubber details. 35

4-9 Electrical schematic of F/C scrubber demonstration 36 system. 36

4-10 Furnace crossover duct to F/C scrubber demonstration system. 37

4-11 Front view of F/C demonstration scrubber 38

4-12 View of F/C scrubber system and metals recovery furnace 38

4-13 Crossover duct from furnace stack to F/C demonstration scrubber. 39

4-14 View of secondary metals recovery furnace and charging process 39

4-15 Sieve plate scrubber of F/C demonstration system . . . 40

4-16 Quencher unit of F/C scrubber system. 40

5-1 F/C scrubber system instrumentation sheet 42

FIGURES (continued)

Number Page

5-2 Modified EPA sampling train with ex-stack cascade impactor. Scrubber outlet sampling system 45

5-3 Modified EPA sampling train with ex-stack cascade impactor. Quencher inlet sampling system. 46

6-1 Particle penetration versus aerodynamic diameter for run 3. 60

6-2 Particle penetration versus aerodynamic diameter for run 4. 60

6-3 Particle penetration versus aerodynamic diameter for run 42 61

6-4 Particle penetration versus aerodynamic diameter (scrubber only) for run 43 61

6-5 Particle penetration versus aerodynamic diameter for run 56 62

6-6 Particle penetration versus aerodynamic diameter for run 58 62

6-7 Particle penetration versus aerodynamic diameter for run 59 63

6-8 Particle penetration versus aerodynamic diameter for run 61 63

6-9 Particle penetration versus aerodynamic diameter for run 62 64

6-10 Particle penetration versus aerodynamic diameter for run 64 64

6-11 Particle penetration versus aerodynamic diameter for run 66 65

6-12 Particle penetration versus aerodynamic diameter for run 69 65

6-13 Particle penetration versus aerodynamic diameter for run 72 66

6-14 Particle penetration versus aerodynamic diameter for run 73 66

FIGURES (continued)

Number Page

6-15 Particle penetration versus aerodynamic diameter for run 74 67

6-16 Particle penetration versus aerodynamic diameter for run 75 67

6-17 Particle penetration versus aerodynamic diameter for run 76 68

6-18 Particle penetration versus aerodynamic diameter for run 77 68

6-19 Effect of calculated particle number concentration on agreement between predicted and experimental for 0.5 μmA diameter particles 74

7-1 Generalized F/C scrubber system. 79

7-2 Multiple plate F/C scrubbing system. 81

7-3 Predicted particle condensation ratio (f_p) as a function of particle diameter 87

7-4 Predicted particle condensation rates (f_p) as a function of liquid bulk temperature. 87

7-5 Predicted particle condensation ratio (f_p) as a function of gas phase (saturated) temperature. 88

7-6 Predicted particle condensation ratio (f_p) as a function of particle number concentration. 88

7-7 Predicted particle condensation ratio (f_p) as a function of liquid phase heat transfer coefficient . . 89

8-1 Flowsheet for F/C scrubber optimum design at metals recovery furnace 100

8-2 Saturator for F/C optimum design 103

8-3 Predicted grown particle size distribution for F/C scrubber optimum design. 105

8-4 Condenser for F/C optimum design 106

8-5 Predicted penetration for venturi scrubber as designed for optimum system 108

FIGURES (continued)

Number Page

8-6 Venturi scrubber for F/C optimum design 109

8-7 Assumed cumulative scrubber entrainment versus drop diameter for optimum system. 111

8-8 Cooling tower of F/C optimum design at metals recovery furnace 113

C-1 Inlet and outlet size distributions for run 3. 145

C-2 Inlet and outlet size distributions for run 4 (scrubber only) 145

C-3 Inlet and outlet size distributions for run 7. 146

C-4 Inlet and outlet size distributions for run 42 (scrubber only) 146

C-5 Inlet and outlet size distributions for run 43 (scrubber only) 147

C-6 Inlet and outlet size distributions for run 56 147

C-7 Inlet and outlet size distributions for run 58 148

C-8 Inlet and outlet size distributions for run 59 148

C-9 Inlet and outlet size distributions for run 61 149

C-10 Inlet and outlet size distributions for run 62 149

C-11 Inlet and outlet size distributions for run 64 150

C-12 Inlet and outlet size distributions for run 66 150

C-13 Inlet and outlet size distributions for run 69 151

C-14 Inlet size distribution for run 71 151

C-15 Inlet and outlet size distributions for run 72 152

C-16 Inlet and outlet size distributions for run 73 152

C-17 Inlet and outlet size distributions for run 74 153

C-18 Inlet and outlet size distributions for run 75 153

FIGURES (continued)

Number Page

C-19 Inlet and outlet size distributions for run 76 154

C-20 Inlet and outlet size distributions for run 77 154

C-21 Inlet size distribution for run 78 155

E-1 Particle penetration versus aerodynamic diameter for run 56 163

E-2 Inlet and outlet size distribution for run 56 168

F-1 Scrubber penetrations for collection by inertial impaction as computed from equations 7-18 and 7-19 for different operating configurations. 175

F-2. Predicted grown particle size distribution for run 56 data. 175

F-3. Particle penetration versus aerodynamic diameter for run 56 176

F-4. Prediction of overall penetration for run 56 using graphical integration. 176

TABLES

Number Page

1-1 F/C scrubbing studies by A.P.T. for EPA 2

3-1 Summary of test data from stack sampling metal recovery furnace 15

3-2 Performance of 1.4 m^3/min pilot plant 20

3-3 Particulate characteristics at 1.4 m^3/min pilot plant . 20

6-1 Total particulate loadings at furnace stack during different stages of F/C scrubbing demonstration program 52

6-2 F/C scrubber demonstration plant operating configurations 54

6-3 F/C scrubber demonstration plant system performance . . 55

6-4 Particulate and impinger data*, F/C scrubber demonstration plant 59

6-5 Comparison of experimental data versus predicted penetrations for F/C scrubber demonstration 72

6-6 Measured variables, definition, precision and test case nominal values for total efficiency calculation 76

6-7 Measured variables, definition, precision and test case nominal values for size distribution calculation . . . 76

8-1 Design criteria summary 99

8-2 Process streams for F/C scrubber optimum design at metals recovery furnace 101

8-3 Total equipment cost estimate for F/C optimum design. 115

8-4 Direct and indirect cost estimate for F/C optimum design. 116

8-5 Operating cost of optimum F/C design. 117

8-6 High energy scrubber costs for regular no. 1 wire . . 120

TABLES (continued)

Number Page

8-7 Cost comparison for premium wire recovery. 122

9-1 Major industrial particulate sources for which F/C scrubbing is attractive. 127

A-1 Process data F/C scrubber demonstration 135

B-1 Inlet and outlet sample particle data for run 3. . . .138

B-2 Inlet and outlet sample particle data for run 4 (scrubber only) 139

B-3 Inlet and outlet sample particle data for run 7 (scrubber only). .139

B-4 Inlet and outlet sample particle data for run 42 (scrubber only). .139

B-5 Inlet and outlet sample particle data for run 43 (scrubber only). .139

B-6 Inlet and outlet sample particle data for run 56 . . .140

B-7 Inlet and outlet sample particle data for run 58 . . .140

B-8 Inlet and outlet sample particle data for run 59 . . .140

B-9 Inlet and outlet sample particle data for run 61 . . .140

B-10 Inlet and outlet sample particle data for run 62 . . .141

B-11 Inlet and outlet sample particle data for run 64 . . .141

B-12 Inlet and outlet sample particle data for run 66 . . .141

B-13 Inlet and outlet sample particle data for run 69 . . .141

B-14 Inlet and outlet sample particle data for run 71 . . .142

B-15 Inlet and outlet sample particle data for run 72 . . .142

B-16 Inlet and outlet sample particle data for run 73 . . .142

B-17 Inlet and outlet sample particle data for run 74 . . .142

B-18 Inlet and outlet sample particle data for run 75 . . .143

TABLES (continued)

Number Page

B-19 Inlet and outlet sample particle data for run 76. . . .143

B-20 Inlet and outlet sample particle data for run 77. . . .143

B-21 Inlet and outlet sample particle data for run 78. . . .143

D-1 Impinger data and results 157

E-1 Particulate data F/C scrubber demonstration 165

E-2 Inlet and outlet sample data for run 56 167

F-1 Example calculations for prediction of overall penetration of F/C scrubber system (run 56). 174

LIST OF ABBREVIATIONS AND SYMBOLS

a_t - Interfacial area of bubble, cm^{-1}
A_p - Cross sectional area of scrubber, cm^2
c - Mass concentration kg/m^3, g/cm^3 or $g/DNcm^3$
C - Dependent variable
C - Cumulative particle mass loading, g/DNm^3
C - Total particle mass loading, g/DNm^3
C' - Cunningham correction factor, dimensionless
C_{pp} - Heat capacity of gas, cal/g-°K
d - Diameter, m or cm
d_h - Diameter of perforation, cm
d_m - Mass mean diameter of particle, cm
d_{pa} - Aerodynamic particle diameter, $\mu mA \equiv d_p \, (C' \, \rho_p)^{1/2}$
d_{pc} - Performance cut diameter (aerodynamic), μmA
d_{pg} - Geometric mean particle diameter, μm or μmA
d_s - Sauter mean diameter, μm
D - Diffusivity, cm^2/s
DNm^3 - Dry normal cubic meter, at 0°C and 1 atm
E - Efficiency, fraction or %
f_p - Fraction of vapor condensing on particles, fraction
f_v - Volume fraction of gas condensing, fraction
F - Foam density, ratio of clear liquid height to total foam height
G - Gas flow rate, m^3/s
h - Heat transfer coefficient, cal/s-cm - °C
H - Humidity, g/g
k' - Mass transfer coefficient, $gmol/cm^2$-s-atm
L - Liquor flow rate, ℓ/s
L_M - Latent heat of vaporization cal/gmol
m - Mass, kg or g
mg - Sample weight, mg

LIST OF ABBREVIATIONS AND SYMBOLS (continued)

M - Molecular weight, kg/kgmol or g/gmol
M_{cum} - Cumulative mass loading collected on that stage and those below, gm/DNm^3
n - Particle number concentration, #/DNcm^3
n_p - Particle number concentration #/cm^3
N - Number of scrubber stages
p_b - Vapor partial pressure, cm H_2O
p_{BM} - Mean partial pressure of non-transferring gas, atm
P - Pressure, cm W.C., dynes/cm^2, kg/cm^2, N/m^2 or atm
P_b - Barometric pressure atm
P_s - Orifice pressure, cm H_2O
Pt - Penetration, fraction or percent
$\overline{Pt}$ - Overall penetration, fraction or percent
Pt^* - Constant penetration value for particles below about 0.5 μmA size, fraction
Pt_a - Penetration due to impaction in the saturator, fraction
Pt_b - Penetration due to impaction in the condenser, fraction
Pt_c - Penetration due to diffusiophoretic in the condenser, fraction
Pt_d - Penetration due to impaction in the stages after the condenser, fraction
ΔP - Pressure drop, cm W.C. or atm
q' - Mass H_2O condensed/mass dry air, g/g
q_p - Mass H_2O condensed on particles/mass dry air, g/g
Q_G - Gas volumetric flow rate, m^3/s
Q_L - Liquid volumetric flow rate, m^3/s or ℓ/s
r - Radius, cm or μm
r - Distance, cm
R - Ideal gas law constant (82 atm-cm^3/gmol-°K)
S - Saturation ratio, atm/atm
S - Sensitivity of error dC/C to an error ∂X
t - Time, s
T - Temperature, °K (or °C, where specified)
T_A - Impactor temperature, °C

LIST OF ABBREVIATIONS AND SYMBOLS (continued)

u - Velocity, m/s or cm/s
u_h - Gas velocity in perforations, cm/s
u_{pD} - Diffusiophoretic deposition velocity, cm/s
V - Volume, m^3 or cm^3
V_{DGM} - Volume of dry gas read by gas meters, m^3
W_s - Weight of dryer, g
X - Independent variable
y - Mole fraction, gmol/gmol
y - Mass H_2O/mass dry air, g/g
Z - Distance in "Z" direction, cm or m

Greek

μ - Viscosity, g/cm-s
μm - Micrometer (micron)
μmA - Aerodynamic diameter $d_p(C' \rho_p)^{1/2}$, μm $(g/cm^3)^{1/2}$
ρ - Density, kg/m^3 or g/cm
ρ_m - Molal density, $gmole/cm^3$
ρ_p - Particle density
σ_g - Geometric standard deviation of particle size distribution
Σ - Summation

Subscripts

G - Gas phase
i - Interface
i - In
i - Initial
i - Individual particle size
i - Inertial impaction
L - Liquid phase
o - Outlet
p - Particle
pa - Aerodynamic
t - Total

ACKNOWLEDGMENTS

A.P.T. appreciated the perceptive and helpful critical review of the demonstration program by EPA personnel concerned with this project: Dr. Leslie E. Sparks and Mr. Dale L. Harmon, under the direction of Mr. James H. Abbott.

Several members of the A.P.T. staff other than the authors of this report have contributed significantly to the demonstration plant program. They are: Messrs. Nikhil Jhaveri, Russell Lyon, Willard Roper, Chuck Nguyen, and Ms. Verne McAdams.

CHAPTER 1

INTRODUCTION

Flux force/condensation (F/C) scrubbing can, under the proper circumstances, achieve high efficiency fine particle collection at appreciably lower power input than conventional high energy scrubbing. This advantage applies especially to the particle diameter range between about 0.1 to 1.0 micron. For smaller particles Brownian diffusion becomes an important collection mechanism and for larger particles inertial impaction is more effective.

F/C effects are those which accompany the condensation of water vapor from the gas and are generally caused by contacting hot, humid gas with colder liquid and/or by injecting steam into saturated gas. The transfer of water vapor toward the cold liquid surface sweeps particles with it and is referred to as diffusiophoresis. Heat transfer from the gas to the liquid also causes particle movement toward the cold liquid and this is called thermophoresis. The condensation of water on the suspended particles causes their mass (particle plus condensate) to increase and this is referred to as particle growth. The particles are easier to collect by inertial impaction after they have grown by condensation.

The research and development series which preceded the presently reported program was based on the prior scientific and engineering literature, which was inadequate for engineering design purposes. A summary of the EPA-sponsored contract programs carried out by A.P.T. is given in Table 1-1.

The demonstration plant study which is reported here followed the laboratory pilot-plant program. The objective of the demonstration was to test an F/C scrubbing system in

Table 1-1

F/C SCRUBBING STUDIES BY A.P.T. FOR EPA

Title	Contract	Report # & Date	Subject
Wet Scrubber System Study - Scrubber Handbook (Vol. 1) Final Report (Vol.2)	CPA-70-95	NTIS #PB 213-016 (1972)	F/C scrubbing principles and potential discussed.
Feasibility of Flux Force/ Condensation Scrubbing for Fine Particulate Control	68-02-0256	EPA 650/2-73-036 NTIS #PB 227-307 (1973)	Theoretical analysis, mathematical modeling, computer predictions, experimental data from bench-scale F/C scrubbers.
Study of Flux Force/ Condensation Scrubbing of Fine Particles	68-02-1082	EPA 600/2-75-018 (1975)	Laboratory pilot-plant study of F/C scrubbing in sieve plate and spray apparatus.
Study of Horizontal Spray Flux Force/Condensation Scrubber	68-02-1328 Task # 10	EPA 600/2-76-200 (1976)	Laboratory pilot-plant study of F/C scrubbing in horizontal spray apparatus.

an actual industrial setting and to obtain information on performance and costs. A survey of prospective sources yielded several candidates which were in the pilot plant (1975) report. Detailed follow-up of these candidates led to the selection of a secondary metals recovery plant, mainly on the basis of its being the only available opportunity for a definite commitment by the host company.

The following report presents the details of the demonstration plant design and the experimental program. A refined, near-optimum design was made on the basis of the experimental data and a revised design model. The process design and cost estimates for F/C scrubbing are presented in comparison with conventional scrubbing. As will be seen, this pollution source cannot be satisfactorily controlled by conventional scrubbing but can be by F/C scrubbing.

CHAPTER 2

SUMMARY, CONCLUSIONS AND RECOMMENDATIONS

SUMMARY

Flux force and water vapor condensation effects enhance fine particle scrubber efficiency and therby provide a means for reducing air pollution control costs. Flux force/condensation (F/C) scrubbing is applicable in situations where the gas is hot or where low cost waste steam is available. A series of EPA contract research and development programs proceeded from scientific principles to develop the engineering basis for the study reported here: a pilot-scale demonstration plant.

The objective of the demonstration was to test an F/C scrubbing system in an industrial situation and obtain information on performance and costs. Based on source test data, the gas temperature, and the importance of this type of source, a secondary metal recovery furnace was selected for control in the demonstration. The furnace is used to burn insulation material from various types of scrap wire and the emissions are small particles of insulation components, condensed metal chloride fume, hydrocarbons, and halogen gases.

An F/C scrubbing system composed principally of a spray-type quencher, a sieve plate column, a spray-type cooling tower, and an induced draft fan was designed on the basis of preceding phases of our research. A maximum flow of 200 Am^3/min (7,000) ACFM) of flue gas was cooled and saturated by a sodium carbonate solution spray in the quencher and then further cooled to provide F/C effects in the 5-plate column. During the program it became necessary to modify the system in order to cope with corrosion of the hot gas duct and to increase particle collection efficiency to compensate for an increase of source emissions.

The system was generally capable of about 90% to 95% efficiency on particles with a mass median aerodynamic diameter of 0.7 to 0.8 µmA (about 0.3 µm physical diameter for particles with a density of 4.0 g/cm^3). This efficiency was achieved with a 68 cm (27 in.) W.C. gas phase pressure drop. A conventional high energy scrubber without F/C effects would require pressure drops of roughly 250 cm (98 in.) W.C. for 90% and 535 cm (210 in.) W.C. for 95% particle collection efficiency.

Demonstration plant particle collection efficiency data were in line with those obtained previously in our bench-scale and laboratory pilot-plant experiments. A mathematical model which is a simplified version of that previously developed yielded predicted efficiencies which compared well with the demonstration plant data. The revised model is much easier to use than the old one and requires only a hand-held type calculator for the prediction of F/C scrubber efficiency.

The uncontrolled source characteristics proved to be exceedingly variable, depending on interactions of several factors. The type of scrap being reclaimed changes the amount and kind of insulation in an individual charge to the furnace. Operator technique determines the size of a charge, furnace temperature, air rate into the furnace and afterburners, and the timing of operations. There is a large change in emission rate as batch-wise burning cycle proceeds.

A refined F/C scrubbing system was designed on the conservative basis of the worst anticipated source emissions and utilizing the lessons learned in the demonstration program. With the re-designed F/C system the control of particulate matter from the incineration of premium no. 1 wire would require a scrubber pressure drop of about 70 cm (28 in.) W.C.

and a condensation ratio of about 0.3 g water vapor per g day gas. The control of lower grade scrap emissions would require about 115 cm (45 in.) W.C. pressure drop and a condensation ratio of 0.3 g/g.

An optimized F/C system for the control of emissions from the incineration of no. 1 regular grade wire would cost $111,000 installed. The annual operating costs for one shift/day based on 10-year straight line depreciation and electric power at 4.5¢ kWh would be $24,100/yr. This optimized F/C system would probably be capable of controlling emisssions from no. 2 and 3 wire incineration, based on the limited amount of test data available for operation with no. 2 and 3 wire.

A conventional high energy scrubber system to control no. 1 regular wire incineration would be impractical because of the extremely high pressure drop which would be needed. In order to make a comparison between F/C and conventional scrubbing costs, two system designs were made on the basis of controlling no. 1 premium wire incineration (although this would be inadequate for commercial use). For this service a F/C system would require a 70 cm W.C. overall pressure drop and would cost $103,120 installed and $20,695/yr to operate. A conventional system would require a 238 cm W.C. overall pressure drop and would cost $111,240 installed and $31,160/yr to operate.

CONCLUSIONS

The following conclusions can be drawn from the results of this study:

1. The performance of the demonstration plant was consistent with previous results in bench-scale and pilot-plant studies.

2. The plant as built was capable of controlling emissions from no. 1 premium wire incineration within air pollution emissions regulations. It was marginally adequate for no. 1 regular wire, depending on source operation conditions.

3. A conventional high energy scrubbing system would require a pressure drop of at least 250 cm (98 in.) W.C. to give the same efficiency as the F/C demonstration plant did at 68 cm (27 in.) W.C.

4. Particle number concentration is very important in F/C scrubbing because the more particles sharing a given amount of condensing water, the smaller their final size. In the metal recovery demonstration the particle number concentration was extremely high, making it a severe test of F/C scrubbing.

5. Source operation in terms of numerous parameters is variable over a wide range and has a great influence on the nature of the emissions to be controlled.

6. A design procedure which has been improved and simplified from the previous version gives predictions which are in good agreement with experimental results. The new mathematical model is convenient to use and can be solved with only a hand-held electronic computer.

7. The spray cooling tower performance was satisfactory in the demonstration plant. Less power and a less efficient entrainment (drift) separator would be required if a filled cooling tower were used. Observation of the solids behavior in the demonstration plant indicated little or no problem with deposition on tank and tower surfaces.

8. Liquid waste disposal was no problem after the scrubber liquid was neutralized with sodium carbonate.

9. The tube bank entrainment separator following the scrubber performed satisfactorily.

10. Refinement of the F/C scrubbing system design after the demonstration program yielded a more nearly optimum design for the control of this source. An F/C scrubber capable of controlling no. 1 regular wire incineration would cost $111,000 to install and $24,100/yr to operate. The efficiency requirement would be beyond the practical capability of a conventional high energy scrubber.

RECOMMENDATIONS

Recommendations based on the experience gained in the demonstration plant program are as follow:

A. Regarding design revisions for a secondary metals recovery air pollution control system:

1. The source operation should be studied carefully and modified so as to minimize the level of emissions and the variation in emissions. Close control of charging and firing practices is needed.

2. The saturator (quencher) should be located immediately adjacent to the incinerator stack in order to reduce the temperature and corrosion burden on the duct work.

3. High mass transfer efficiency is required to control the acid gases so the total combination of saturator, condenser, scrubber, and entrainment separator must be designed to provide it.

4. A venturi scrubber appears to be the best choice for particle collection after condensation and growth. Because the mass transfer capacity of a venturi and its entrainment separator is limited, the quencher and/or condenser must be efficient for gas absorption.

B. Regarding future research and development on F/C scrubbing:

1. Laboratory research on particle growth in bench-scale prototypes of condensers and scrubbers is necessary to provide

data which can be used in validating and/or revising the mathematical model. At present the model involves several significant assumptions.

2. Field measurements of particle number concentration and growth characteristics for a number of important air pollution sources would provide the key information needed to assess the suitability of F/C scrubbing for the specific source. Apparatus of the same general size and nature as that used for making performance tests could be taken anywhere in the U.S. and operated by a 3-man crew.

3. Field studies of solids deposition on surfaces of various materials which could be used for cooling tower construction would give the most important piece of information needed in selecting the type of cooler to use. These tests would be done at the same sites as described in 2, above, and could most efficiently be done concurrently with the particle characterization tests.

4. The use of steam injection into saturated gas is an attractive but insufficiently explored ramification of F/C scrubbing. A bench-scale laboratory study could yield the information needed to determine the optimum balance between the quantity of steam to inject and the amount of condensation by cooling. Engineering design studies followed by pilot tests are needed to identify the best way of generating steam inexpensively.

5. F/C scrubbing is highly suited to the control of fine particles from basic oxygen furnace emissions and a demonstration plant would be valuable.

CHAPTER 3

DEMONSTRATION PLANT SITE SELECTION

The main point of this study was to conduct a pilot-scale demonstration of a flux force/condensation scrubber system for collection of fine particulate emissions from an industrial source. Thus, it was important to find a company which operated a suitable plant and which was willing to allow access to the plant for the pilot-scale demonstration.

The following criteria were used for selecting the industrial source:

1. The type of source must be classified nationally as a major pollutant.

2. F/C scrubbing must be applicable to the source in terms of the technical and economic feasibility. Ideally, the pollutant gas for F/C scrubbing is characterized by hot or humid conditions with a major portion of the particulates in the submicron range.

3. The source should be either difficult or expensive to control with presently available particulate control devices.

A secondary non-ferrous metals recovery furnace was selected based on the above criteria for selection of the F/C demonstration scrubber. This chapter describes the nature of the process and the characteristics of the pollutants at the source. In addition, the results of a 1.4 m^3/min pilot-plant setup at the site is discussed in greater detail.

Alternate Sites Studied

Several companies operating metal melting furnaces were visited. During each visit, the demonstration program was explained and the specifics of a possible F/C scrubber system on their emission sources were discussed. The pertinent information on some of the alternate emission sources is described below while the particulars on the actual site selected are given in the next section.

1. Emission source: cupola furnace pair
   Existing control equipment: a spray chamber followed by a baghouse

The exhaust gas was at about 958°C. From the cupola the gas entered the spray chamber where 150 liters per minute of water was sprayed in. The large particles were removed by the water spray and the gas was cooled to 163°C. The gas then entered the baghouse and was subsequently emitted to the atmosphere. The total gas flow rate from a cupola was about 315 m^3/min @ 163°C and the cupolas were used alternately. The baghouse had frequent operating problems due to the high gas temperature and the pressure drop through the bags. The possibility of installing the F/C scrubber system downstream of the spray chamber was discussed with the company.

2. Emission source: electric arc furnace
   Existing control equipment: baghouse

The arc furnace was charged every two hours with scrap iron. The exhaust gas, about 200 m^3/min at 140°C, entered the baghouse through a 20-HP fan and was subsequently emitted to the atmosphere. The particulates were mainly iron oxides in the submicron range. The possibility of installing the F/C scrubber system in place of the baghouse was discussed with the company.

3. Emission source: metal sweating furnace (incinerator)
   Existing control equipment: afterburner for unburned gas.

The gas-fired incinerator was charged approximately every 20 minutes with utility electrical wires and some synthetic with utility electrical wires and some synthetic materials such materials, such as PVC. There was no particulate control equipment for the exhaust gas except for the afterburners.

4. Emission source: metal sweating furnace (incinerator)
   Existing control equipment: afterburner for unburned gas.

The incinerator burned propane and was continuously charged by a conveyer arrangement with aluminum, zinc, lead, and synthetic materials such as PVC. The exhaust gas flow rate was about 142 m^3/min @ 482°C. The particulates emitted are fines, mainly metal oxides and carbon. The possibility of installing the F/C scrubber system on these incinerators was discussed with the owner.

DISCUSSION OF ACTUAL SITE SELECTED

The Metal Recovery Furnace

After consulting with the Project Officer, it was decided to pursue the possibility of evaluating the demonstration scrubber system on the secondary non-ferrous metal recovery furnace (incinerator). An agreement was worked out between A.P.T., Inc. and the company operating the furnace, detailing the scope of participation and task responsibilities of the parties. A description of the furnace operation and emission was as follows:

Emission Source:	Secondary non-ferrous metal recovery furnace.
Existing Control Equipment:	Afterburners for un-burned gas and combustibles.

The gas-fired furnace was used for the recovery of copper from utility electrical wires and the recovery of aluminum, zinc, and lead by the metal sweating process from the corresponding scrap material. Two gas-fired afterburners were located immediately downstream of the furnace to control emissions of unburned gas and combustibles. However, the afterburners had not been adequate to control particulate emissions. especially during the copper wire reclamation.

Previous emission data indicated that the particulate loading was dependent on the charge being burned (maximum for copper wire reclamation, lower for metal sweating operations) and the operation of the afterburners. The furnace was charged approximately every 20 minutes. Particulate emissions were also higher during the first few minutes of a charging cycle. Thus, the stack conditions and emissions varied significantly, as illustrated, from the following two sets of emission data available at the time of site selection:

Type of operation: Copper wire reclamation

	Run 1	Run 2
1. Emission rate, g/Nm^3 @ 12% CO_2	0.17	0.5
kg/hr	0.15	0.38
2. Gas flow rate, actual m^3/min	193	158
3. Stack Temperature, °C	859	782
4. Process load, kg/hr	1816	1816

Both the afterburners were operated during the runs.

The wire reclamation industry classifies the scrap wire as follows:

No. 1 Premium - This grade contains mostly weather stripping, such as power lines. 80% by weight of charge is reclaimed as copper.

No. 1 Regular - This grade of #1 wire contains 60% copper and 40% plastic.

No. 2 This grade contains mainly thin wires below 16 gauge with thick rubber, P.V.C., nylon, etc. insulations.

No. 3 No. 3 wire contains mostly heavier wire than 16 gauge with much heavy insulation.

EMISSION DATA FROM STACK SAMPLING

Emissions tests were scheduled to determine particle loading and size distributions at various furnace operating modes. The variables for the different operating modes were reclamation of different grades of wire and furnace operation with and without afterburners.

The method used for particle loadings and size distributions was a modified EPA Method No. 5 with an out-of-stack

University of Washington Mark III cascade impactor in place of the filter. The particulate loadings, along with the total emission rates, are given in Table 3-1.

Preliminary testing of the non-ferrous metal recovery furnace supplied information on the type of particulate, the particulate size, and the nature of the exhaust products. The sampling tests did show that the particles were very fine and perhaps partly volatile in the 650°C gas stream in the furnace exhaust stack, indicating that control of the source would be a demanding, if not extreme test, of the F/C scrubbing process.

Miniature Pilot-Scale Scrubber System

A multiple plate column with a capacity to scrub 1.4 m^3/min was selected for a small scale study of the source in order to evaluate the best F/C system for the specific characteristics of the selected plant. A process flow sheet of this pilot scrubber system is shown in Figure 3-1. The hot stack gas was cooled and humidified in the quencher and then passed through the F/C scrubber. The liquor system was designed such that the temperature of scrubber inlet water can be controlled in tank number 2 by selective mixing of stream 5 and 11. The amount of vapor condensed in the scrubber was controlled by the appropriate selection of the scrubber inlet water temperature.

A schematic drawing of the system is shown in Figure 3-2. The pilot scale scrubber as assembled had the following dimensions and specifications:

A. Probe and Duct to Quencher --

Function -- To draw 2.5 m^3/min (90 ACFM) of stack gas at 650°C (1,200°F) isokinetically into the system from the furnace stack and carry it without appreciable heat loss into the quencher.

Construction -- Probe tip: 10 cm I.D., 60° sloped sharp entrance. Gas duct: 6.4 cm I.D., insulated 10 m long steel pipe.

B. Quencher --

Function -- To cool 2.5 m^3/min (90 ACFM) of stack gas at 650°C (1,200°F) down to 1.4 m^3/min (50 SCFM) at 75°C (168°F)

TABLE 3-1. SUMMARY OF TEST DATA FROM STACK SAMPLING METAL RECOVERY FURNACE

Case No.	Furnace Operation and Load	Impactor Load g/DNm³	Impinger Load g/DNm³	d_{pg} µmA	σ_g	Emission Rate Kg/hr
1	Aluminum scrap	0.0204	--	0.93	4.6	0.086
	No afterburners	0.0243	--	0.90	5.2	0.104
2	#1 wire No afterburners	0.492	--	0.48	5.8	2.45
3	#1 wire 2 afterburners	0.172	--	0.47	4.0	0.85
4	#2 wire	0.306	1.31	--	--	7.81
	2 afterburners	0.686	1.40	--	--	10.1
5	#3 wire	0.988	3.16	--	--	20.1
	2 afterburners	1.61	3.50	--	--	29.7

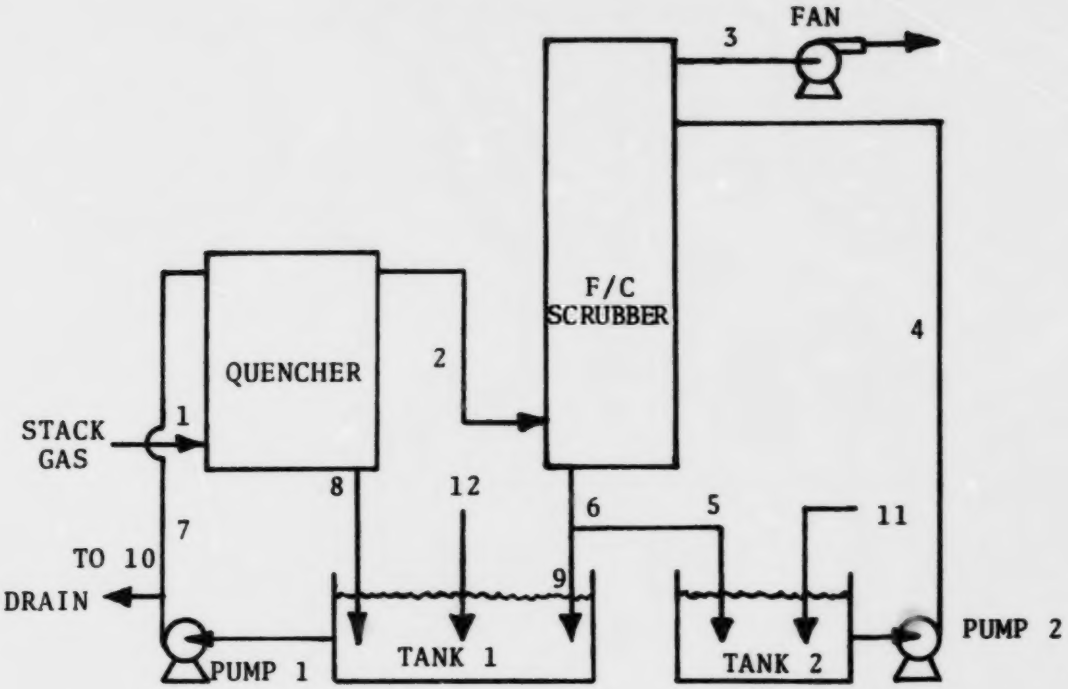
FAN
3
F/C SCRUBBER
4
QUENCHER
2
STACK GAS
1
8
12
6
5
11
7
TO 10
DRAIN
9
PUMP 1
TANK 1
TANK 2
PUMP 2

Stream No.		Temp. (°C)	Volume Flow		Flow	g vapor / g dry gas
			m^3/min	ℓ/min	kg/hr	
1	Stack gas	871	3.14	--	--	--
2	Saturated gas	75	1.42	--	73.8	0.40
3	Outlet gas	63	1.08	--	62.7	0.18
4	Water	38	--	5.68	341.0	--
5	Water	66	--	2.12	127.0	--
6	Water	66	--	5.98	359.0	--
7	Water	68	--	1.51	90.6	--
8	Water	75	--	1.21	72.6	--
9	Water	66	--	3.86	232.0	--
10	Water	68	--	3.56	214.0	--
11	City water	21	--	3.56	214.0	--
12	City water	21	--	start-up only		--

Figure 3-1. Flowsheet for the 1.4 m^3/min pilot scale F/C scrubber system.

and nearly saturated condition. This conditioning and cooling was accomplished by direct evaporation of recirculated liquor.

Construction -- Overall size: 46 cm I.D., 69 cm high. Flow: counter current. Spray requirements: 1.51 ℓ/min of recirculated liquor sprayed evenly through 3 spray heads at 1,100 dynes/cm^2 (160 psi) gauge. Holding tank: 56 cm diameter by 51 cm deep, located 2 m below quencher with an open top. The intake to the pump was 10 cm below the liquor level. Pump: Piston pump with 370 watt motor, capacity of 8 ℓ/min at 14,000 dynes/cm^2 (200 psi).

C. F/C Scrubber --

Function -- To remove particulates from the gas by F/C mechanisms.

Design -- A cylindrical four-sieve plate scrubber was chosen for the 1.4 m^3/min pilot test. Partially recirculated liquor was introduced at the top plate and cascades down to the bottom plate, maintaining cross flow on the sieve plates. Conditioned gas from the quencher, introduced under the bottom plate, flowed upward through the sieve plates.

Construction -- Overall size: 15.25 cm (6 in.) I.D., 183 cm (6 ft) high glass column. Liquid requirements: 5.7 ℓ/min of partially recirculated liquor introduced behind inlet weir of top plate. Sieve plates: Four sieve plates with round perforations. The perforations were 0.318 cm diameter spaced triangularly 0.95 cm apart. Inlet and outlet weirs on each plate were 6.4 cm high by 12 cm wide. Entrainment separator: Fine mesh screen placed across column. Pump: Centrifugal type with 250 watt mator, capacity of 22 ℓ/min. Fan: Direct drive, centrifugal type with 1.5 kW motor, capacity of 1.2 cm^3/min at 64 cm of water. Holding tank: 56 cm diameter by 51 cm deep, located under scrubber liquid level of 51 cm deep was maintained by city water line with float control. The scrubber return line was extended 46 cm below the liquid line.

D. Instrumentation --

Function -- To provide data on the liquid and gas flow rates, temperatures, pressures, and composition. Measurement locations: The points in the system where the measurements were made continuously during a run are shown in Figure 3-2.

Method -- Temperatures: Type T thermocouples for 0 to 100°C, and type K for 100°C to 650°C, connected to a 24-point recorder. Pressure: Bourdon tube gauges were used for the high pressure measurements, Magnehelic gauges were used for low pressure measurments. Volume flow: total volumes of liquid added or removed from the holding tanks were measured by positive displacement rotor-type meters. Liquid flow rate: Measured by rotameters. Gas flow rate: Measured by orfice connected to manometer. Particulate loading in gas streams: Loadings and size distributions were measured by sampling the streams with cascade impactors.

E. Liquor Conditioning --

Function -- To condition the scrubbing and quenching liquor such that it was suitable for dumping into the municipal sewer line.

Method -- The liquor was treated in a batch process manner at the end of a run.

DISCUSSION OF RESULTS FROM 1.4 m^3/min PILOT TESTS

Results of the eight performance tests are presented in Tables 3-2 and 3-3. Runs 1 to 3 were made when the furnace was operated for aluminum sweating and the results from these runs are not included. The remaining five runs were made during copper wire reclamation (no. 1 regular grade).

Overall, when the impinger catch was included in determining penetrations, the quencher performance appeared to be comparable or better than the scrubber performance. However, when the results were compared for the collection of particulates by excluding the impinger catch, the scrubber proved to have a better performance as would be expected. Both devices were efficient for the removal of the vapor phase of the stack gas, but it should be noted that due to the small capacity of the quencher requirement in the pilot tests, the quencher behavior and design were not representative of a full-scale system.

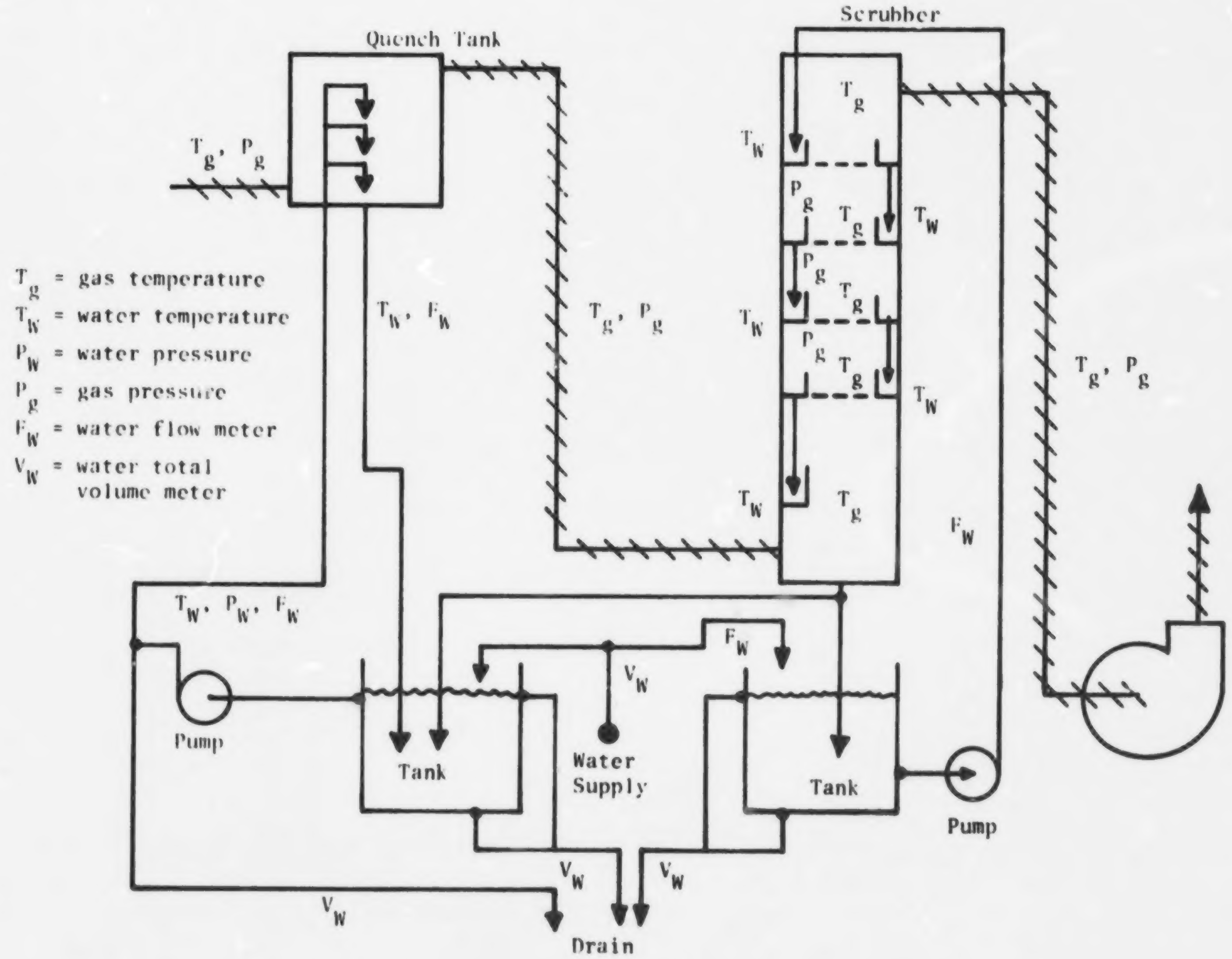
Quench Tank
Scrubber
T_g, P_g
T_g = gas temperature
T_W = water temperature
P_W = water pressure
P_g = gas pressure
F_W = water flow meter
V_W = water total volume meter
T_W, F_W
T_g, P_g
T_g
T_W
P_g
T_g
T_W
P_g
T_g
T_W
P_g
T_g
T_W
T_W
T_g
T_g, P_g
F_W
T_W, P_W, F_W
F_W
V_W
Pump
Tank
Water Supply
Tank
Pump
V_W
V_W
V_W
Drain

Figure 3-2. Schematic of 1.4 m³/min pilot scrubber.

TABLE 3-2. PERFORMANCE OF 1.4 m^3/min PILOT PLANT

Run No.	Loading mg/DNm^3			Overall $\overline{Pt}$		Scrubber $\overline{Pt}$	
	Quencher Inlet	Scrubber Inlet	Scrubber Outlet	With Impinger Catch	Without Impinger Catch	With Impinger Catch	Without Impinger Catch
4	1,566	1,004	437	27.9	31.9	43.5	44.3
5	1,150	358	201	17.4	47.2	56.1	56.7
6	774	338	179	23.1	45.0	53.0	77.9
7	1,383	537	303	21.9	43.3	56.4	67.3
8	--	130	46	--	--	35.4	74.9

TABLE 3-3. PARTICULATE CHARACTERISTICS AT 1.4 m^3/min PILOT PLANT

Run No.	q'	Quencher Inlet		Scrubber Inlet		Scrubber Outlet	
	g H_2O/ g D.A.	d_{pg} µmA	σ_g	d_{pg} µmA	σ_g	d_{pg} µmA	σ_g
4	0.06	0.84	1.1	0.70	1.6	0.60	1.7
5	0.067	0.70	1.7	0.60	1.9	0.50	1.8
6	0.073	0.80	1.2	0.55	1.9	0.45	1.6
7	0.088	0.85	1.1	0.53	1.5	0.53	1.5
8	--	--	--	0.44	1.7	0.40	1.7

Performance of the four-plate F/C scrubber was comparable to the results obtained earlier for a 14.0 m^3/min (500 CFM) four-plate scrubber tested under a previous EPA contract (Calvert et al., 1975). Due to substantial heat loss in the small diameter gas line from the furnace stack to the quencher in the pilot system, the condensation ratio, q', (g H_2O condensed/g dry air) in the F/C pilot scrubber was low. For higher condensation ratio, the particle penetration across the scrubber would be lower.

CONCLUSIONS FROM 1.4 m^3/min PILOT TESTS

The pilot scale experimentation yielded information on the source, the emissions, and the F/C scrubber design. These may be summarized as follow:

1. Particulate and gaseous emissions from the furnace change significantly with the nature of the charge and with time within the charging cycle. However, the gas flow rate and temperature remained constant during the charging cycle and depend only on the nature of the charge.

2. Particulate loading and the concentration of the corrosive condensable gas (consisting of metal chlorides, HCl, fluorides etc., depending on the charge) were the highest for #3 wire reclamation and decrease successively for #2 and #1 wire.

3. Emissions from the recovery of aluminium, zinc, and lead can be adequately controlled by afterburners. However, the afterburners were inadequate to control emissions from the copper wire reclamation, which presently exceed the control standards. Due to the amount of copper reclaimable (~80%) from the no. 1 wire and its availability, controlling emissions from no. 1 wire reclamation with F/C scrubbing was assigned the highest priority.

4. During the wire reclamation operation, significant amounts of corrosive acidic gases were emitted and appropriate measures were used to cope with this condition. It was decided to build the quencher with type 316 stainless steel and the gas duct from the quencher to the scrubber of fiberglass-reinforced plastic.

5. In order to absorb the acidic gases and to ease the demands on materials of construction, sodium carbonate was added to the quencher and the scrubber water to maintain the pH above 6. The quencher capacity was increased above the initial design in order to assure adequate mass transfer capacity as well as other benefits.

6. The mass loading as monitored during pilot plant testing was somewhat higher than previously encountered. Therefore, initial demonstration was made with five plates in the scrubber rather than starting with four and then adding the fifth. Insulation for the gas duct from the furnace to the quencher was used to minimize heat loss so that a condensation ratio, q, of 0.2 to 0.3 can be maintained in the scrubber. These conditions were expected to result in adequate particle collection in the scrubber, based on the pilot system results and projections from the earlier data.

CHAPTER 4

ENGINEERING DESIGN

After conclusion of the pilot scale tests, the program proceeded to the installation of the demonstration plant at the metal recovery facility. The pilot scale experimentation had yielded information on the source, the emissions, and the F/C scrubbing system design. This section describes the overall process design and the detailed mechanical features of the F/C scrubbing demonstration plant.

PROCESS DESIGN

A flow diagram of the F/C scrubbing system along with the major equipment items is given in Figure 4-1. The system was designed to scrub 198 Am^3/min (7,000 ACFM) of flue gas, this volume being the maximum measured flow of gases from the furnace.

The gases were drawn from the furnace stack to the quencher and through the scrubbing system by a fan located at the outlet of the system. The gases were preconditioned in the quencher by circulating water sprays to reduce the volume and to saturate the gases with moisture. They were then cleaned by a scrubber with five perforated plates which was designed with provisions for locating a sixth plate inside the shell. The cleaned gas was then vented to the atmosphere through a stack.

Water from the quencher was drained to a holding tank and recirculated to the quencher inlet. Liquor from the scrubber was collected in another holding tank and sprayed in the cooling tower which utilized ambient air for evaporative cooling. The outlet liquid from the cooling towers was then recirculated to the scrubber. City water was provided for the scrubber and cooling tower holding tanks for make up and start up.

Water used to quench and scrub the gas in the system was treated periodically and chlorides in the gases were controlled by the adjustment of pH of the scrubbing liquor with sodium carbonate as required.

As indicated in Figure 4-1, the scrubbing system consisted of three major vessels which included the quencher, scrubber, and cooling tower. The primary function of each major vessel in the F/C scrubbing system was as follows:

Quencher: The major objective was to cool 198 Am^3/min (7,000 ACFM) of stack gas at 650°C (1,200 °F) down to 105 Am^3/min (3,700 ACFM) at 71.0°C (160°F). This cooling was accomplished by evaporating recirculated water. In addition, the quencher absorbed and neutralized the acid gases which are emitted during the reclamation of insulated wire. See Figure 4-2.

F/C Scrubber: The F/C scrubber served to remove particulates from the stack gas and to absorb acid gas. The F/C scrubber had a design capacity of 105 Am^3/min (3,700 ACFM) and its major function was to remove fine particulate emissions from the gas stream. See Figure 4-3.

Cooling Tower: The purpose of the cooling tower was to reduce temperature of the scrubber liquor with a flow rate of 570 ℓ/min (150 GPM) from about 59.4°C (139°F) to 40.6°C (106°F). This was accomplished by means of evaporative cooling. See Figure 4-4.

MEACHANICAL DESIGN

The mechanical details of the F/C scrubbing system are shown in the construction drawings which are presented in Figures 4-5 through 4-10. Photographs of the physical system are given in Figures 4-11 through 4-16. A brief description on the mechanical design for each of the quencher major vessels is given below.

Quencher

The quencher included a 1.52 m (60 in.) diameter and 3.7 m (12') long vertical cylindrical spray chamber with co-current

Water used to quench and scrub the gas in the system was treated periodically and chlorides in the gases were controlled by the adjustment of pH of the scrubbing liquor with sodium carbonate as required.

As indicated in Figure 4-1, the scrubbing system consisted of three major vessels which included the quencher, scrubber, and cooling tower. The primary function of each major vessel in the F/C scrubbing system was as follows:

Quencher: The major objective was to cool 198 Am^3/min (7,000 ACFM) of stack gas at 650°C (1,200 °F) down to 105 Am^3/min (3,700 ACFM) at 71.0°C (160°F). This cooling was accomplished by evaporating recirculated water. In addition, the quencher absorbed and neutralized the acid gases which are emitted during the reclamation of insulated wire. See Figure 4-2.

F/C Scrubber: The F/C scrubber served to remove particulates from the stack gas and to absorb acid gas. The F/C scrubber had a design capacity of 105 Am^3/min (3,700 ACFM) and its major function was to remove fine particulate emissions from the gas stream. See Figure 4-3.

Cooling Tower: The purpose of the cooling tower was to reduce temperature of the scrubber liquor with a flow rate of 570 ℓ/min (150 GPM) from about 59.4°C (139°F) to 40.6°C (106°F). This was accomplished by means of evaporative cooling. See Figure 4-4.

MEACHANICAL DESIGN

The mechanical details of the F/C scrubbing system are shown in the construction drawings which are presented in Figures 4-5 through 4-10. Photographs of the physical system are given in Figures 4-11 through 4-16. A brief description on the mechanical design for each of the quencher major vessels is given below.

Quencher

The quencher included a 1.52 m (60 in.) diameter and 3.7 m (12') long vertical cylindrical spray chamber with co-current gas-liquid contact. The shell was assembled from rolled 316 stainless steel sheets, with stainless steel angle support. The inlet and outlet ducting was 46 cm (18") diameter, and a hollow cylindrical entrainment separator was built, packed with 1.6 cm pall rings, and placed at the bottom of the quencher upstream of the outlet.

Initially, the quencher spray requirement was 57 ℓ/min (15.0 GPM) of recirculated liquor which was sprayed evenly through spray manifolds at 2.8 kg/cm^2 (40 psig). Later, the spray flow rate was increased to 90 ℓ/min (24 GPM) in order to improve the collection efficiency of the system. A holding tank measuring 1.2 m x 1.2 m x 60.0 cm located under the quencher unit and a self-priming, centrifugal-type pump at 2.8 kg/cm^2 (40 psig) was provided for this purpose. The inlet piping was 3.8 cm (1-1/2") I.D. while the internal arrangement included a 3.2 cm square stainless steel tubing. The water inside the quencher then drained through a 7.6 cm (3") I.D. pipe into the cooling tower sump tank and eventually was recirculated.

F/C Scrubber

The F/C scrubber consisted of a cylindrical 2.3 m (7'6") diameter and 3.0 m (10') high, five-plate structure with provisions for locating a sixth plate in a split-tower design. The inside walls were coated with Epoxy paint for protection against corrosion and leaks. The stainless steel sieve plates were identical and had triangularly pitched 0.48 cm (3/16") perforations. (Note: The perforation size for plates 4 and 5 were reduced to 0.32 cm (1/8") at a later stage of the project.) The inlet and outlet weirs were 0.46 m (1'6") long and 5 cm (2") high.

The gas was transported from the quencher by a 46 cm (18") diameter duct and introduced under the bottom of plate 1. The gas flowed vertically upward through plates 1 to 3, down through a rectangular compartment into bottom of plate 4, and then vertically upward through plates 4 to 6. The gas then entered the entrainment separator consisting of two tube banks, constructed from 1.9 cm diameter PVC pipe. It was eventually vented to the atmosphere by a 25-HP, belt-driven, centrifugal-type fan which was capable of 142 Am^3/min (5,000 SCFM) at 56.0 cm (22") W.C.

The liquor requirements of the F/C scrubber included a maximum of 56.0 ℓ/min (150 GPM) water on plates 3 and 6. Two self-priming, centrifugal-type pumps of 560 ℓ/min (150 GPM) capacity and 0.91 kg/cm^2 (13 psig) head and a holding tank measuring 1.8 m x 1.8 m x 0.61 m (6' x 6' x 2') was provided for this purpose. Water was introduced at both plates 3 and 6 positions, and it cascaded down to the bottom plates 1 and 4, respectively, maintaining cross flow on the sieve plates. The inlet piping to the F/C scrubber was 7.62 cm (3") I.D. while the water was drained out from the unit into the holding tank through a 15.3 cm (6") drain.

Cooling Tower

The cooling tower consisted of a 5.3 m x 3.0 m x 2.7 m (17'6" x 10' x 9') counter-current spray chamber. Ambient air was induced through the spray chamber by an air-foil, blade-type, belt-driven, tube-axial fan with a 3.7 kw (5 HP) motor and capacity of 650 Am^3/min (23,000 SCFM). During the tests it was found that a high efficiency entrainment separator was required before the air could be vented to the atmosphere. The entrainment separator consisted of 3 rows of wave-plate baffles with spacing of 1.3 cm (1/2") and a wave amplitude of 2.2 cm (7/8"). Baffle rows were offset 0.65 cm (1/4") and baffle direction in each row was also reversed.

The liquor to be cooled was sprayed from the top at a rate of 560 ℓ/min (150 GPM) at 2.8 kg/cm^2 (40 psig) through a spray manifold. This liquor was pumped from the scrubber holding tank and utilized a self-priming, centrifugal-type pump with a capacity of 662 ℓ/min at 2.8 kg/cm^2 (40 psig). The cold water was then collected in a 3 m x 2.7 m x 0.46 m (10' x 9' x 1'6") holding tank under the tower and sprayed back to the scrubber unit.

Piping

Polyvinyl chloride (PVC) piping was selected for the F/C scrubbing system, due to its superior resistance to acidic and brine solutions. Chlorinated PVC piping was specified for the quencher circuit due to the higher liquid temperatures. The liquor piping system was based on the scrubber operating configurations, while the layout was based on accessibility and eases of measurement and control.

The flow control system with valves and bypass lines were designed to provide for accuracy and protection from transients and water hammer effects. Relay systems and level controls were specified for the pump electrical wiring to protect against pump cavitation, and to ensure that the hot furnace gas flow will be cut off if the quencher pump failed.

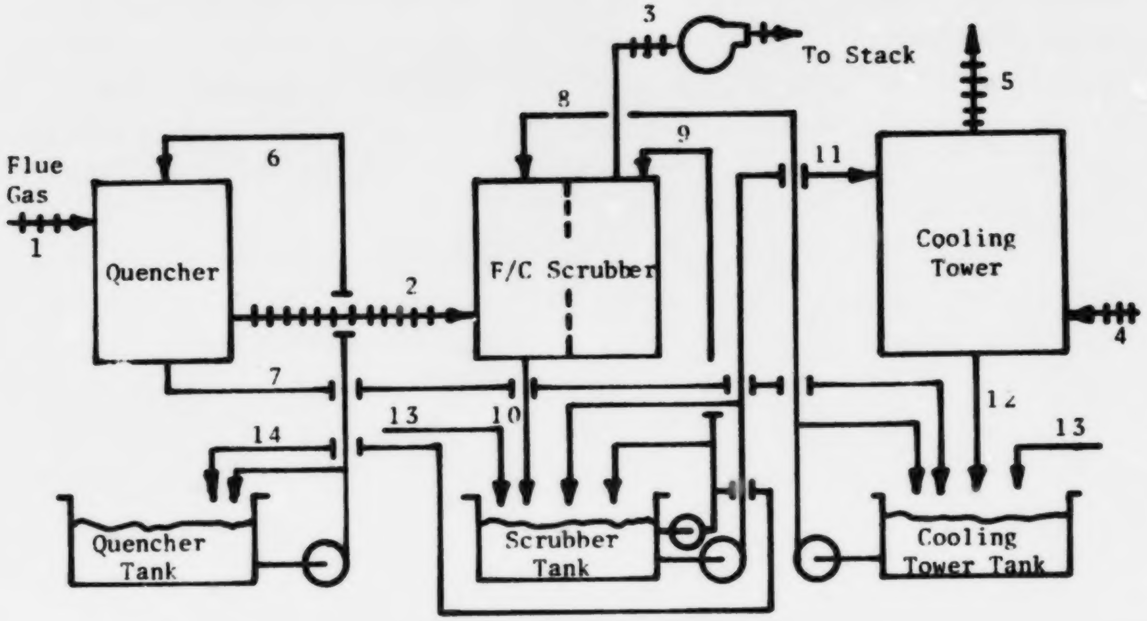
3
To Stack
5
8
9
11
Flue Gas
1
6
Quencher
2
F/C Scrubber
Cooling Tower
4
7
12
13
10
14
13
Quencher Tank
Scrubber Tank
Cooling Tower Tank

STREAM NO.	COMPOSITION	TEMP. °C	VOL.FLOW Am^3/min (G) or ℓ/min (L)	MASS FLOW kg/hr	ENTHALPY (0°C BASE) kcal/kg	y g water / g d.gas
1	Flue Gas	649	198	4,400	226(d.g.)	0.07
2	Gas Mixture	71.7	100	5,384	211(d.g.)	0.31
3	Gas Mixture	50.6	71.8	4,480	67.5(d.g.)	0.09
4	Ambient Air	31.4	850	58,700	19	0.011
5	Gas Mixture	-	-	60,000	30.5	0.033
6	Water	59.4	59.0	3,540	68.4	-
7	Water	71.1	43.3	2,600	71.1	-
8	Water	40.6	568	34,100	40.6	-
9	Water	59.4	568	34,100	59.4	-
10	Water	59.4	1150	69,000	59.4	-
11	Water	59.4	568	34,100	59.4	-
12	Water	40.6	549	32,900	40.6	-
13	City Water	21.1	18.9	1,140	21.1	-
14	Make-up Water	59.4	13.6	818	59.4	-

Figure 4-1. Flow diagram of F/C scrubbing system.

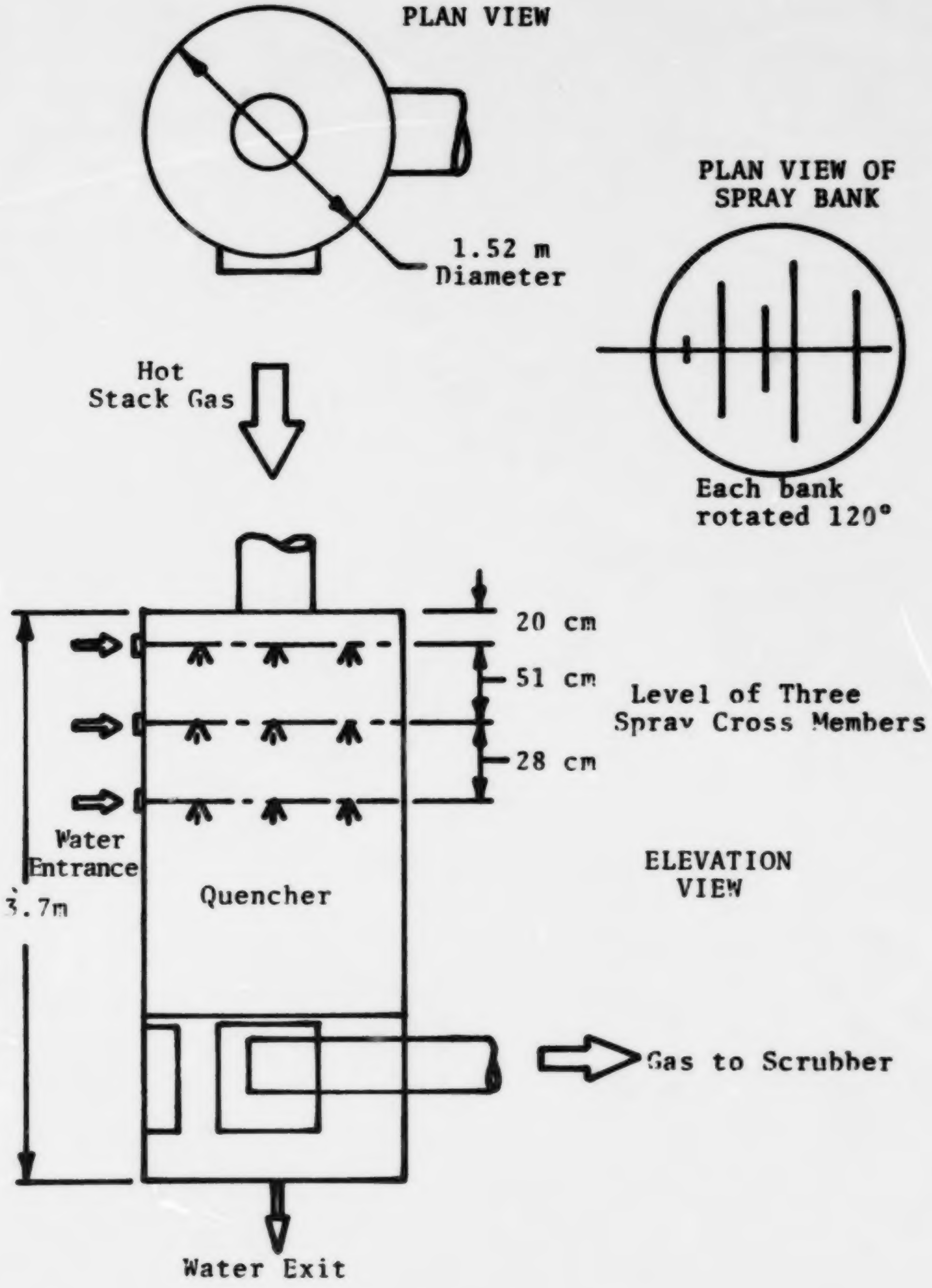
PLAN VIEW
1.52 m Diameter
PLAN VIEW OF SPRAY BANK
Each bank rotated 120°
Hot Stack Gas
20 cm
51 cm
28 cm
Level of Three Spray Cross Members
Water Entrance
3.7m
Quencher
ELEVATION VIEW
Gas to Scrubber
Water Exit

Figure 4-2. Quencher unit of F/C demonstration system.

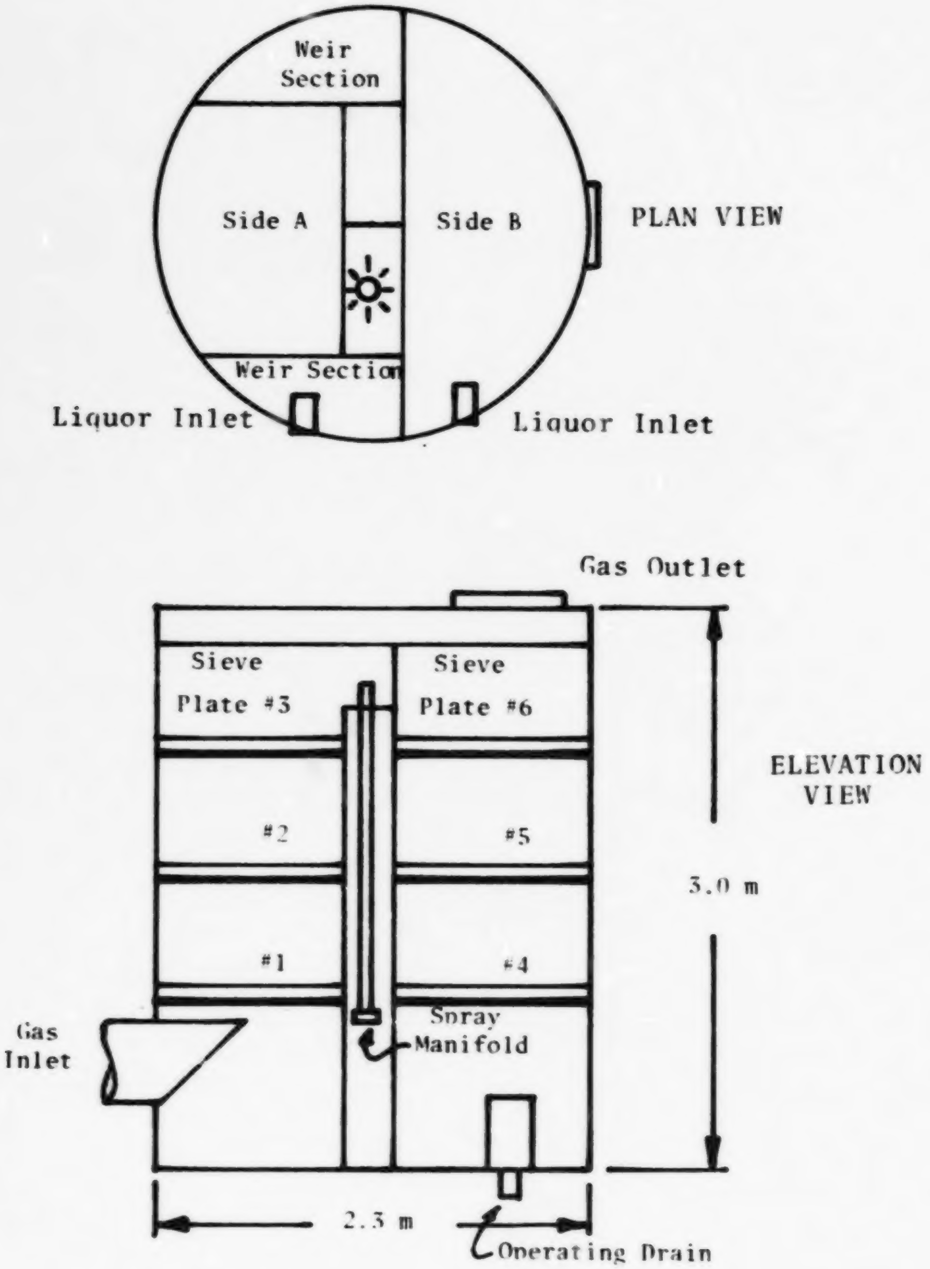
Weir Section
Side A
Side B
PLAN VIEW
Weir Section
Liquor Inlet
Liquor Inlet
Gas Outlet
Sieve Plate #3
Sieve Plate #6
ELEVATION VIEW
#2
#5
3.0 m
#1
#4
Gas Inlet
Spray Manifold
2.3 m
Operating Drain

Figure 4-3. Scrubber unit of F/C demonstration plant.

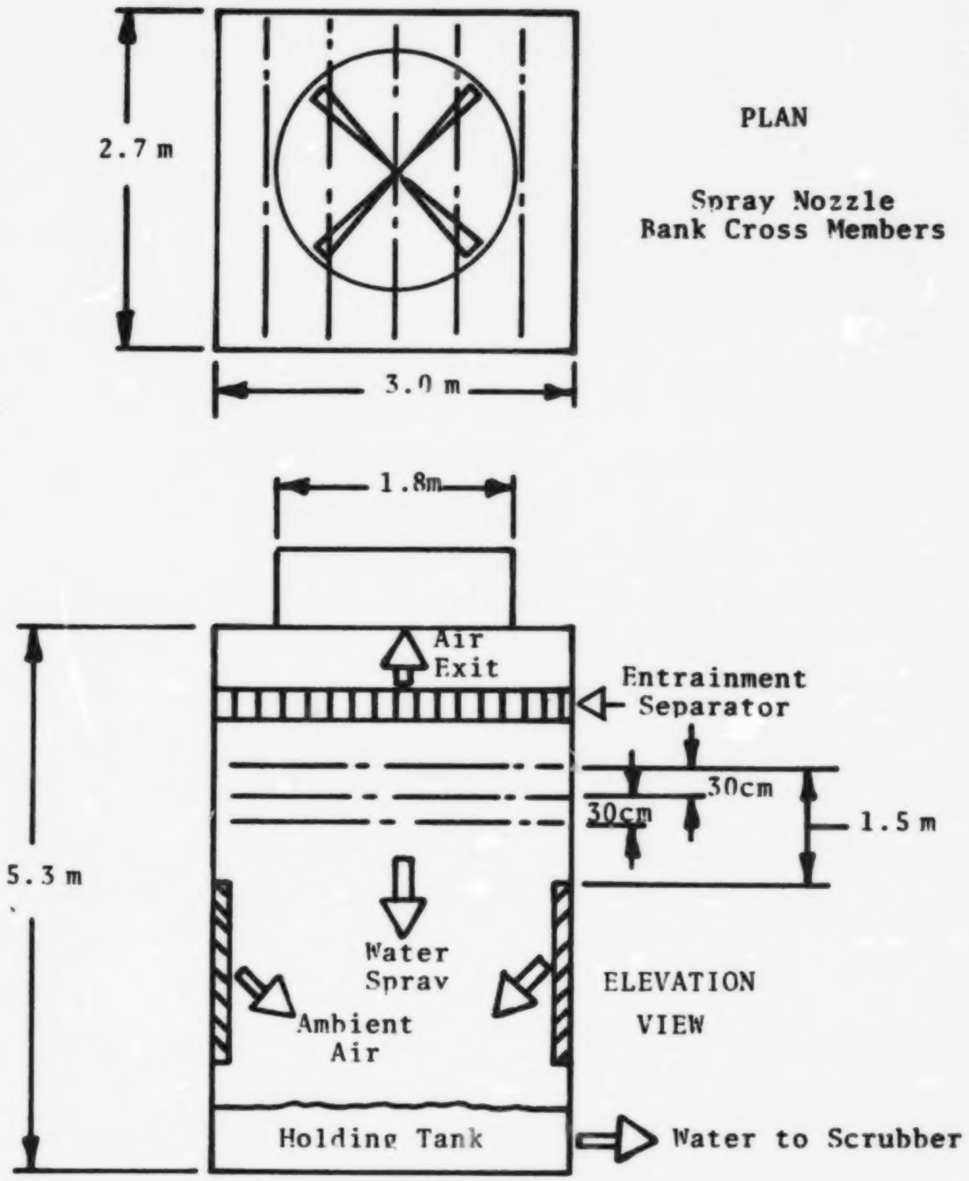
2.7 m
PLAN
Spray Nozzle
Bank Cross Members
3.0 m
1.8m
Air
Exit
Entrainment
Separator
30cm
30cm
1.5 m
5.3 m
Water
Spray
ELEVATION
VIEW
Ambient
Air
Holding Tank
Water to Scrubber

Figure 4-4. Cooling tower of F/C demonstration scrubbing system.

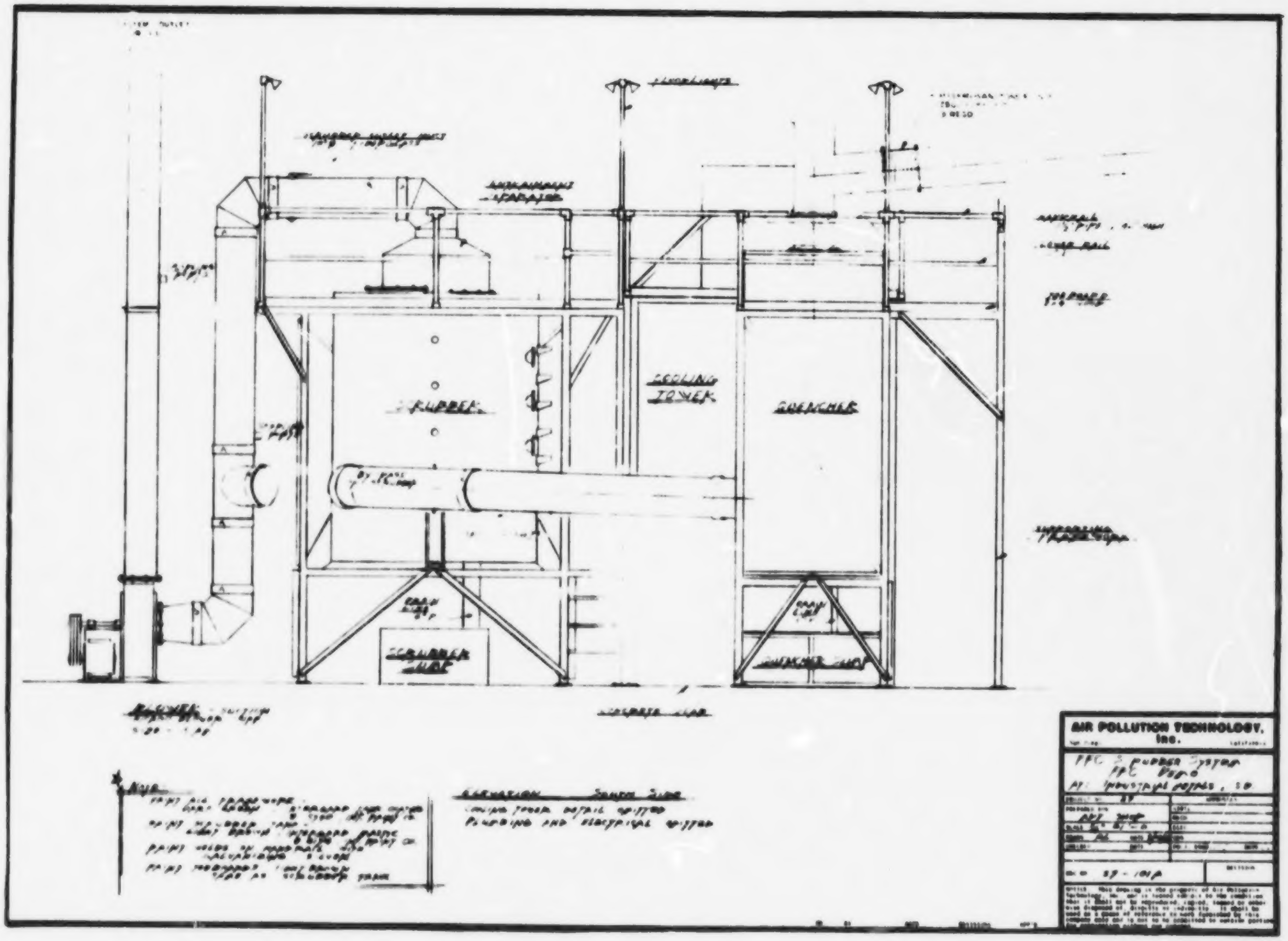
SCRUBBER
COOLING TOWER
QUENCHER
SCRUBBER SUMP
QUENCHER SUMP
CONCRETE SLAB
ELEVATION SOUTH SIDE
AIR POLLUTION TECHNOLOGY, Inc.

Figure 4-5. General elevation, F/C scrubber demonstration system.

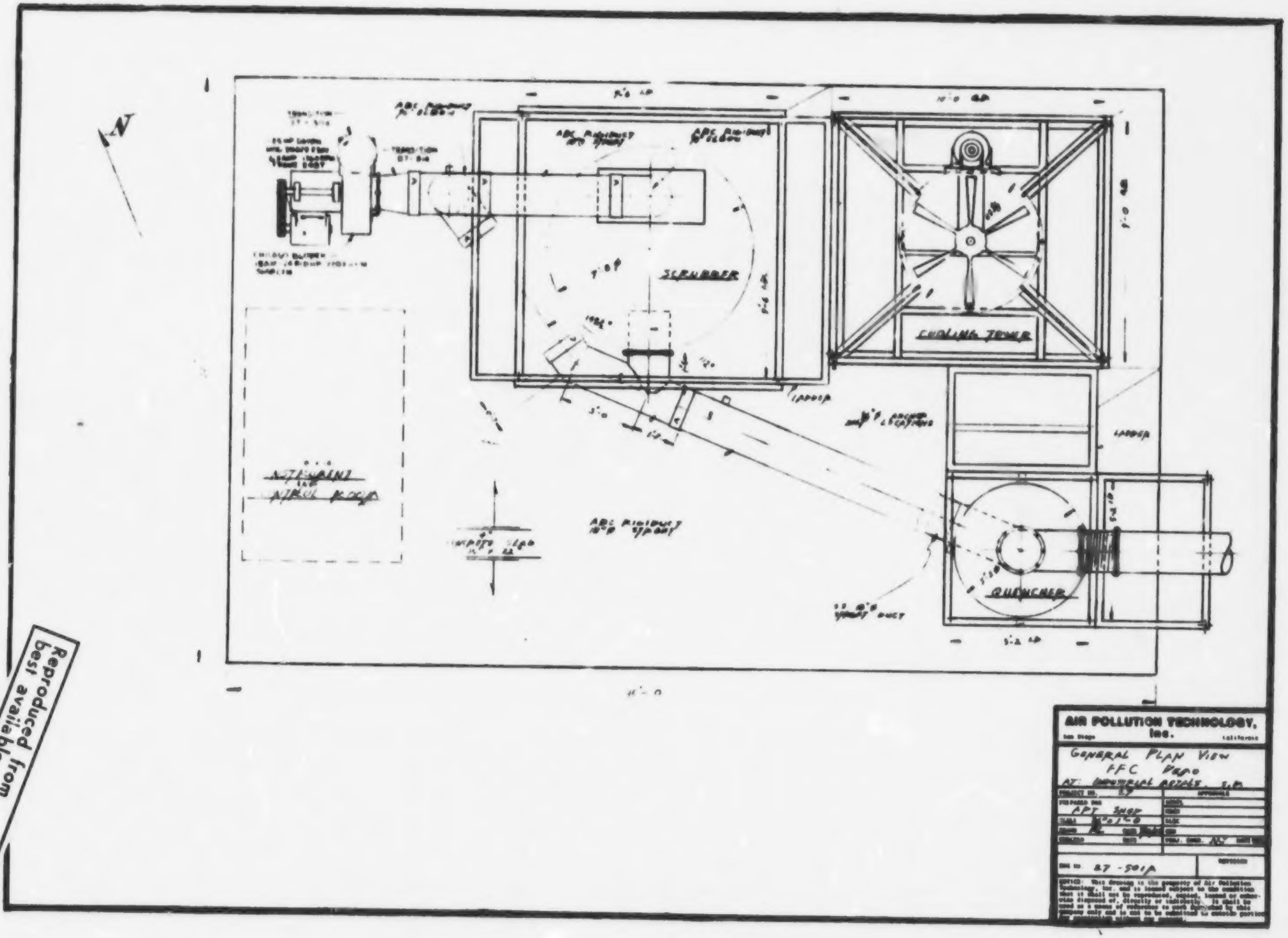
N
SCRUBBER
COOLING TOWER
QUENCHER
LADDER
AIR POLLUTION TECHNOLOGY, Inc.
San Diego
California
GENERAL PLAN VIEW
FFC Demo
APT SHOP
27-501A

Figure 4-6. Top view, F/C scrubber demonstration system.

Reproduced from best available copy.

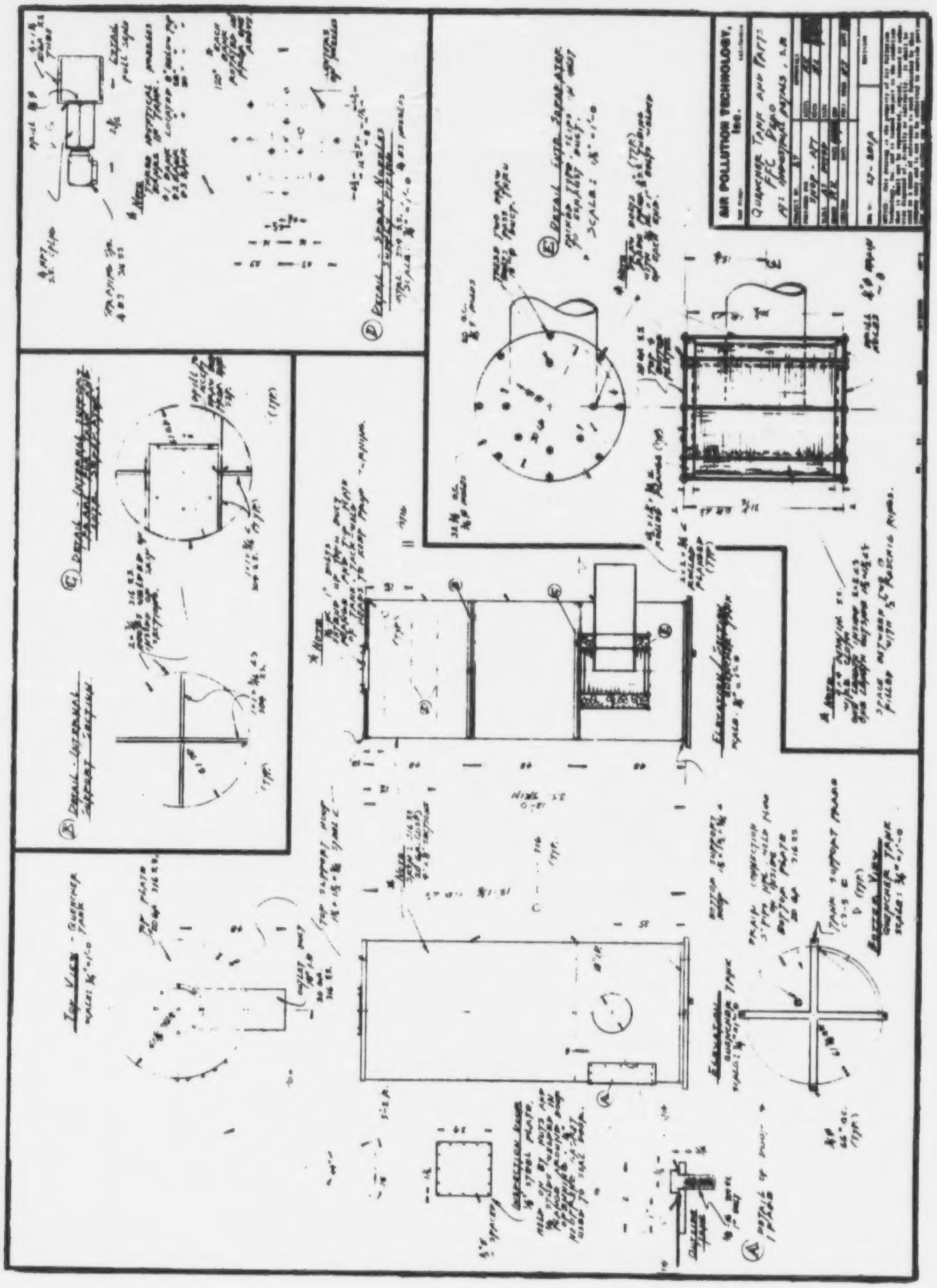
AIR POLLUTION TECHNOLOGY, Inc.

Figure 4-7. Quencher details.

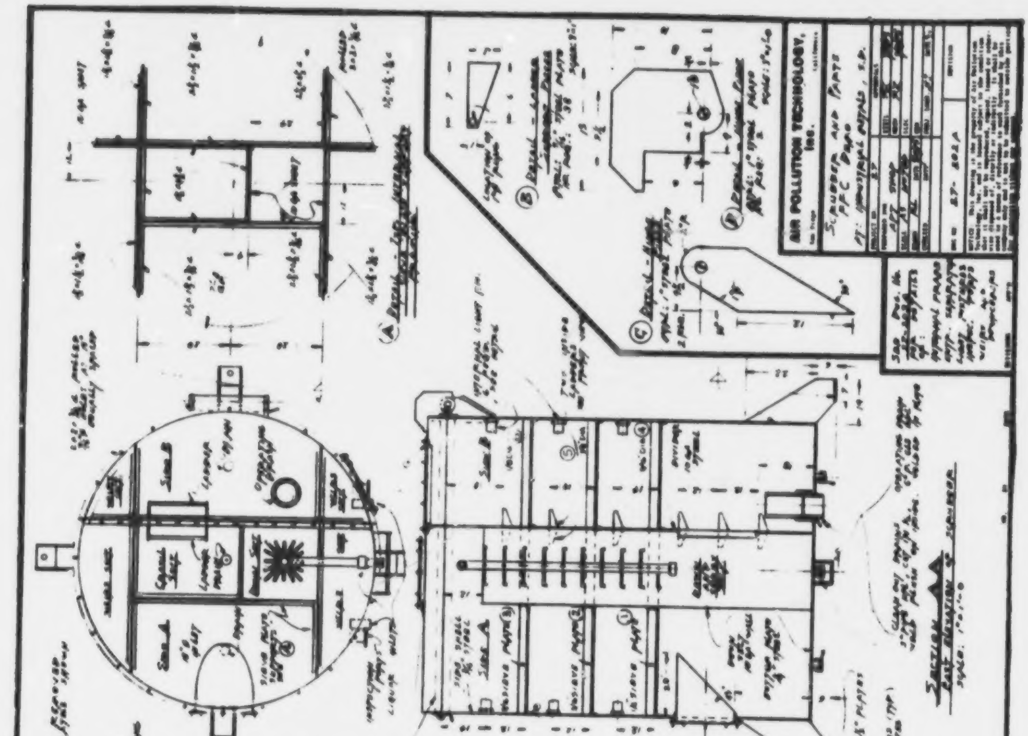
AIR POLLUTION TECHNOLOGY, Inc.
TOP VIEW
ELEVATION
SECTION A-A

Figure 4-8.F/C scrubber details.

Reproduced from best available copy.

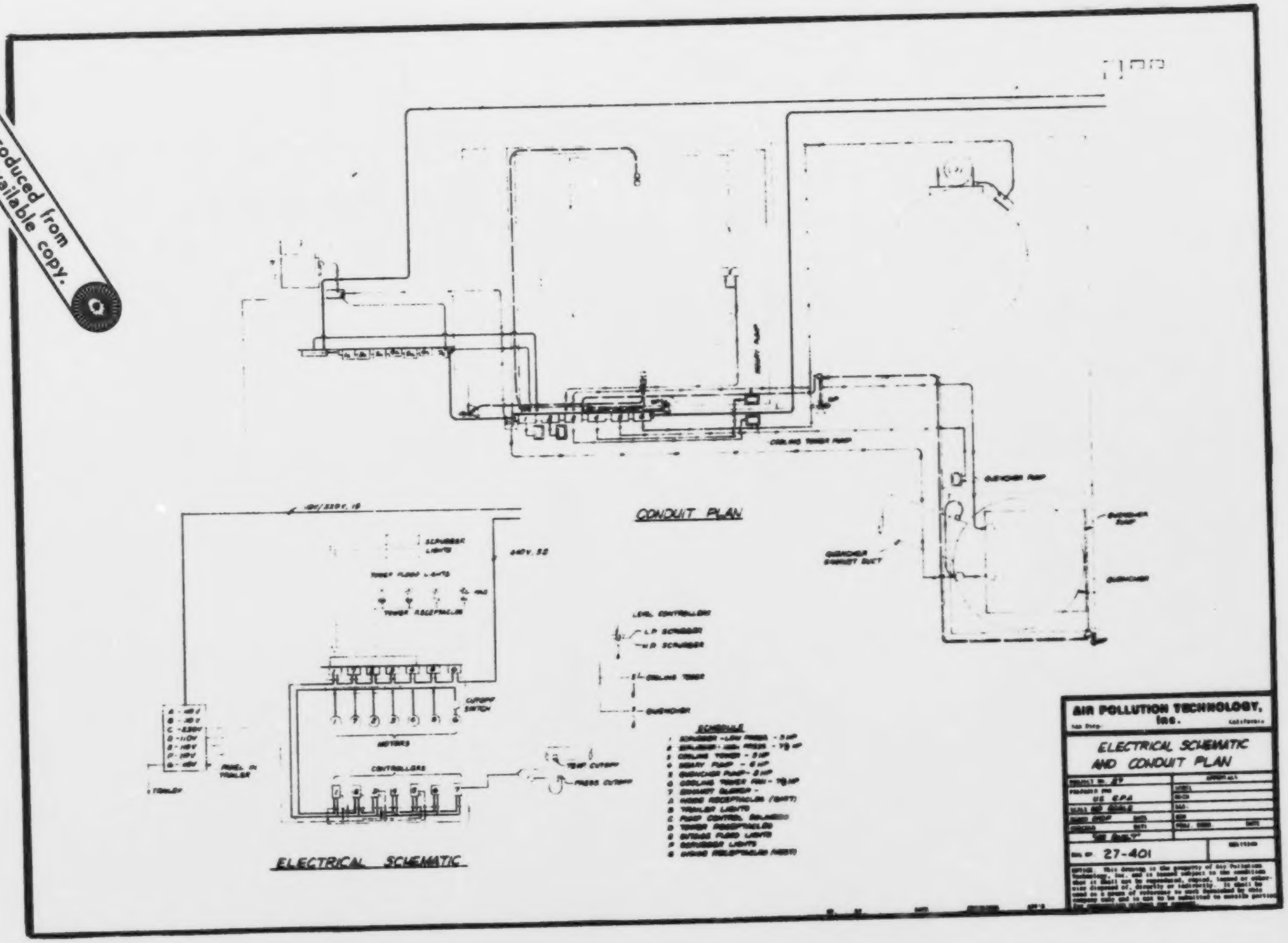
CONDUIT PLAN
COOLING TOWER PUMP
QUENCHER PUMP
QUENCHER EXHAUST DUCT
QUENCHER
ELECTRICAL SCHEMATIC
SCRUBBER LIGHTS
TOWER FLOOD LIGHTS
TOWER RECEPTACLE
440V. 3Ø
CUTOFF SWITCH
MOTORS
CONTROLLERS
PANEL IN TRAILER
TRAILER
TEMP CUTOFF
PRESS CUTOFF
LEVEL CONTROLLER
L.P. SCRUBBER
H.P. SCRUBBER
COOLING TOWER
QUENCHER
SCHEDULE
AIR POLLUTION TECHNOLOGY, Inc.
ELECTRICAL SCHEMATIC AND CONDUIT PLAN
US EPA
27-401

Reproduced from best available copy.

Figure 4-9. Electrical schematic of F/C scrubber demonstration system.

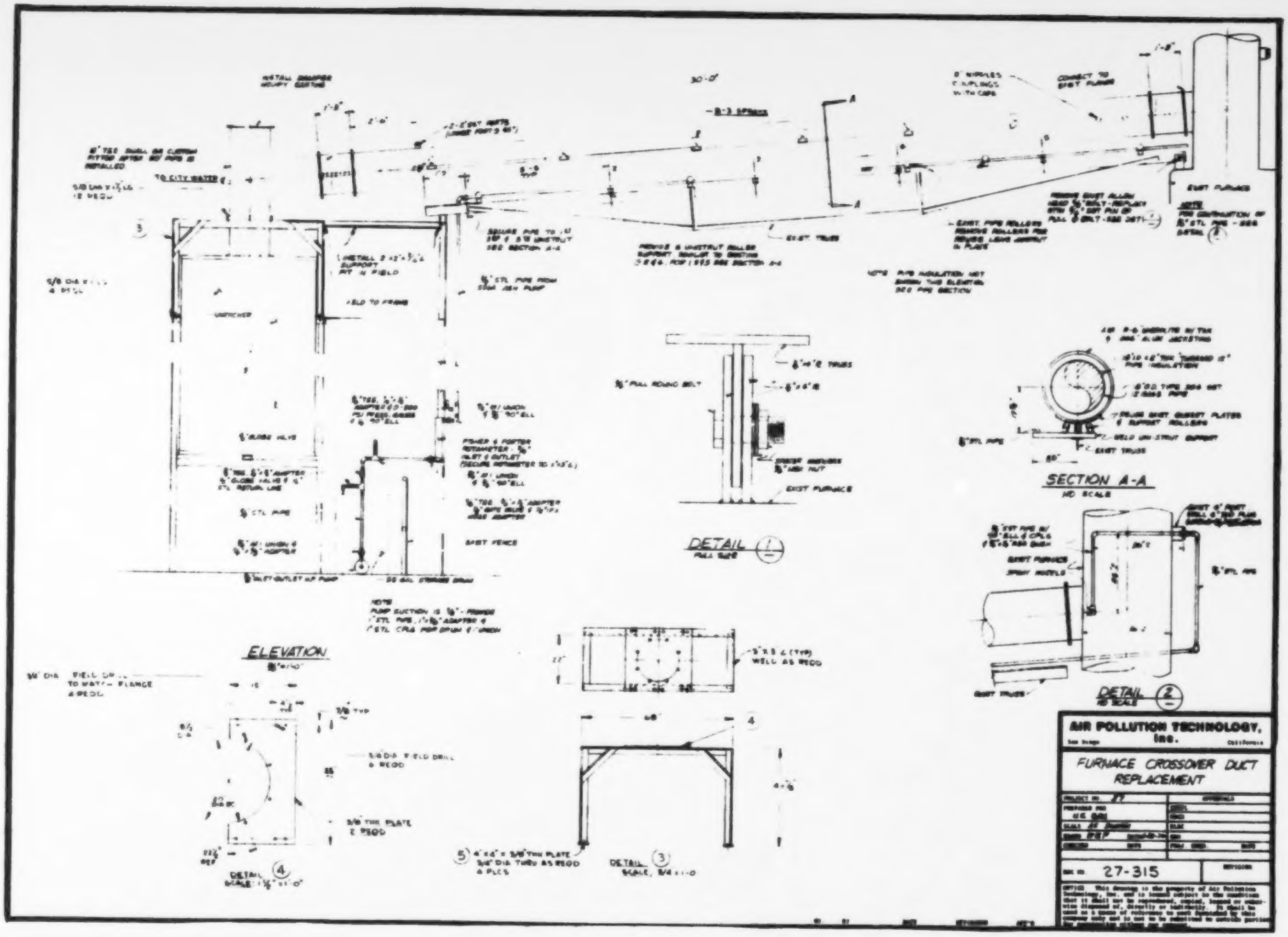
30'-0"
TO CITY WATER
ELEVATION
DETAIL 1
FULL SIZE
SECTION A-A
NO SCALE
DETAIL 2
NO SCALE
DETAIL 3
SCALE 3/4"=1'-0
DETAIL 4
AIR POLLUTION TECHNOLOGY, Inc.
San Diego California
FURNACE CROSSOVER DUCT REPLACEMENT
27-315

Figure 4-10. Furnace crossover duct to F/C scrubber demonstration system.

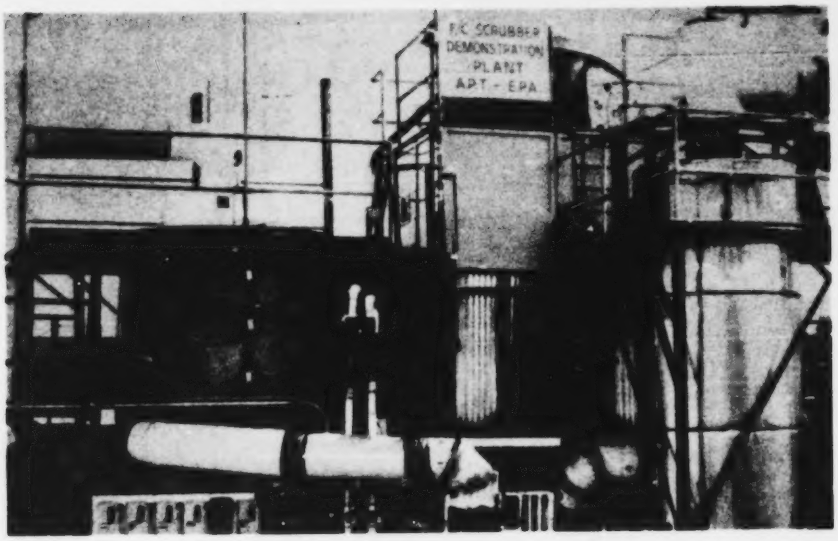
F/C SCRUBBER
DEMONSTRATION
PLANT
APT - EPA

Figure 4-11. Front view of F/C demonstration scrubber.

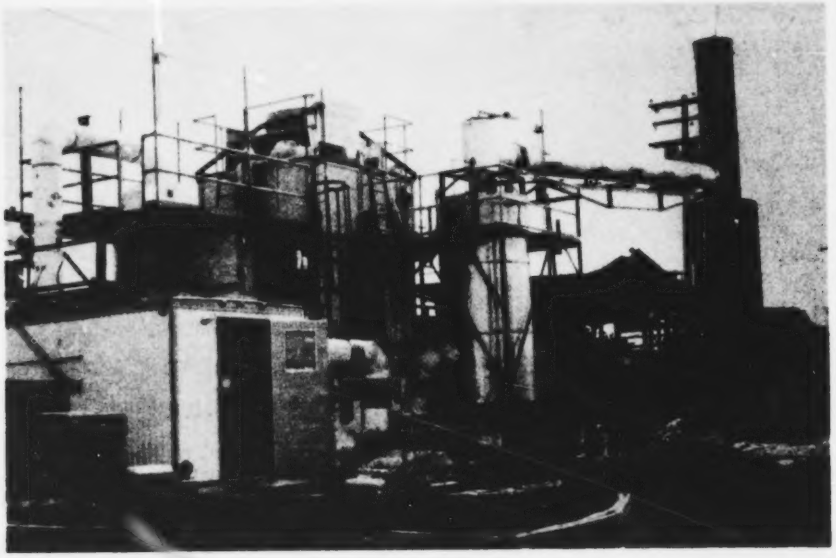

Figure 4-12. View of F/C scrubber system and metals recovery furnace.

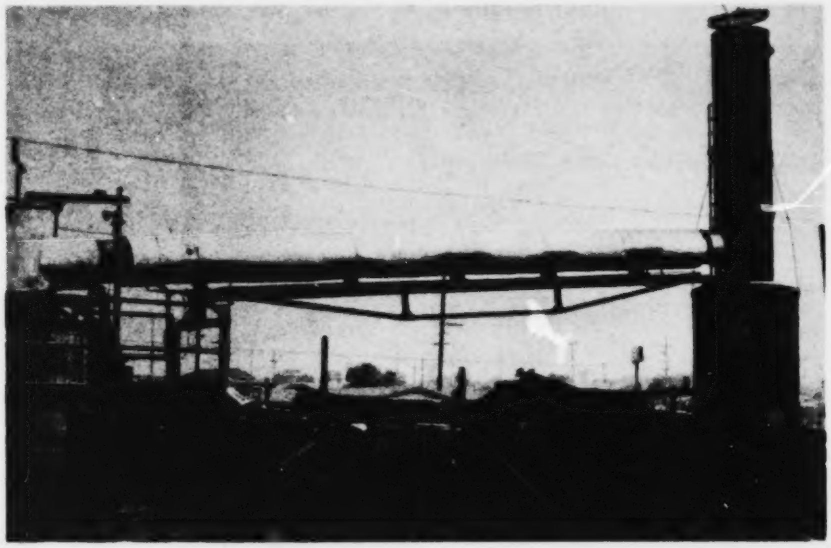

Figure 4-13. Crossover duct from furnace stack to F/C demonstration scrubber.

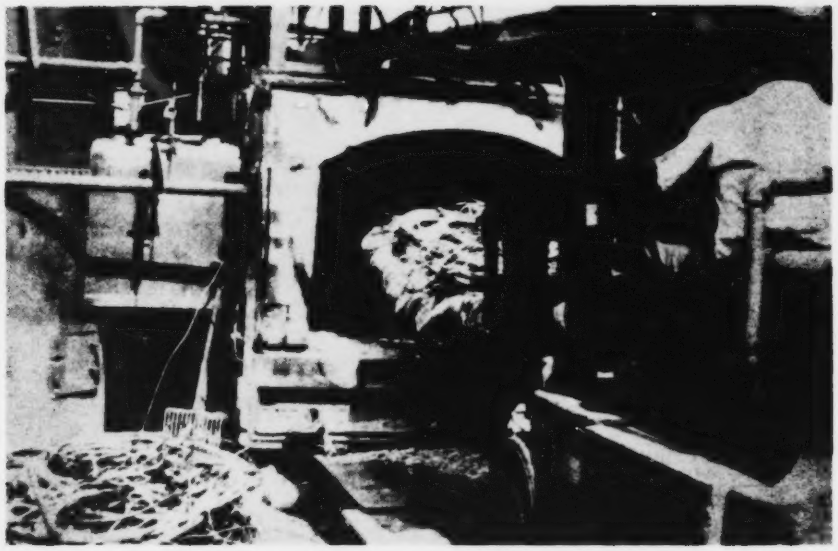

Figure 4-14. View of secondary metals recovery furnace and charging process.

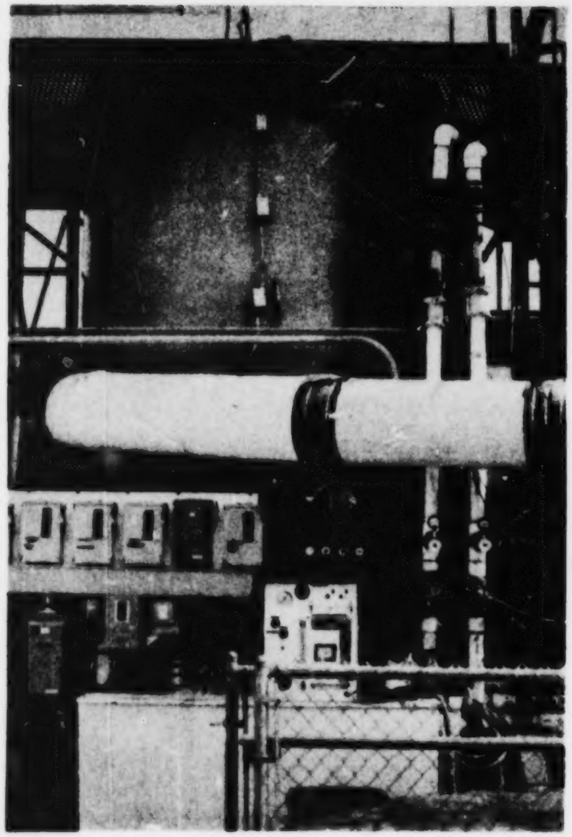

Figure 4-15. Sieve plate scrubber of F/C demonstration system.

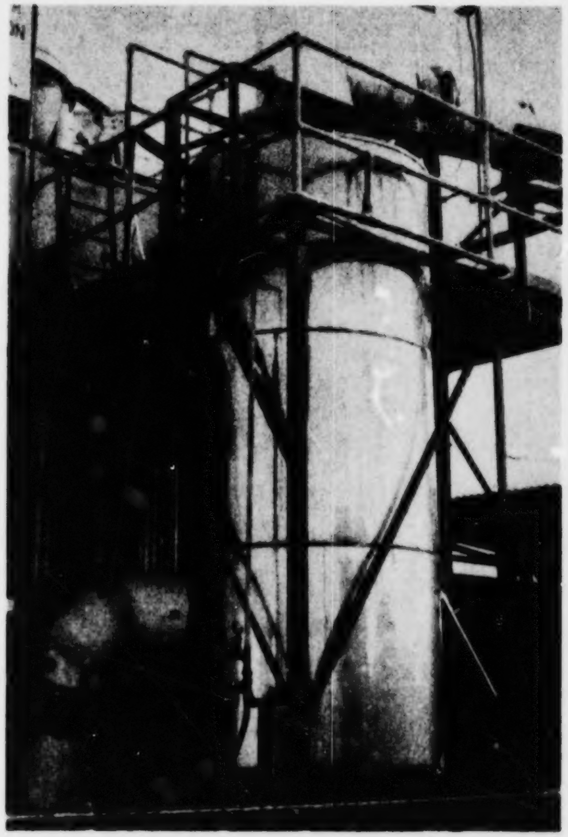

Figure 4-16. Quencher unit of F/C scrubber system.

CHAPTER 5

SYSTEM PERFORMANCE TESTING

After the installation of the scrubbing system, peripheral equipment was installed for monitoring the different process parameters and testing the performance of the system. On completion of this task, startup of the demonstration plant was initiated, and thereafter the system was evaluated by compiling process and performance data under different operating modes. The following information regarding the F/C demonstration plant is described in this section of the report:

1. Instrumentation system of the demonstration plant.
2. Performance testing equipment.
3. Demonstration unit operating procedures.
4. Testing procedures.
5. Data analysis and calculations.

INSTRUMENTATION SYSTEM

Instrumentation for the scrubber system provided for measurements of flow rates, temperatures, pressures and humidity in the gas and liquid streams as indicated in Figure 5-1.

Three venturi meters were fabricated out of polyvinyl chloride material and were used to measure flow rates in the scrubber low pressure, scrubber high pressure, and cooling tower liquor piping. Two fluid manometers with mercury as the indicating fluid were used to measure the pressure drop across these venturi meters.

Two rotameters with flow ranges of 0-150 ℓ/min (0-40 GPM) were installed and used for measuring flow rates in the liquid lines going to the scrubber center duct and quencher spray manifold. Rotameters were also used to monitor the liquor flow rate of the sodium carbonate spray system and water spray

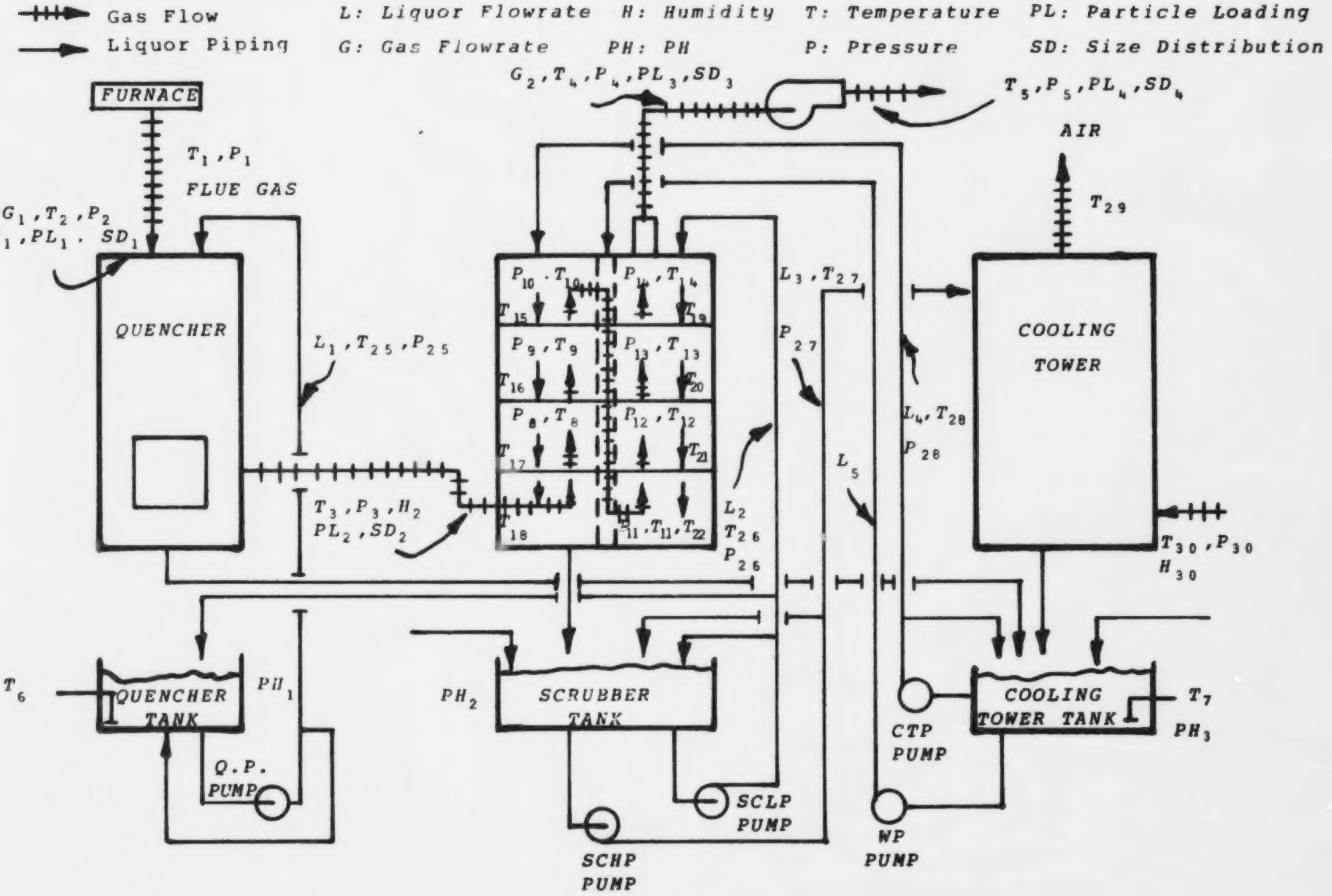
Gas Flow
Liquor Piping
L: Liquor Flowrate
H: Humidity
T: Temperature
PL: Particle Loading
G: Gas Flowrate
PH: PH
P: Pressure
SD: Size Distribution
FURNACE
T_1, P_1
FLUE GAS
G_1, T_2, P_2
$H_1, PL_1 . SD_1$
QUENCHER
L_1, T_{25}, P_{25}
T_3, P_3, H_2
PL_2, SD_2
$G_2, T_4, P_4, PL_3, SD_3$
T_5, P_5, PL_4, SD_4
$P_{10} . T_{10}$
P_{14}, T_{14}
T_{15}
T_{19}
P_9, T_9
P_{13}, T_{13}
T_{16}
T_{20}
P_8, T_8
P_{12}, T_{12}
T_{17}
T_{21}
T_{18}
P_{11}, T_{11}, T_{22}
L_2
T_{26}
P_{26}
L_3, T_{27}
P_{27}
L_5
L_4, T_{28}
P_{28}
AIR
T_{29}
COOLING TOWER
T_{30}, P_{30}
H_{30}
T_6
QUENCHER TANK
PH_1
Q.P. PUMP
PH_2
SCRUBBER TANK
SCHP PUMP
SCLP PUMP
WP PUMP
CTP PUMP
COOLING TOWER TANK
T_7
PH_3

Figure 5-1. F/C scrubber system instrumentation sheet.

inside the cross-over duct from the furnace stack to the quencher.

The gas flow rates were measured with standard pitot tubes. These measurements were made at the inlet to the quencher and at the inlet to the blower.

The gas temperature was measured with thermocouples, utilizing type T (copper/constantan) at temperatures below 200°C and type K (chromel/alumel) at temperatures above 200°C. The thermocouples were wired to a multipoint, millivolt recorder which was located in the scrubber system control room.

Water temperatures in the scrubber unit were measured with copper constantan (type T) thermocouples. In the high pressure liquid lines, dial thermometers were used for measurement of the liquor temperature.

Pressures in the gas lines were measured with either inclined, straight-well-type manometers or Magnehelic gauges. This selection was based on the accuracy and sensitivity of the measurement required. Pressure in the liquor lines was measured by standard type pressure gauges.

The moisture content in the quencher inlet gas was determined from a wet and dry bulb thermometer measurements. The scrubber inlet and outlet gas streams were considered saturated and the moisture content was determined from the temperature of the gas.

PERFORMANCE TESTING EQUIPMENT

The performance of the demonstration plant was evaluated by measuring the total particle collection efficiency of the system by using a modified EPA Method 5 technique. In addition, A.P.T. cascade impactors were used to measure the particle size distribution in the gas stream and obtain the demonstration plant efficiency as a function of particle size. The apparatus used is described as follows:

1. Four identical particle sampling trains (see Figures 5-2 and 5-3) were fabricated and utilized at the furnace stack, quencher inlet, scrubber inlet, and scrubber outlet locations.

2. All the sampling equipment was operated with inlet nozzles appropriately sized to give isokinetic sampling. In the majority of the runs, a pre-cutter with an approximate cut diameter of 6 μmA was used to remove both the larger particle loading and the entrained liquid.

3. The sampling probes were constructed of 1.27 cm (0.5") stainless steel tubing and installed in the sampling ports of the scrubbing systems.

4. The total particulate loadings were measured by using 10.2 cm (4") ex-stack filter holders, while the particle size distributions were determined by ex-stack A.P.T. cascade impactors. The collection device in each case was followed by 4 impingers for gas absorption and 1 silica gel dryer to remove moisture.

5. The sampling probes and collection device were heated with insulated heating tape controlled with variable transformers to prevent water condensation in the system. The dry gas sample flow rate was measured with a dry gas meter, a rotameter, and an orifice meter in each train.

6. Impactor substrates and filters were weighed with an analytical balance to the nearest tenth milligram. Tare weights were taken after drying in an electrical oven and desiccator. Glass fiber filter paper (Gelman type "A") was used for impactor substrates and filters.

SCRUBBER SYSTEM OPERATING PROCEDURE

This section summarizes the procedure for the operation of the F/C scrubber demonstration unit. For brevity, the periodic routine maintenance functions are not included here, and only the normal startup, operation,and shutdown procedures are given.

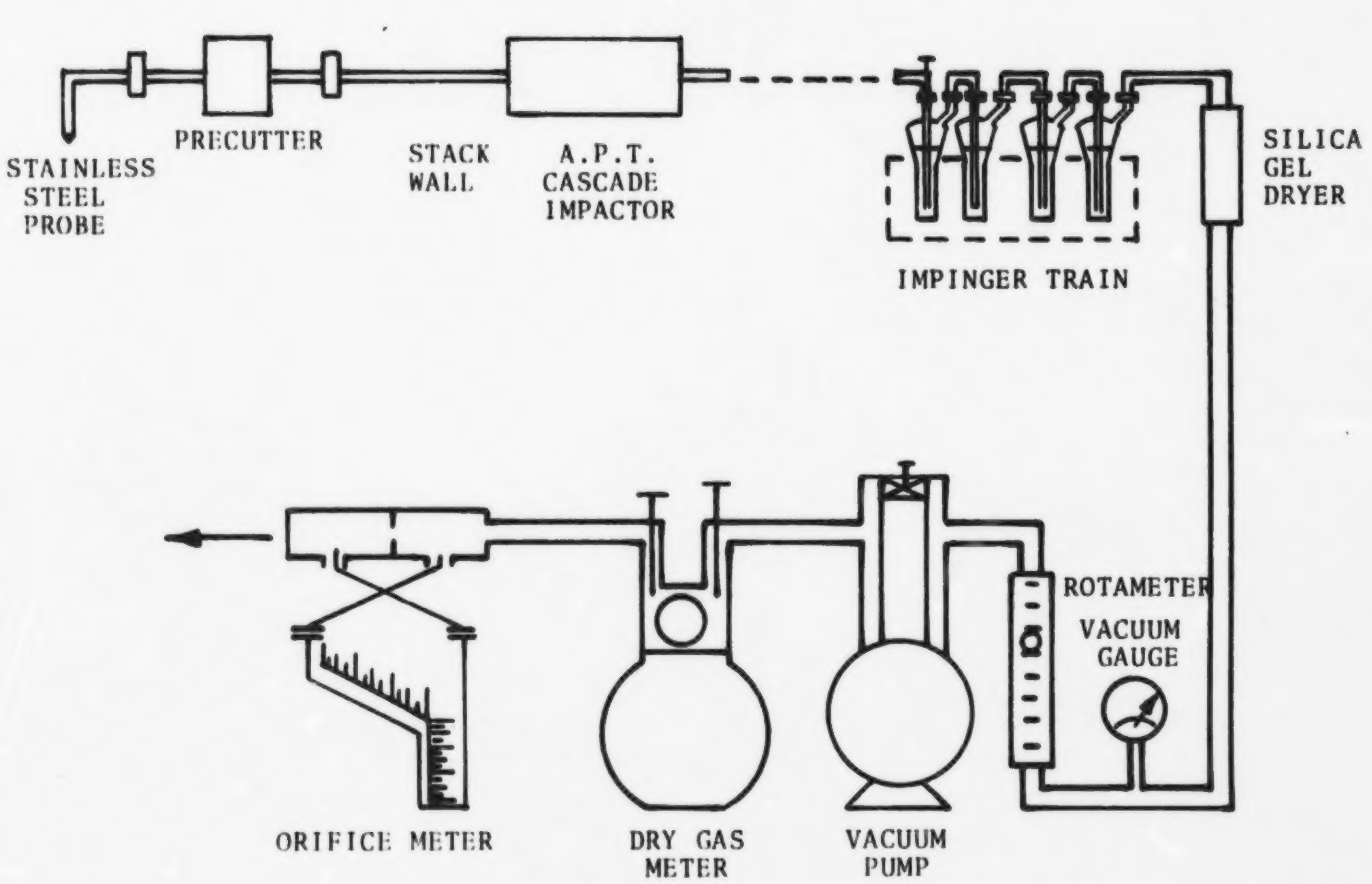
STAINLESS STEEL PROBE
PRECUTTER
STACK WALL
A.P.T. CASCADE IMPACTOR
IMPINGER TRAIN
SILICA GEL DRYER
ROTAMETER
VACUUM GAUGE
VACUUM PUMP
DRY GAS METER
ORIFICE METER

Figure 5-2. Modified E.P.A. sampling train with ex-stack cascade impactor. Scrubber outlet sampling system.

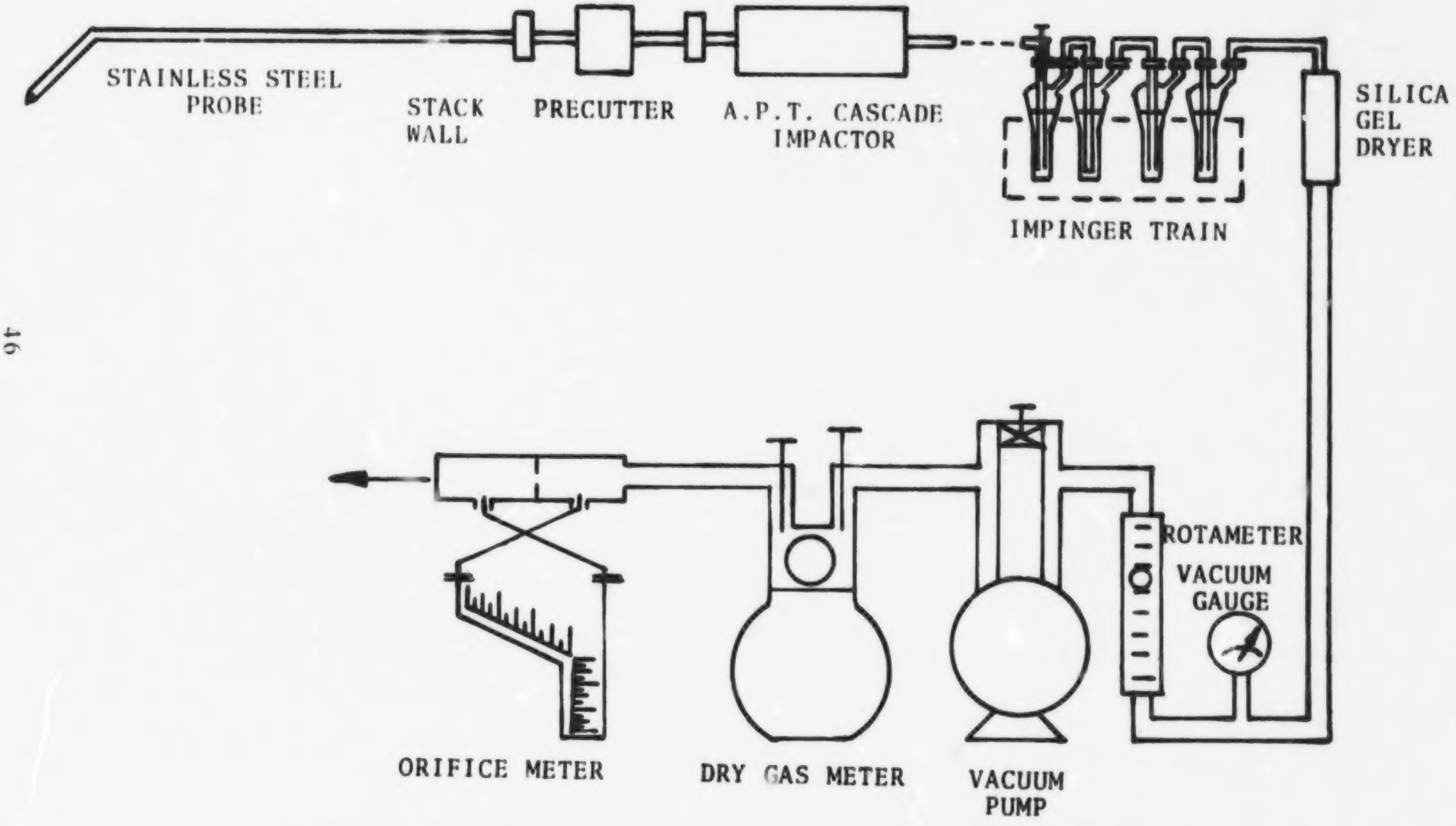
STAINLESS STEEL PROBE
STACK WALL
PRECUTTER
A.P.T. CASCADE IMPACTOR
IMPINGER TRAIN
SILICA GEL DRYER
ROTAMETER
VACUUM GAUGE
ORIFICE METER
DRY GAS METER
VACUUM PUMP

Figure 5-3. Modified E.P.A. sampling train with ex-stack cascade impactor. Quencher inlet sampling system.

During startup, initially all the liquor tanks were filled with city water and then the water was circulated from the scrubber to the cooling tower. Cold water from the cooling tower was pumped back into the scrubber. Simultaneously, the quencher pump was started and this activated the water sprays in the quencher unit. At this time the cooling tower fan was turned on, followed by the main blower which draws the gas from the furnace through the F/C system. This completed the startup of the F/C scrubbing unit.

The operation of the F/C unit required little attention and only routine visual inspection was necessary to ensure that all equipment was performing as described. Fail-safe circuits were provided so that the pumps would cease operation in case of low water level in the liquor tanks. Similarly, the blower would stop in case of liquor failure to the quencher. During operation of the F/C scrubber unit, adjustments to ensure adequate water rate and gas flow through the system were made but were necessary only occasionally.

The shutdown procedure was simple. The main blower and the cooling tower fan were turned off and all the pumps were deactivated. This then stopped the operation of the scrubber system.

PERFORMANCE TEST PROCEDURES

This section describes the test procedures that were used to determine the performance of the F/C scrubber unit. The particle and contaminant gas collection efficiency of the system were measured by a combination of tests described below. All tests were run after the scrubber system was in operation and had achieved a steady state condition.

Modified EPA Method 5 (Filter Runs)

A modified EPA Method 5 test procedure was utilized to determine overall particulate loading, particulate penetration and gas absorption in the system. The samples were obtained at the furnace stack, quencher inlet, scrubber inlet, and scrubber outlet.

Impaction Runs

The particle characteristics in the gas streams were measured by A.P.T. cascade impactors. The impactors were heated to prevent vapor condensation on the impactor walls. Pre-cutters were also used preceding the impactor in order to remove the larger particles.

For both the filter and the impactor runs, the impinger catch was analyzed to determine chloride ion concentration, pH and total solids. The efficiency of the scrubber system for the absorption of contaminant gases can be determined from these data.

METHODS OF CALCULATION

The F/C scrubber system performance was measured by sampling with both absolute filters and cascade impactors. The filter runs provided information on the total particulate loading, and the overall scrubber efficiency. The impactor runs provided particle characteristics such as the particle size distribution, cumulative mass loading, particle penetration, and the particle number concentration.

Particle Loading and Overall Efficiency

The total particulate loading inlet and outlet to the system and the overall efficiency were calculated as follows:

1. The dry sample volume flow rate was converted to normal conditions at 0°C and 1 atm (DNm^3/min).
2. Total weight gain on the sampling elements were combined into one quantity (g).
3. The total particle mass loading, "C", (g/DNm^3) was calculated from:

$$C = \frac{\text{total weight gain (g)}}{\text{sampling rate }(DNm^3/min) \times \text{sampling time (min)}} \qquad (5\text{-}1)$$

4. The overall penetration was calculated from:

$$\overline{Pt} = \frac{C_o}{C_i} \qquad (5\text{-}2)$$

where "C_i " and "C_o " were the inlet and outlet particle loadings measured simultaneously.

5. The overall efficiency (E%) was calculated from:

$$E\% = (1-\overline{Pt})\ 100\% \qquad (5\text{-}3)$$

Particle Size Distribution

The particle size distributions were measured gravimetrically using the cascade impactor as a device to fractionate particles of different size. Cumulative mass of particles collection on each stage and all the stages below, including the absolute filter were calculated as a percentage of the total weight gain. The cut diameters for the impactor stages were calculated from the sampling rate in conjunction with the calibration data for A.P.T. impactors.

Cumulative Mass Loading and Particle Penetration

The penetration as a function of particle size, or the fractional penetration through the system, was determined by a stepwise graphical procedure. The procedure is based on the following equation:

$$Pt\ (d_{pa}) = \frac{f(d_{pa})_o}{f(d_{pa})_i} = \frac{\left[\frac{dC}{d(d_{pa})}\right]\ \text{outlet}}{\left[\frac{dC}{d(d_{pa})}\right]\ \text{inlet}} \qquad (5\text{-}4)$$

where "$dC/d(d_{pa})$" is the slope of cumulative mass loading less than "d_{pa}" versus the aerodynamic particle diameter curve at "d_{pa}" and equals "$f(d_{pa})$", and "Pt (d_{pa}) is the penetration for particle diameter "d_{pa}".

To determine the penetration as a function of particle size the following procedure was followed:

1. Cumulative mass loading for all the stages and the filter, below the stage with a cut diameter of "d_{pa}", were plotted against "d_{pa}" from the inlet and outlet cascade impactor samples.
2. Slopes of the inlet and outlet plots above were determined for several "d_{pa}" values in the range of 0.5 μmA to 3.0 μmA. The fractional penetration was determined for each "d_{pa}" from the ratio of the slopes as described above. The fractional penetration was then plotted over the entire size range ($Pt(d_{pa})$ versus d_{pa}) to give the penetration grade curve.

CHAPTER 6

EXPERIMENTAL RESULTS AND DISCUSSION

After the construction of the F/C scrubber demonstration plant, startup and performance testing were begun. Initial startup runs were made with ambient air through the F/C scrubber system. Once satisfactory performance of all mechanical equipment had been achieved the hot flue gas from the furnace was hooked up to the F/C scrubber unit. The system operated close to the design conditions but higher particulate emission rate was encountered at the source tnan previously monitored. Table 6-1 presents a brief summary of total particulate loadings at the furnace stack for #1 grade copper wire at different stages of the demonstration program. The emissions from the processing of both #1 premium and #1 regular grade went up from those measured before the initial site selection to the operation of the demonstration plant.

The purpose of the testing phase of the program was to obtain the overall mass efficiency of the system, the particle collection efficiency across the F/C scrubber, the operational reliability of the demonstration plant, and the economics of F/C scrubbing. Thus, both performance and process data along with operational information were determined and analyzed. The measurement techniques and methods of data analysis and calculations of results are described in the preceding chapter. The purpose of this section of the report is to present the results and discuss the salient features of the test program. The economics of the F/C scrubbing system are discussed in Chapter 8.

Overall, the F/C demonstration scrubber was capable of controlling the emissions from the processing of #1 premium grade copper wire. The performance was marginal for #1 regular grade

TABLE 6-1. TOTAL PARTICULATE LOADINGS AT FURNACE STACK DURING DIFFERENT STAGES OF F/C SCRUBBING DEMONSTRATION PROGRAM.

Stage of F/C Program	Number of Runs for Averaging	Type of Wire Processed	Average * Loading (g/DNm^3)
Site Selection	2	Premium #1	0.36**
Pilot Plant	4	Regular #1	1.3
Demonstration F/C Scrubber	4	Premium #1	0.78
	20	Regular #1	1.8

* Mass loadings are based on overall average emissions over charging cycle and include impinger catch.

** Corrected to 12% CO_2

copper wire but the demonstration scrubber was not capable of controlling the emissions from #2 and #3 grades of copper wire.

EXPERIMENTAL RESULTS

The F/C demonstration plant was evaluated at ten operating modes as listed in Table 6-2. The purpose of the changes from mode to mode was both to increase the efficiency of the F/C system to cope with the higher emission rate than previously monitored and to obtain collection efficiency data for different modes of operation.

The performance of the system, based on mass concentration data for different operating modes, is presented in Table 6-3. This table gives the inlet and outlet concentrations of particulate matter, the corresponding penetrations, and the total pressure drop across the system. The process data for these runs are summarized in Table A-1 of the Appendix "A".

Cascade impactor data were taken in order to determine collection efficiency as a function of particle size. The cumulative loading data are presented in Table 6-4, while the corresponding impactor stage data are given in Appendix "B". The cascade impactor data were utilized to calculate the fractional penetrations as a function of particle aerodynamic diameter. The calculation procedure was previously discussed in Chapter 5. The resulting fractional penetrations for the test along with the predicted penetration curves are presented in Figures 6-1 to 6-18.

TABLE 6-2. F/C SCRUBBER DEMONSTRATION PLANT OPERATING CONFIGURATIONS

Conf. No.	Description of System
A	5 plates in scrubber, 0.48 cm hole diameter, cold water on pass A of scrubber.
B	5 plates in scrubber, 0.48 cm hole diameter, cold water on pass B of scrubber.
C	6 plates in scrubber, 4 plates with 0.48 cm hole diameter, 2 plates with 0.32 cm hole diameter, cold water on pass B of scrubber.
D	5 plates in scrubber, 3 plates with 0.48 cm hole diameter, 2 plates with 0.32 cm hole diameter, cold water on pass B of scrubber.
E	5 plates in scrubber, 3 plates with 0.48 cm hole diameter, 2 plates with 0.32 cm hole diameter, cold water on pass A of scrubber.
F	5 plates in scrubber, 3 plates with 0.48 cm hole diameter, 2 plates with 0.32 cm hole diameter, cold water on pass B of scrubber, sodium carbonate solution spray in crossover duct, charge wetted with water.
G	Sampling at peak of emissions only, 5 plates in scrubber, 3 plates with 0.48 cm hole diameter, 2 plates with 0.32 cm hole diameter, cold water on pass B of scrubber, sodium carbonate solution spray in crossover duct, charge wetted with water.
H	Sampling at peak of emissions only, 5 plates in scrubber, 3 plates with 0.48 cm hole diameter, 2 plates with 0.32 cm hole diameter, cold water on pass B of scrubber, sodium carbonate solution spray in crossover duct, charge wetted with water, water spray in crossover duct.
I	Sampling at peak of emissions only, 6 plates in scrubber, 4 plates with 0.48 cm hole diameter, 2 plates with 0.32 cm hole diameter, cold water on pass B of scrubber, sodium carbonate solution spray in crossover duct, charge wetted with water, water spray in crossover duct.
J	6 plates in scrubber, 4 plates with 0.48 cm hole diameter, 2 plates with 0.32 cm hole diameter, cold water on pass B of scrubber, sodium carbonate solution spray in crossover duct, charge wetted with water, water spray in cross over duct.

TABLE 6-3. F/C SCRUBBER DEMONSTRATION PLANT SYSTEM PERFORMANCE

Run No.	Configuration	$\Delta P \times 10^{-3}$ N/m^2	Total Part. Conc.(g/DNm^3)			Pt, Qu&Scr. %	Pt, Scrub. %
			Qu.In	Scr.In	Scr.Out		
1	A	4.2	1.3		0.24	18.5	
2	A	4.2	1.6		0.35	21.9	
3*	A	4.3	1.7	0.93	0.29	17.0	31.2
4*	A	4.2		2.00	0.35		17.5
5	A	4.3		0.97	0.37		38.1
6	B	4.2		0.30	0.11		36.7
7*	B	4.2		0.20	0.057		28.5
8	C	5.0			0.18		
9	C	5.0			0.076		
10	D	5.0			0.37		
11	D	5.0			0.23		
12	D	5.0			0.39		
13	D	5.0			0.099		
14	D	5.0			0.30		
15	D	5.0			0.28		
16	D	5.0			0.22		
17	D	5.0	2.1		0.060	2.9	
18	D	5.0	1.2		0.096	8.0	
19	D**	5.0	5.7		0.73	12.8	
20	D**	5.0	1.2		0.22	18.3	
21	E	5.0	2.6		0.18	6.9	
22	E	5.0	1.1		0.090	8.2	

Qu.In = quencher inlet, Scr.In = scrubber inlet,
Scr.Out = scrubber outlet

* Cascade impactor run ** Liquor to pass A only

Note: [a] Runs 1-56: Wire quality - number 1, regular grade

[b] Runs 57-78: Wire quality - number 1, premium grade

[c] Total particulate concentration includes both filter and impinger catch.

TABLE 6-3 (continued)

Run No.	Configuration	$\Delta P \times 10^{-3}$ N/m^2	Total Part. Conc.(g/DNm^3)			Pt, Qu&Scr. %	Pt, Scrub. %
			Qu.In	Scr.In	Scr.Out		
23	E	4.7	2.6		0.66	25.4	
24	E	4.7	2.6		0.83	31.9	
25	E	4.7	1.9		0.41	21.6	
26	D	4.7	1.2		0.20	16.7	
27	D	5.0	1.6		0.12	7.5	
28	D	5.0	2.0		0.22	11.0	
29	D	5.0	0.79		0.13	16.4	
30	D	5.0	0.32		0.098	30.6	
31	D	5.0	1.6		0.31	19.4	
32	D	5.0	0.92		0.22	23.9	
33	D	5.0	1.2		0.36	30.0	
34	F	4.7	0.96				
35	F	5.0	0.52		0.090	17.3	
36	F	4.8	1.6		0.096	6.0	
37	F	4.7	1.2		0.13	10.8	
38	G	4.7	3.2		0.18	5.6	
39	G	4.7	3.5		0.21	6.0	
40	G	4.7	2.6	0.231	0.054	2.1	23.4
41	G	4.7	2.6		0.14	5.4	
42*	G	4.7		0.40	0.12		30.0
43*	G	4.7		0.27	0.11		40.7
44	H	5.0	6.4		0.29	4.5	

Qu.In = quencher inlet, Scr.In = scrubber inlet
Scr.Out = scrubber outlet

* Cascade impactor run

Note:
[a] Runs 1-56: Wire quality - number 1, regular grade
[b] Runs 57-78: Wire quality - number 1, premium grade
[c] Total particulate concentration includes both filter and impinger catch.

TABLE 6-3 (Continued)

Run No.	Configuration	$\Delta P \times 10^{-3}$ N/m^2	Total Part. Conc. (g/DNm^3)			Pt, Overall Syst. % ***	Pt, Qu&Scr. %
			Furn. Out	Qu.In	Scr.Out		
45	H	5.0	4.0		0.22	5.5	
46	H	5.0	4.5		0.27	6.0	
47	H	5.0	3.8		0.15	3.9	
48	H	5.0	2.7		0.17	6.3	
49	H	5.0	3.5		0.24	6.9	
50	H	5.0	4.1		0.21	5.1	
51	I	6.9	2.2		0.12	5.4	
52	I	6.9	1.4		0.10	7.1	
53	I	6.9	2.3		0.094	4.1	
54	I	6.4	1.6		0.19	11.9	
55	I	5.3	2.3		0.20	8.7	
56*	I	5.7		1.3	0.077		5.9
57*	I	6.0		0.68	0.023		3.4
58*	I	6.1		0.83	0.030		3.6
59*	I	6.0		1.4	0.031		2.2

Furn.Out = furnace outlet, Qu.In = quencher inlet,
Scr.Out = scrubber outlet

* Cascade impactor run

*** Overall system penetration based on inlet mass concentration measured at furnace out (upstream of sodium carbonate spray) and outlet mass concentration measured at scrubber outlet.

Note: [a] Runs 1-56: Wire quality - number 1, regular grade

[b] Runs 57-78: Wire quality - number 1, premium grade

[c] Total particulate concentration includes both filter and impinger catch.

[d] Total particulate concentrations were measured at the furnace outlet and not at the scrubber inlet for run 45 and those following it.

TABLE 6-3. (Continued)

Run No.	Configuration	$\Delta P x 10^{-3}$ N/m	Total Part. Conc. (g/DNm^3)			Pt, Overall Syst. % ***	Pt, Qu&Scr. %
			Furn. Out	Qu.In	Scr.Out		
60	J	6.1	1.4		0.068	4.9	
61*	J	5.8		0.89	0.055		6.2
62*	J	6.1		1.1	0.052		4.7
63	J	6.0	0.53		0.083	15.7	
64*	J	6.0		2.8	0.16		5.7
65	J	5.8	0.67		0.087	13.0	
66*	J	5.8		1.2	0.048		4.0
67**	J	6.1		1.9	0.055		2.9
68	J	5.8	0.53		0.038	7.2	
69*	J	6.0		1.0	0.077		7.7
70**	J	6.1					
71*	J	6.0		1.6			
72*	J	6.1		1.3	0.080		6.2
73*	J	6.8		1.3	0.037		2.8
74*	J	6.8		1.2	0.049		4.1
75*	J	6.3		1.5	0.056		3.7
76*	J	6.1		2.5	0.039		1.6
77*	J	6.5		1.2	0.059		4.9
78*	J	6.5		1.2	0.052		4.3

Furn.Out = furnace outlet, Qu.In = quencher inlet,
Scr.Out = scrubber outlet

* Cascade impactor run
** Blank run
*** Overall system penetration based on inlet mass concentration measured at furnace out (upstream of sodium carbonate spray) and outlet mass concentration measured at scrubber outlet.

Note: [a] Runs 1-56: Wire quality - number 1, regular grade

[b] Runs 57-78: Wire quality - number 1, premium grade

[c] Total particulate concentration includes both filter and impinger catch.

[d] Total particulate concentrations were measured at the furnace outlet and not at the scrubber inlet for run 45 and those following it.

TABLE 6-4. PARTICULATE AND IMPINGER DATA*, F/C SCRUBBER DEMONSTRATION PLANT

Run No.	Total Particulate Conc.		Impactor Part.Conc.		Impt.Pt	Impinger Conc.	
	In(g/DNm³)	Out(g/DNm³)	In(g/DNm³)	Out(g/DNm³)	%	In(g/DNm³)	Out(g/DNm³)
3	1.7	0.29	0.089	0.024	27.0	1.6	0.26
4**	2.0	0.35	1.9	0.34	17.9	0.09	0.01
7**	0.20	0.057	0.11	0.034	30.9	0.09	0.02
42**	0.40	0.12	0.39	0.12	30.8	0.01	0.0
43**	0.27	0.11	0.27	0.11	40.7	0.0	0.0
56	1.3	0.077	1.2	0.048	4.0	0.09	0.03
58	0.83	0.030	0.83	0.030	3.6	0.0	0.0
59	1.4	0.031	1.3	0.031	2.4	0.12	0.0
61	0.89	0.055	0.89	0.053	5.9	0.0	0.0
62	1.1	0.052	1.1	0.052	4.7	--	--
64	2.8	0.16	2.5	0.14	5.6	0.28	0.02
66	1.2	0.048	1.2	0.048	4.0	0.01	0.0
69	1.0	0.077	0.70	0.077	11.0	0.32	0.0
71	1.6	--	1.2	--	--	0.36	--
72	1.3	0.081	0.97	0.081	8.3	0.36	0.0
73	1.3	0.037	1.1	0.037	3.4	0.19	0.0
74	1.2	0.049	1.1	0.049	4.4	0.034	0.0
75	1.5	0.056	1.2	0.048	4.0	0.27	0.01
76	2.5	0.039	2.2	0.036	1.6	0.27	0.0
77	1.2	0.059	0.76	0.051	6.7	0.43	0.01
78	1.2	0.052	1.2	0.014	1.2	0.02	0.04

* Particulate data taken across quencher inlet and scrubber outlet unless otherwise noted.

** Particulate data taken across plate scrubber only.

Note: [a] Run 7 was a cold impactor run.

[b] Inlet data for run 71 (outlet) was inadequate due to error in test procedure.

[c] Outlet loadings for run 78 were too light to provide adequate size data.

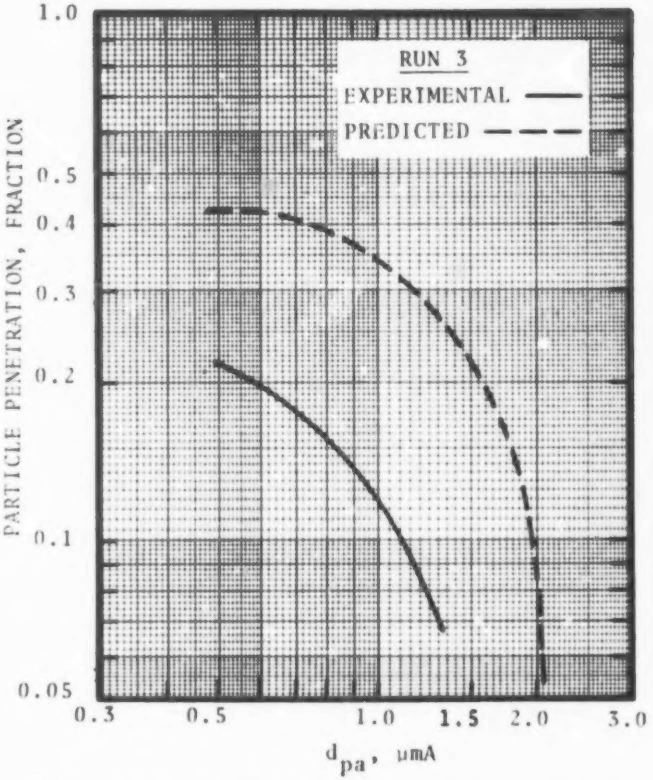

Figure 6-1. Particle penetration versus aerodynamic diameter for run 3.

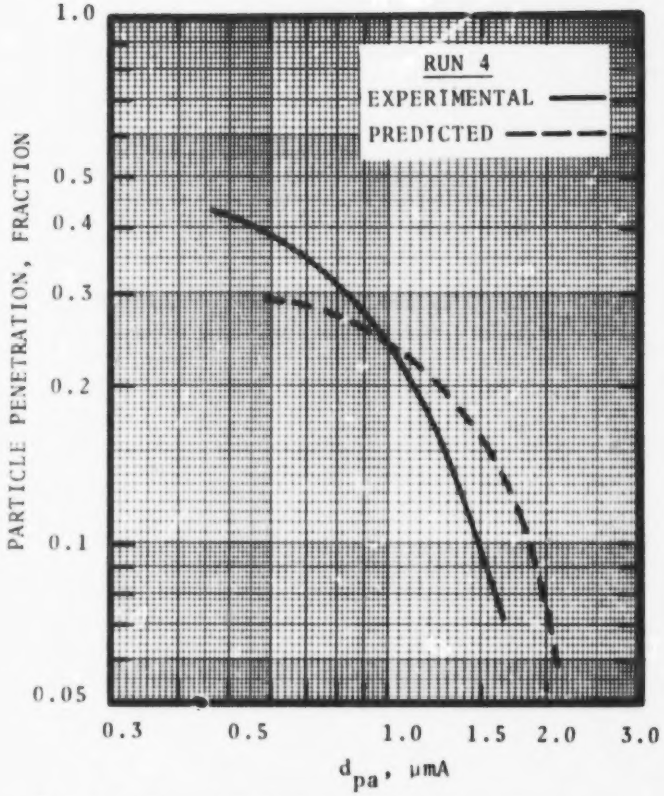

Figure 6-2. Particle penetration versus aerodynamic diameter for run 4.

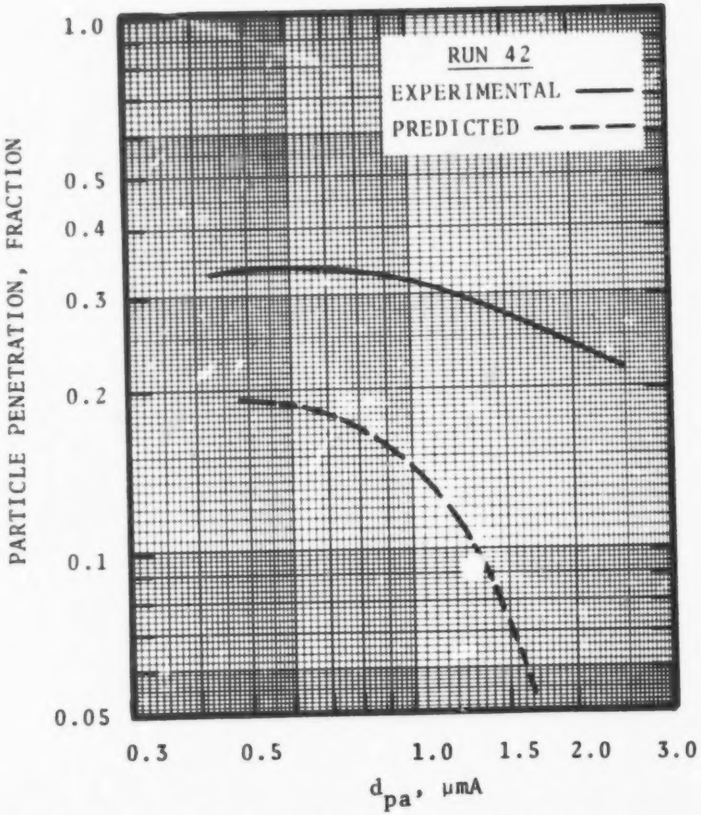

Figure 6-3. Particle penetration versus aerodynamic diameter for run 42.

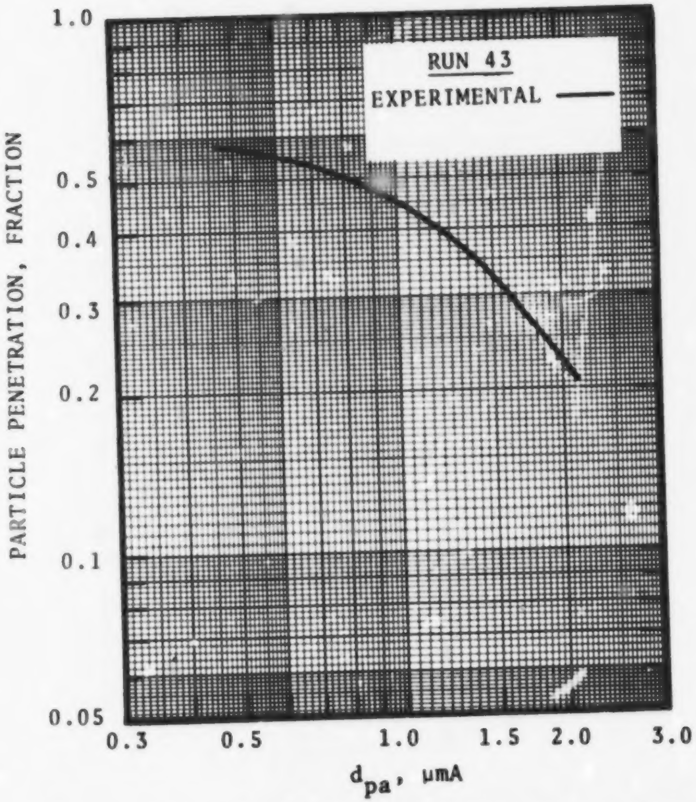

Figure 6-4. Particle penetration versus aerodynamic diameter (scrubber only) for run 43.

Note: Predicted penetration curve was very low due to very low predicted particle number concentration for this run. (See Table E-1 of appendix)

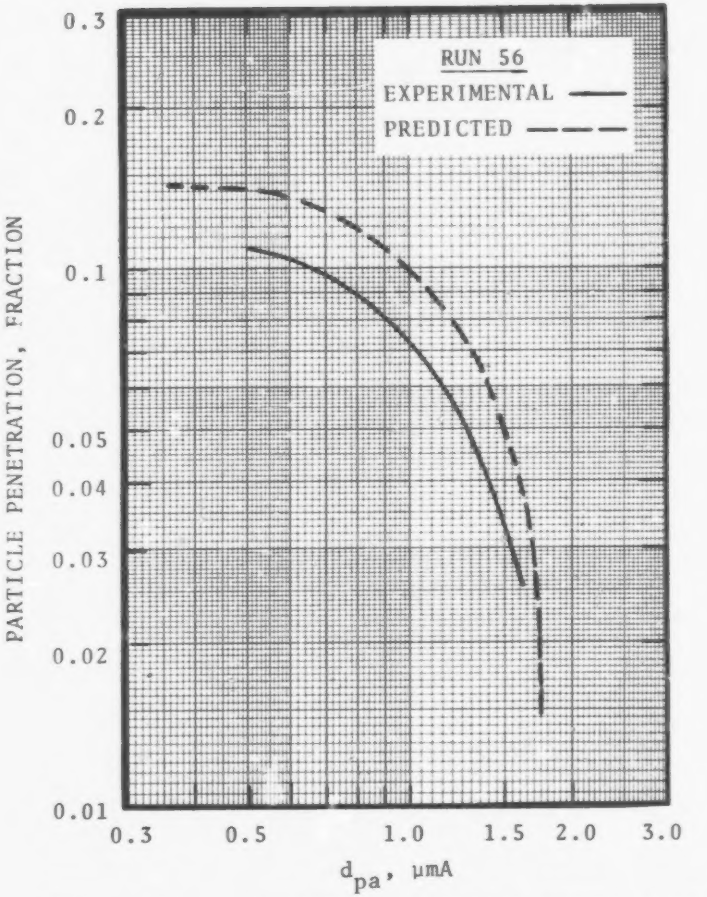

Figure 6-5. Particle penetration versus aerodynamic diameter for run 56.

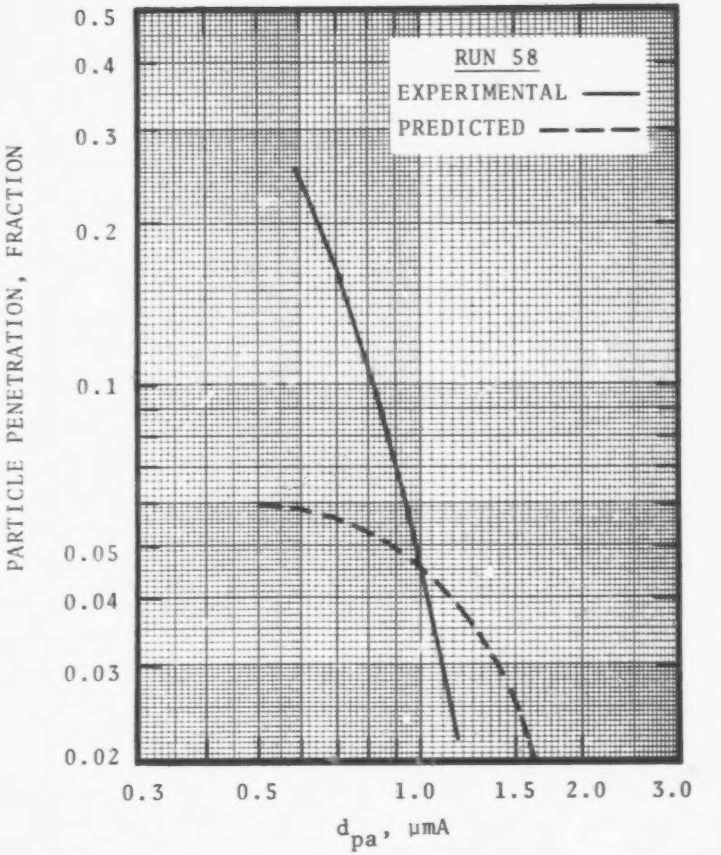

Figure 6-6. Particle penetration versus aerodynamic diameter for run 58.

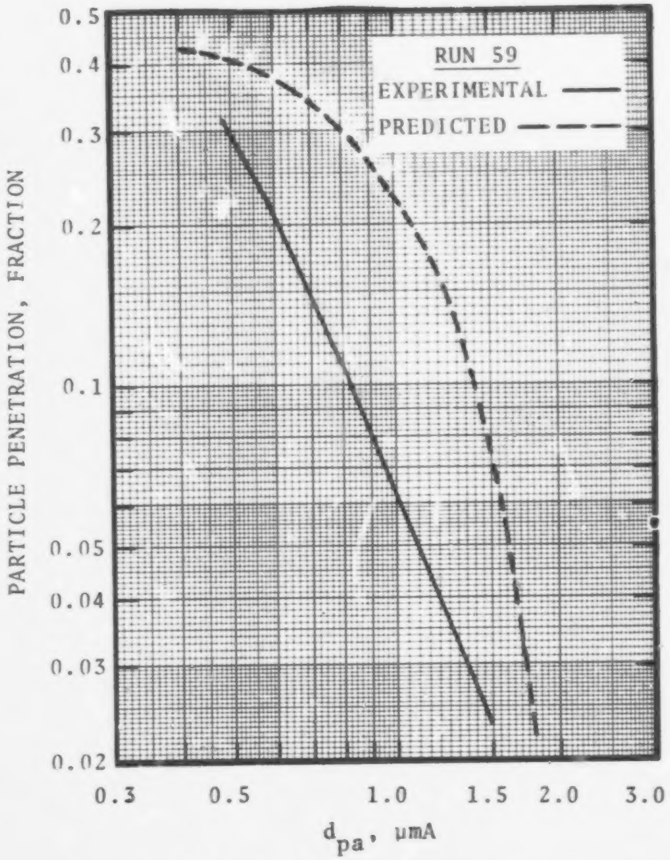

Figure 6-7. Particle penetration versus aerodynamic diameter for run 59.

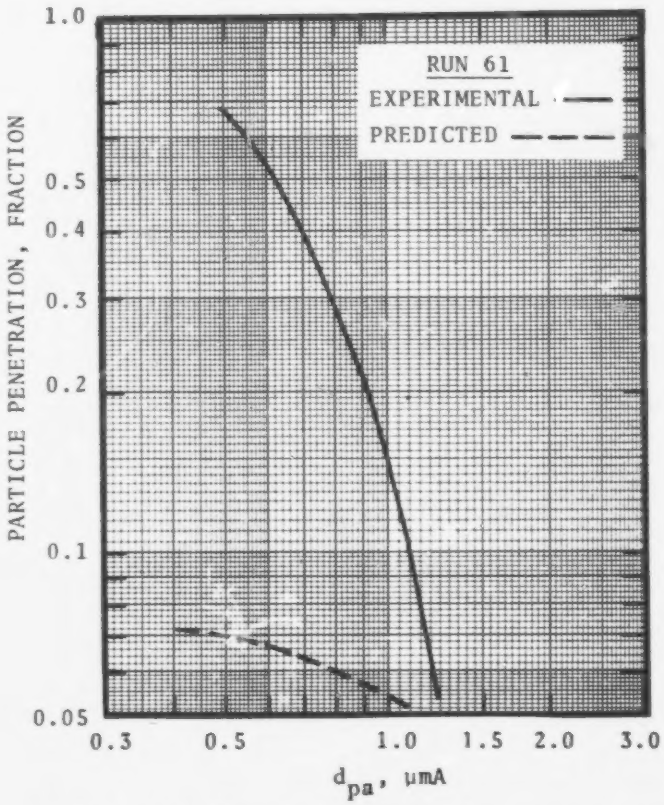

Figure 6-8. Particle penetration versus aerodynamic diameter for run 61.

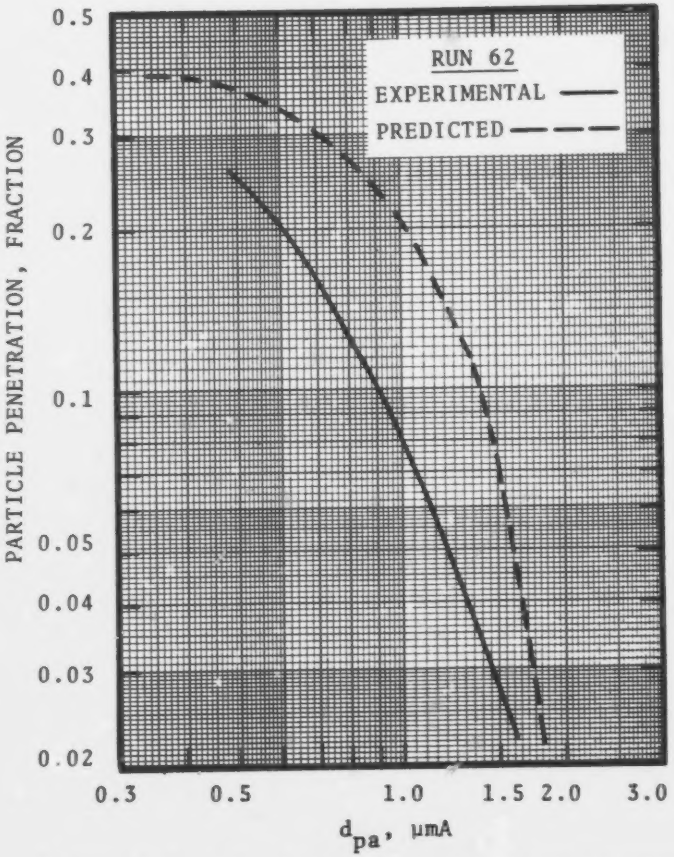

Figure 6-9. Particle penetration versus aerodynamic diameter for run 62.

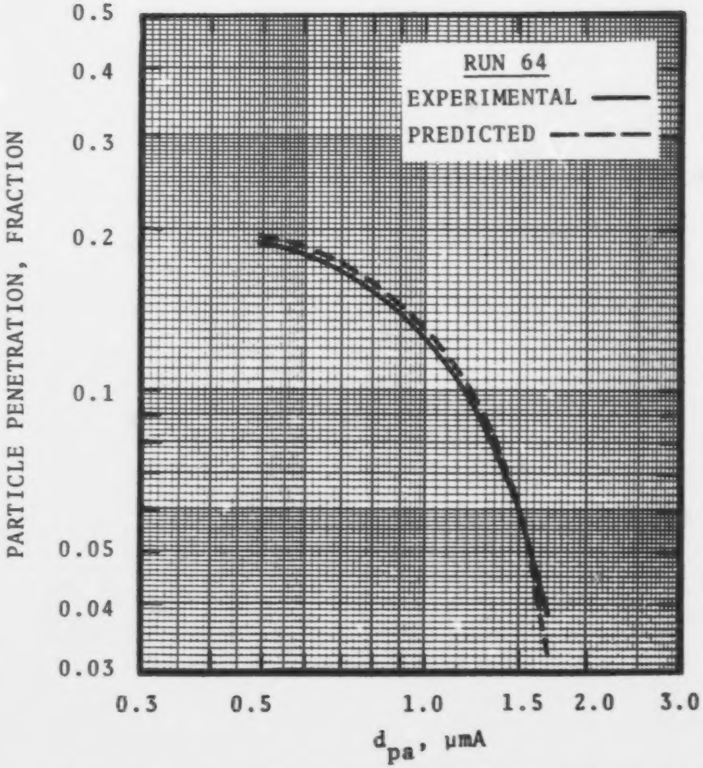

Figure 6-10. Particle penetration versus aerodynamic diameter for run 64.

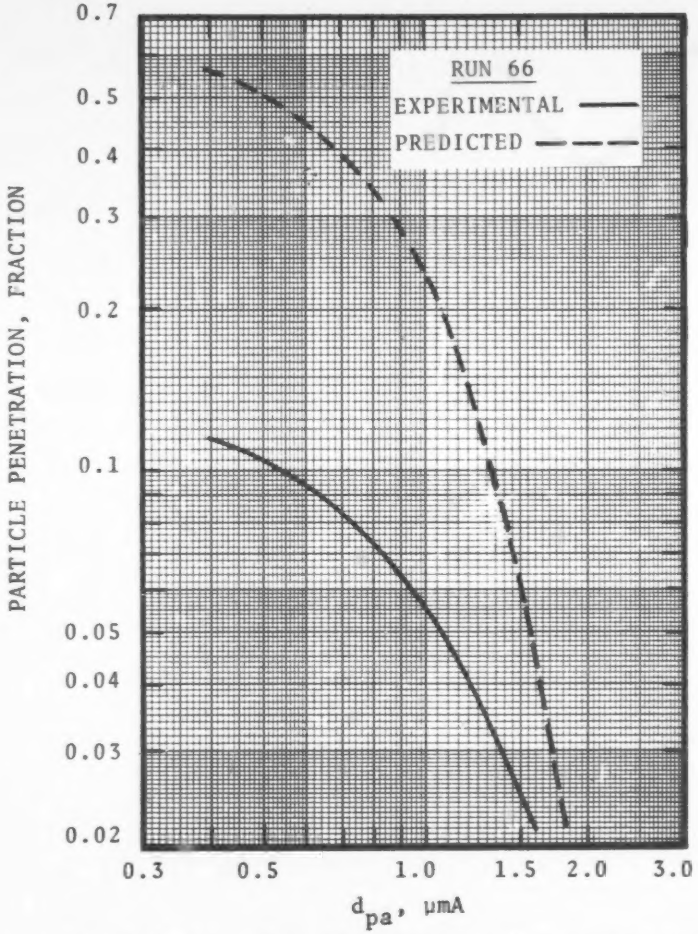

Figure 6-11. Particle penetration versus aerodynamic diameter for run 66.

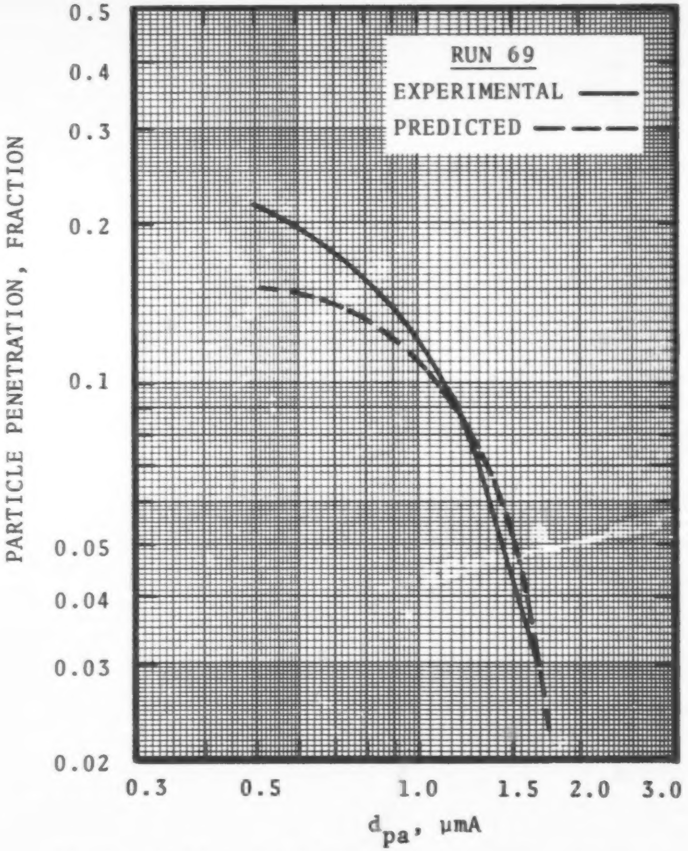

Figure 6-12. Particle penetration versus aerodynamic diameter for run 69.

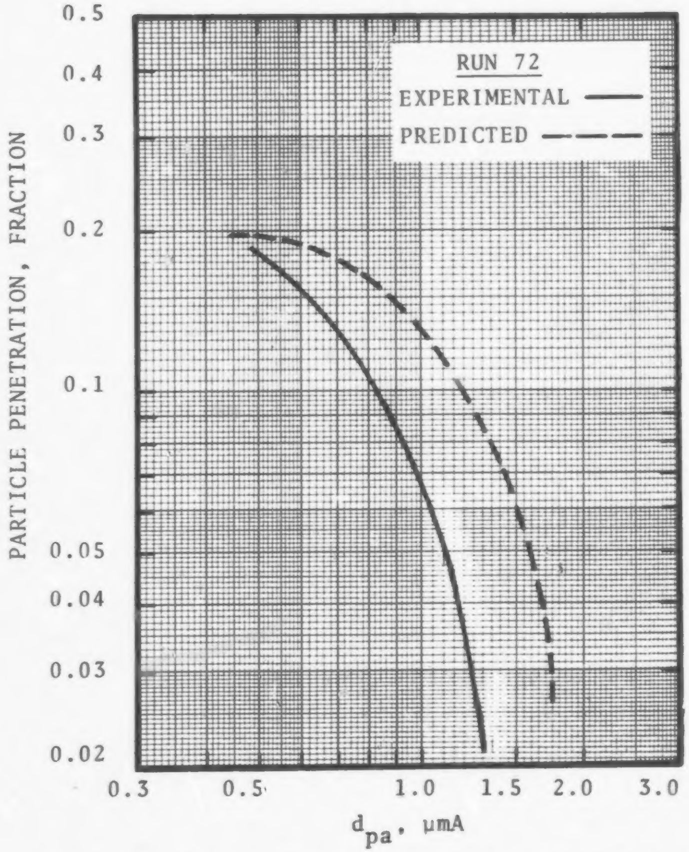

Figure 6-13. Particle penetration versus aerodynamic diameter for run 72.

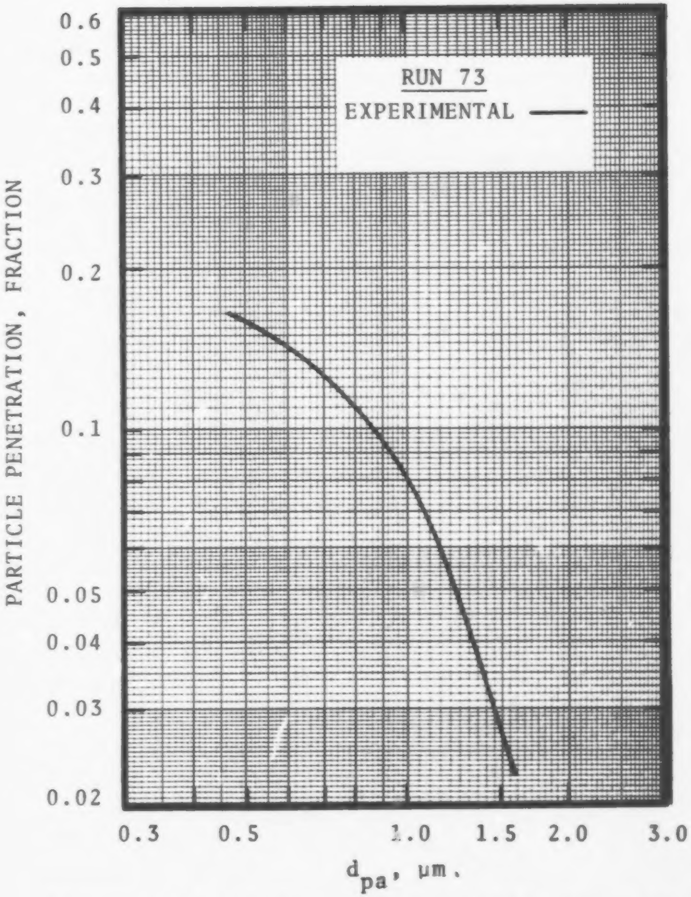

Figure 6-14. Particle penetration versus aerodynamic diameter for run 73.

Note: Predicted penetration curve was very high due to very high predicted particle number concentration for this run. (see Table E-1 of appendix)

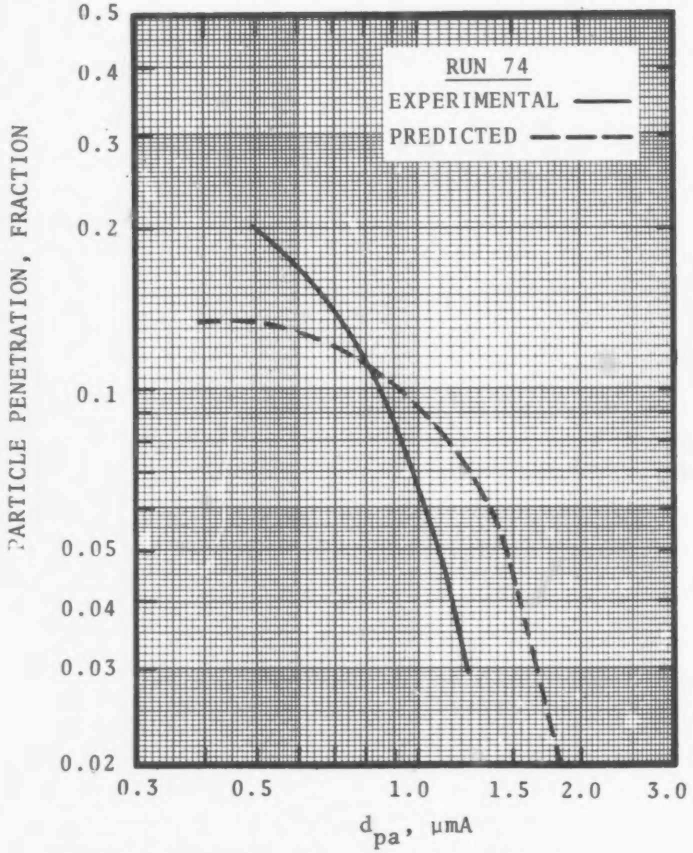

Figure 6-15. Particle penetration versus aerodynamic diameter for run 74.

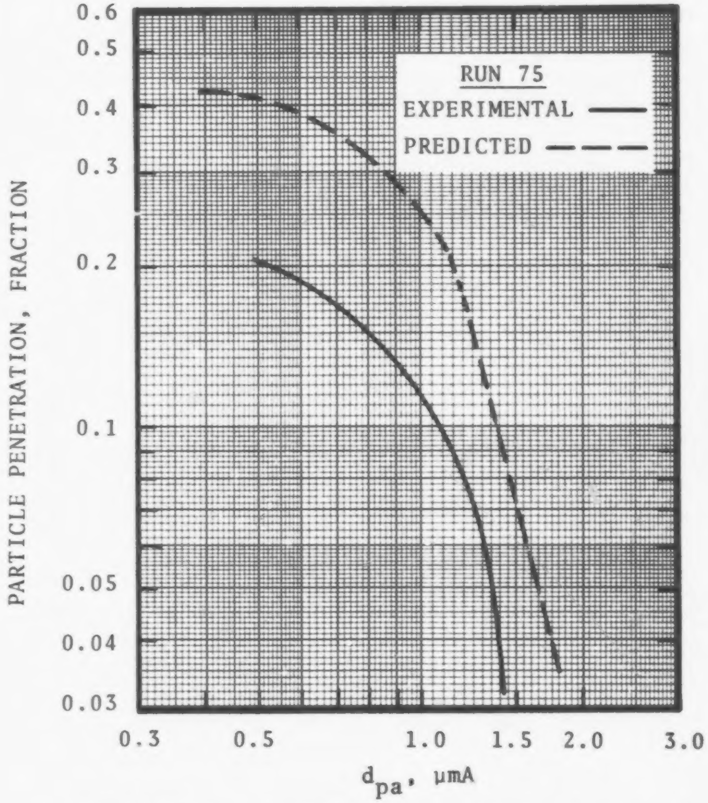

Figure 6-16. Particle penetration versus aerodynamic diameter for run 75.

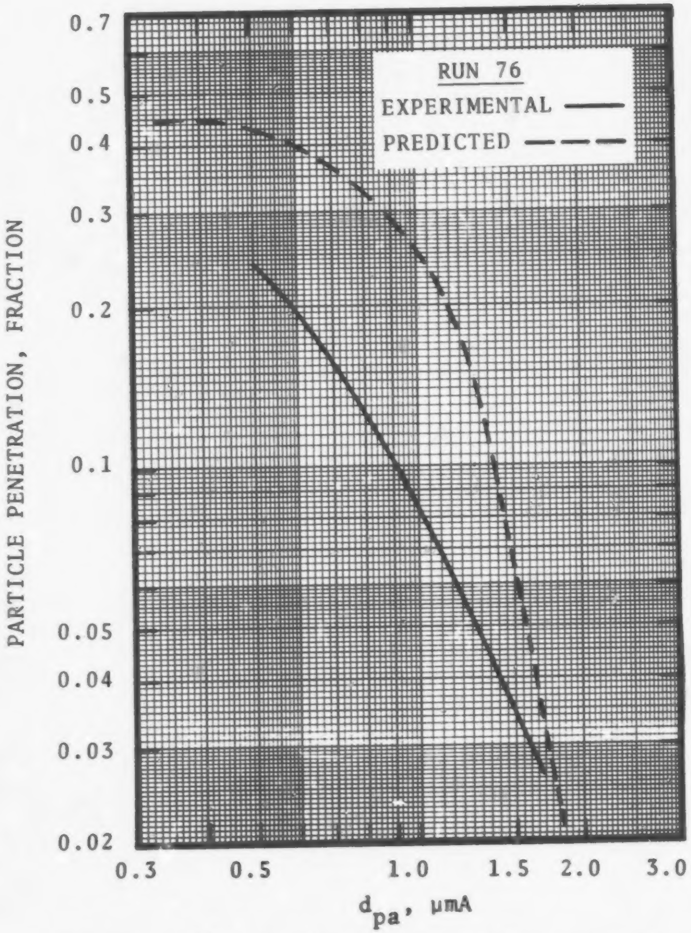

Figure 6-17. Particle penetration versus aerodynamic diameter for run 76.

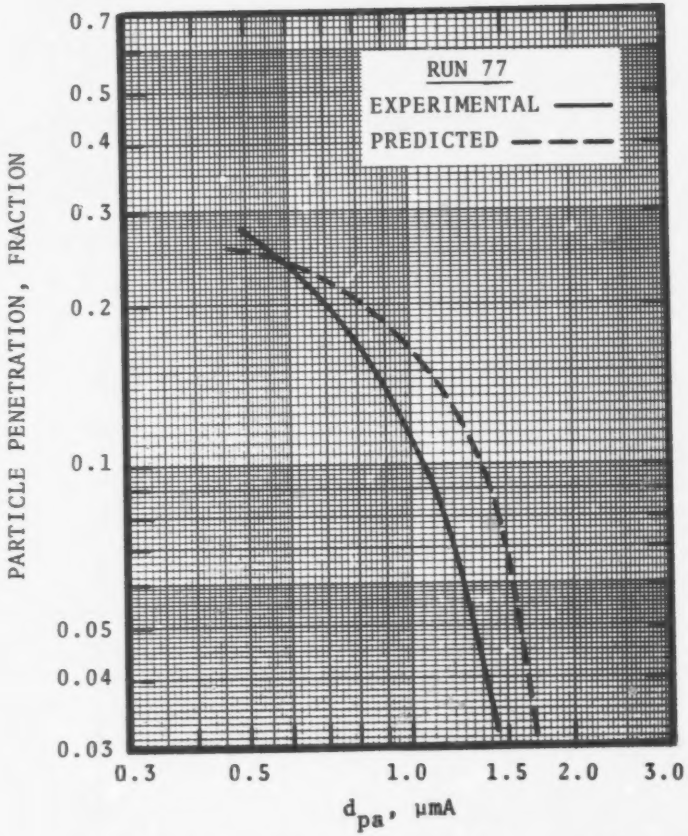

Figure 6-18. Particle penetration versus aerodynamic diameter for run 77.

DISCUSSION OF RESULTS

Operating Modes

Operating modes and scrubber configuration were varied in order to cope with the high emission rates encountered at the source. This provided a base for comparison of performance under different sets of process and equipment parameters. In summary, the following variations were studied.

1. The F/C scrubber system was provided with the provision of adding a sixth plate inside the unit. The purpose of adding the extra plate was to enhance the efficiency of the scrubber through increasing collection of particles by inertial impaction. This in turn resulted in higher pressure drop across the system.

2. The F/C scrubber was modified by installation of sieve plates with perforation of smaller diameter at two positions inside the scrubber. The existing plates had a 0.48 cm (3/16") diameter perforation with 6.0% open area, while the modified plates used 0.32 cm (1/8") perforation with 3.3% open area. This change achieved a greater velocity through the perforation, resulting in higher collection efficiency due to inertial impaction.

3. The sieve plate scrubber consisted of two passes of vertical columns connected in series. The gas flowed into the bottom of pass 'A' equipped with three sieve plates, then into the bottom of pass 'B', which also was provided with three sieve plates. The piping system was designed with the flexibility of injecting the cold water from the cooling tower at either pass of the scrubber, with the other pass receiving the hot water from the scrubber sump tank. The system was operated with cold water injected at pass 'A' during one operational mode and similarly with cold water injected at pass 'B' during another operating mode. It was observed, that for this particular design of the F/C scrubber, introduction of cold liquor at pass 'B' of the scrubber versus hot liquor did reduce emission of excessive steam from the stack of the F/C unit.

4. The emissions from the furnace were cyclic in nature and were higher during the initial part of the charging cycle. Emis-

sion data were collected on both an overall average basis and also on a peak interval time basis only. The peak interval testing provided the emissions data during the worst part of the charging cycle.

5. The scrap charge was also pre-wetted during the later operating modes before introduction into the furance. The purpose was to increase the gas humidity of the flue gas and consequently provide a higher condensation ratio across the F/C unit.

6. Initially the F/C demonstration unit was built with a carbon steel cross-over duct to convey the pollutant gas from the furnace stack to the F/C unit. After corrosion caused its failure, this cross-over duct was replaced with a stainless steel (316) duct. A sodium carbonate spray solution was added inside the cross-over duct for the purpose of reducing the formation of metal chloride particles and to neutralize the acidity of the gas stream at an early stage. Water sprays were also added in the same duct to achieve further improvement in performance.

Mass Loading Versus Wire Scrap Quality

The performance results of the F/C unit under different operating models are given in Table 6-3. The performance results indicate that for a majority of cases, the system operated at an efficiency of over 90%. As regards the mass loading, two grades of #1 wire were processed at the host facility. The two grades were regular #1, which is 60% copper and 40% plastic, and premium #1, which is 80% copper and 20% fabric (with some rubber). This change in wire quality was reflected in the total particulate loadings at both the inlet and outlet to the F/C system. Overall, the performance indicated that the system was well within the local air pollution control district standards during the reclamation of premium #1 copper wire. The performance of the system during the reclamation of #1 copper wire was marginal due to limitations on the fan pressure capacity.

Performance Model

The predictability of the F/C demonstration plant can be judged from a comparison of the actual performance of the system with the predicted performance as determined from the design model. The details on the design model are given in the next chapter. This section compares the results of the F/C plant with the predicted performance.

The observed performance was close to the predicted performance as calculated using the design model. Figures 6-1 to 6-18 give a comparison of experimental particle penetration of the F/C demonstration scrubber to the predicted penetration. Table 6-5 summarized the results, showing the experimental overall penetration of the demonstration scrubber versus the calculated overall penetration. The procedure for predicting penetration is illustrated by an example in Appendix "F".

As indicated by the data, there is some deviation between the experimental and predicted performance. Some of the reasons for this deviation are given in the following list of assumptions and uncertainties in the model and the experimental data.

1. The calculation procedure does not account for collection in the quencher section of the system. The quencher collects the larger particles, but not the submicron particles.

2. The flux force mechanism of thermophoresis and the mechanism of centrifugation were not considered in the calculation of the performance using the model. It was assumed that the effect of inertial impaction and diffusiophoresis would overshadow the effect of other mechanisms.

3. The foam density was considered to be of constant value (F=0.4) in the design model prediction. In actuality, there would be some variation due to changes in plate hydrodynamics under different operating conditions.

4. The design model assumes the particle to be wettable but insoluble. Since the particles were quite soluble in water they will cause more condensation than predicted and the performance for the system should be better than predicted.

5. The fraction of water vapor condensing on the particles

TABLE 6-5. COMPARISON OF EXPERIMENTAL DATA VERSUS PREDICTED PENETRATIONS FOR F/C SCRUBBER DEMONSTRATION

Run No.	Experimental *			Predicted Penetration %
	Loading (mg/DNm)		Penetration %	
	Inlet	Outlet		
3	89.0	23.9	26.8	27.7
4**	1,910.0	338.0	17.7	18.3
42**	395.0	121.0	30.6	14.2
43**	274.0	106.0	38.7	***
56	1,170.0	48.4	4.1	3.7
58	829.0	30.2	3.6	1.3
59	1,250.0	31.2	2.4	4.1
61	886.0	53.3	6.0	2.6
62	1,150.0	51.7	4.5	4.5
64	2,490.0	140.0	5.6	5.1
66	1,230.0	48.2	3.9	8.6
69	701.0	77.1	11.0	4.7
72	969.0	80.7	8.3	8.0
73	1,100.0	36.7	3.3	****
74	1,140.0	49.0	4.3	2.6
75	1,200.0	48.3	4.0	6.0
76	2,240.0	36.0	1.6	2.7
77	763.0	50.5	6.6	4.4

* Particulate data across quencher inlet and scrubber outlet unless otherwise indicated.

** Particulate data across plate scrubber only.

*** Predicted particle number concentration was very low.

**** Predicted particle number concentration was very high.

was approximated to be 0.25 of the total condensation in the scrubber in the design model computations. This approximation was based on simulated computer runs using a model for F/C scrubbing in a sieve plate at conditions comparable to the F/C process parameters at the demonstration plant. This value will vary as indicated in Chapter 7, depending on different process conditions such as the gas-phase temperature, liquid-bulk temperature, number-particle concentration, and liquid-phase heat transfer coefficient.

6. The design model uses as one of its parameters the particle number concentration at the inlet to the F/C system. As discussed in Appendix "E". there is uncertainty in the procedure used to determine number concentration. Any error in these predictions causes deviations between the predicted and actual performance. An attempt is made in Figure 6-19 to to study the effect of the absolute values of the predicted particle number concentration "n" on the agreement between predicted particle penetration and experimental particle penetration. This plot shows that the agreement is best $\left(\frac{\text{Predicted Pt}}{\text{Experimental Pt}} = 1.0\right)$ when the particle no. concentration is about 1.5×10^8 /DNcm^3.

The ratio of penetrations is higher when the predicted particle no. concentration is higher and lower when the predicted particle no. concentration was lower. There is uncertainty and great variation in the absolute values of the particle number concentration. Therefore, the graph indicates that some of the deviations of the model predictions from the experimental prediction could very well be due to the deviations of the predicted particle number concentrations from their true values.

Error Analysis

The accuracy of the experimental results, as discussed in this chapter, is dependent on the independent and cumulative errors of several measurements. The scope of this

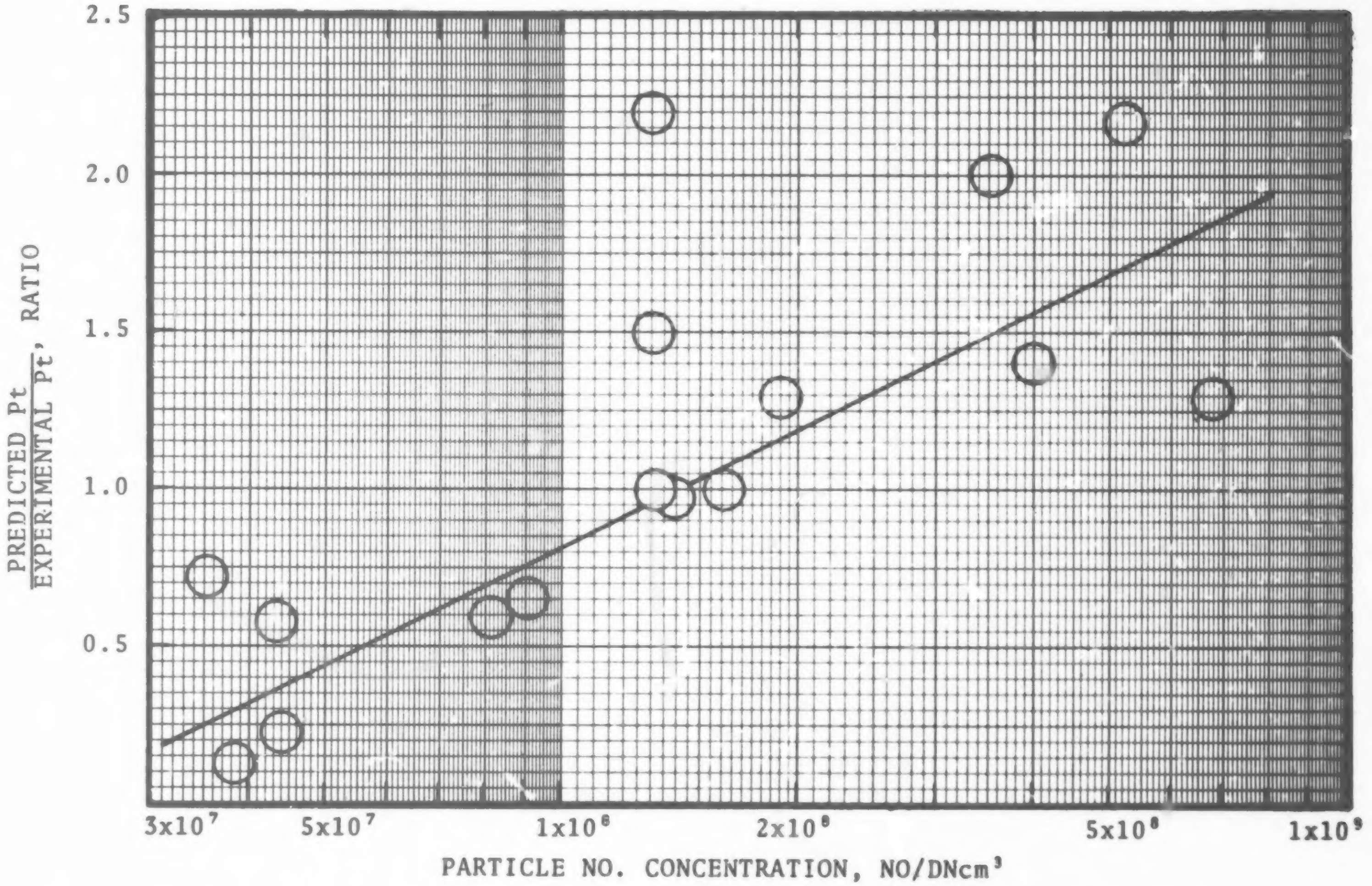

Figure 6-19. Effect of calculated particle number concentration on agreement between predicted and experimental for 0.5 μmA diameter particles.

report does not permit a complete statistical error analysis on all the experimental results. However, the individual errors associated with total filter runs and impactor size distributions are discussed below.

The independent variables involved in the determination, along with their precision and nominal values, are listed in Table 6-6 and 6-7. The equation for calculating the overall penetration and size distribution involves both intermediate variables and multi-appearances of variables. However, if these are replaced with an exact expression, the fractional error in the dependent variable "C" can be calculated as:

$$\frac{dC}{C} = \frac{1}{C}\frac{\partial C}{\partial X_1}\bigg|_{n.} dX_1 + \frac{1}{C}\frac{\partial C}{\partial X_2}\bigg|_{n.} dX_2 + \ldots \frac{\partial C}{\partial X_n}\bigg|_{n.} \partial X_n \quad (6\text{-}1)$$

where $X_1, X_2, \ldots X_n$ = independent variables as listed in Tables 6-6 and 6-7.

C = absolute value of dependent variable calculated at nominal conditions

$\partial X_1, \partial X_2, \ldots \partial X_n$ = precision of independent variable.

$\frac{dC}{C}$ = fractional error of dependent variable

Here the quantity

$$S_1 = \frac{1}{C}\frac{\partial C}{\partial X_1}\,_{n.} \quad (i = 1, 2, \ldots n.) \qquad (6\text{-}2)$$

represents the sensitivity of error $\frac{dC}{C}$ to an error ∂X_i. This value gives a direct indication of the effect of an error in the measured variable on the fractional error of the dependent variable.

The errors involved in the calculation of fractional penetration and inlet number concentration are more subjective in nature for they involve judgment in analyzing graphs and determining slopes.

TABLE 6-6. MEASURED VARIABLES, DEFINITION, PRECISION AND TEST CASE NOMINAL VALUES FOR TOTAL EFFICIENCY CALCULATION

Symbol	Measurement	Unit	Precision	Nominal Value
V_{DGM}	Volume of dry gas read by dry gas meter	ft^3	0.002	10.0
t	Length of time of test	min	.2/60	60.0
mg	Sample weight	mg	0.50	50.0
Ps	Orifice pressure reading dry gas meter	in H_2O	0.02	0.15
P_b	Barometric pressure	in Hg	0.10	29.9

TABLE 6-7. MEASURED VARIABLES, DEFINITION, PRECISION AND TEST CASE NOMINAL VALUES FOR SIZE DISTRIBUTION CALCULATION

Symbol	Measurement	Unit	Precision	Nominal Value
V_{DGM}	Volume of dry gas read by dry gas meter	ft^3	0.002	2.5
t	Length of time of test	min	.2/60	5.0
mg	Sample weight on each impactor substrate	mg	0.02	0.5
Ps	Orifice pressure reading dry gas meter	in H_2O	0.05	0.15
P_b	Barometric pressure	in Hg	0.10	29.9
T_A	Impactor temperature	°C	1.0	50.0
V	Volume of impinger	ml	0.5	200.0
Ws	Weight of dryer	g	0.01	200.0

Note: Tables 6-6 and 6-7 include English units where test apparatus was equipped accordingly.

CHAPTER 7

F/C SCRUBBER PERFORMANCE PREDICTION MODEL

The purpose of the F/C scrubber performance model is to predict the overall efficiency of a flux force condensation scrubber under different sets of operating and process conditions. The model can be used to predict the outlet concentration of particulate matter that would be anticipated from a F/C scrubber installation on a pollutant source with a known particle concentration and size distribution of emissions. In summary the F/C model first predicts the size distribution of the grown particle and then determines the fractional penetrations for different particle sizes. Using these penetration data and the initial inlet size distribution, one can then calculate the anticipated overall efficiency.

Under previous EPA contracts, Air Pollution Technology, Inc conducted detailed studies on the technical and economic feasibilities of applying F/C scrubbing for fine particle collection. These studies (Calvert et al. (1973 and 1975)) included theoretical development of design equations for F/C scrubbing and the development of a computer mathematical model to predict particle collection in a sieve plate F/C scrubber. The predictions compared well with experimetal results, but the computerized model had certain limitations. Its usefulness for quick and overall design calculations was limited since solutions for each sieve plate and for each different set of operating conditions had to be calculated individually. In this study, a revised mathematical model was developed from the same basic relationships and the design procedures were greatly simplified for prediction of F/C scrubber performance.

In the course of refining our design method we arrived at the conclusion that the flux force effects would be treated separately from the condensation effects in many scrubber situations. While the condensation-induced improvement in inertial impaction efficiency could be handled conveniently, the flux force deposition prediction remained cumbersome. Recently we became aware of a concept developed by Whitmore (1977) which provided the key to simplifying the prediction of the flux force effects in F/C scrubbing. By incorporating Whitmore's concept into our model we have developed a much simpler design method which is convenient to use. This revised model will be described below.

BASIC CONCEPTS

Before proceeding to the details of the mathematical model the basic concepts and outline of the approach will be discussed. If we consider a typical F/C scrubbing system, it might have the features shown in Figure 7-1. The gas leaving the source is hot and has a water vapor content which depends on the source process. The first step is to saturate the gas by quenching it with water. This will cause no condensation if the particles are insoluble, but will if they are soluble. There will be a diffusiophoretic force directed away from the liquid surface.

Condensation is required in order to have diffusiophoretic deposition, any growth on insoluble particles, and extensive growth on soluble particles. Contacting with cold water or a cold solid surface is employed to cause condensation. While condensation occurs there will be diffusiophoretic and thermophoretic deposition as well as some inertial impaction (and, perhaps, Brownian diffusion). The particles in the gas leaving the condenser will have grown in mass due to the layer of water they carry.

Subsequent scrubbing of the gas will result in more particle collection by inertial impaction. This will be more efficient than impaction before particle growth because of the

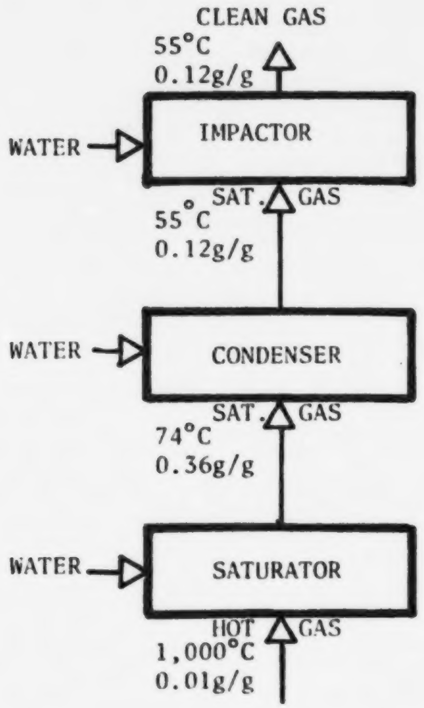
CLEAN GAS
55°C
0.12g/g
WATER
IMPACTOR
SAT. GAS
55°C
0.12g/g
WATER
CONDENSER
SAT. GAS
74°C
0.36g/g
WATER
SATURATOR
HOT GAS
1,000°C
0.01g/g

Figure 7-1. Generalized F/C Scrubber System.

greater inertia of the particles. There may be additional condensation, depending on water and gas temperatures, and its effects can be accounted for as discussed above.

One can apply this general outline of F/C scrubbing to a variety of scrubber types and Figure 7-2 shows a multi-plate F/C scrubber system. It can be seen that the gas is saturated before entering the plate column, although this is not always necessary. The first plate can serve as the saturator and partial condenser. Generally, the efficiency of heat and mass transfer is so high (say, 80%+) on a well designed plate that most of the condensation occurs on the first plate.

In subsequent plates the gas is scrubbed by inertial impaction and there will be a minor amount of additional condensation. We have shown a simple counter-current column but other variations are possible.

The mathematical model is based on the process just described for a plate-type F/C scrubber. It is outlined below:

I. Saturate the gas before it reaches plate 1
    A. Particles are collected at size "d_{p_1}".
    B. No condensation occurs on the particles (they are assumed insoluble).
II. Contact on plate 1
    A. Particles are collected by impaction in the bubble formation zone, still at size "d_{p_1}".
    B. Condensation occurs and particles grow to "d_{p_2}".
    C. Diffusiophoretic deposition removes some particles from the gas in the froth layer on the plate. Thermophoresis and centrifugal deposition are neglected.
III. Contact on plate 2
    A. Particles are collected by impaction in the bubble formation zone at size "d_{p_2}".
    B. Negligible condensation occurs.
IV. Contact on subsequent plates has same characteristics as plate 2.

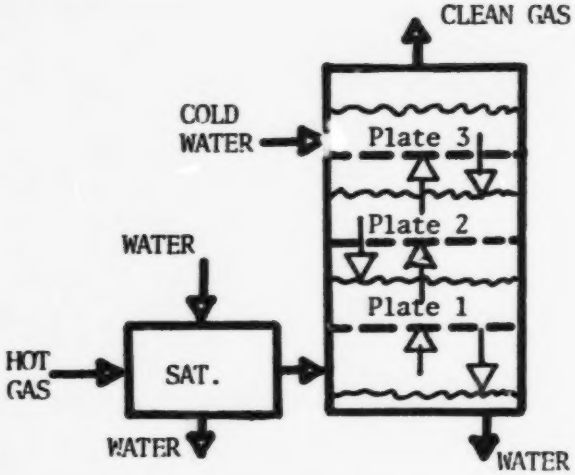
CLEAN GAS
COLD WATER
Plate 3
Plate 2
Plate 1
WATER
HOT GAS
SAT.
WATER
WATER

Figure 7-2. Multiple plate F/C scrubber system.

Although the model is somewhat idealized, it is well within the bounds of engineering accuracy and the precision of experimental measurements. One can always revise any stage of the model with a closer approximation of parameters if one wishes to examine the sensitivity of the method to parametric values. In our evaluations of the model we found that further refinements did not produce significant changes in predictions.

DIFFUSIOPHORETIC DEPOSITION

Particle deposition by diffusiophoresis was described by the following equation in our previous models:

$$u_{pD} = \frac{\sqrt{M_1}\ D_G}{\left| y\sqrt{M_1} + (1-y)\sqrt{M_2} \right| (1-y)} \left(\frac{dy}{dr}\right), \text{ cm/s} \qquad (7\text{-}1)$$

or,

$$u_{pD} = C_1\ D_G \left(\frac{1}{1-y}\right) \frac{dy}{dr} \qquad (7\text{-}2)$$

where D_G = diffusivity of water vapor in carrier gas, cm^2/s

M_1 = molecular weight of water, g/mol

M_2 = molecular weight of non-transferring gas, g/mol

y = mole fraction water vapor, dimensionless

r = distance in the direction of diffusion, cm

The molecular weight and composition function represented by "C_1" describes the effect of molecular weight gradient on the deposition velocity corresponding to the net motion of the gas due to diffusion (the "sweep velocity"). For water mole fraction in air ranging from 0.1 to 0.5, "C_1" varies from 0.8 to 0.88. We used a rough average of 0.85 for "C_1" for computing "U_{pD}" and consequent particle collection efficiency by integrating over the period of condensation.

Whitmore concludes that the fraction of particles removed from the gas by diffusiophoresis is equal to either the mass fraction or the mole fraction condensing, depending on what theory is used for deposition velocity. In other words, it is not necessary to follow the detailed course of the condensation process, computing instantaneous values of deposition velocity, and integrating over the entire time to compute the fraction of particles collected. One can simply observe that if some fraction of the gas is transferred to the liquid phase it will carry along its load of suspended particles.

We have used Whitmore's general concept but with two modifications. First, one can see from equation (7-1) that Whitmore's theory would be comparable to assuming that the particles move with the same velocity as the gas phase. We have chosen to retain the correction for molecular weight gradient, which means that we will compute the particle collection efficiency as 85% of the volume fraction of gas condensing on the cold surface.

The second modification concerns how to compute the proper value of the volume fraction of gas condensing. The problem is that not all of the condensate goes to the heat transfer surface; some of it goes to the suspended particles. As will be shown in detail later, the fraction of the condensate which causes particle growth depends on several factors and ranged from about 0.1 to 0.4 of the total condensate for the range of parameters we explored.

If one is concerned only with diffusiophoretic deposition the particle collection efficiency would, therefore, be 60% to 80% of that computed without accounting for condensation on particles. In the case of a scrubber which also employs inertial impaction the particles would be agglomerated to some extent by the diffusional sweep, so they would have higher mass and be easier to collect.

Without going into a detailed model of this phenomenon one could use either of two simplifying assumptions:

1. Assume that the condensation on particles causes no agglomeration.
2. Assume that the condensation on particles causes agglomeration and that the inertial impaction efficiency is sufficiently high that all of the

particles swept to other particles will be collected by impaction.

The first assumption will lead to too low an efficiency and the second to too high an efficiency. However, the maximum difference between the two for a representative case of 25% of the volume condensing and 25% of that going to the particles would be 5.3%. That is, the percentage of particles which could be swept to other particles = (0.25 x 0.85 x 0.25 x 100). This is a relatively small effect compared to the other uncertainties.

PARTICLE GROWTH

Particle growth is dependent on how well the particles can compete with the cold surface for the condensing water. There are several transport processes at work simultaneously in the condenser section of an F/C scrubber:

1. Heat transfer
    a. From the gas to the cold surface
    b. From the particles to the gas
2. Mass transfer
    a. From the gas to the cold surface
    b. From the gas to the particles

A mathematical model which accounted for these transport processes in addition to particle depostion has been described in EPA reports, see Calvert et al. (1973 and 1975). The portions of that model relating to particle deposition were deleted to provide a model which would describe particle growth in the absence of deposition. The basic relationships involved are as follow:

The rate of change of particle radius is given by a mass balance,

$$\frac{dr_p}{dt} = \frac{k'_{pG}\,(p_G - p_{pi})}{\rho_M}\text{, cm/s} \tag{7-3}$$

where:

$$k'_{pG} = \frac{2\,D_G\,P}{R T_G\,d_p\,p_{BM}} = \text{particle to gas mass transfer coefficient, gmol/cm}^2\text{-s-atm} \tag{7-4}$$

pG = water vapor partial pressure in bulk of gas bubble, atm
p_{BM} = mean partial pressure to non-transferring gas, atm
r_p = particle radius, cm
T_G = gas bulk temperature, °K
ρ_M = molar density of water, gmol/cm^3
p_{pi} = water vapor partial pressure at vapor-particle interface, atm
ρ_m = molal desntiy of water, gmol/cm^3
P = total pressure, atm
R = gas law constant, atm-cm^3/gmol-°K
d_p = particle diameter, cm

Particle temperature can be computed from an energy balance:

$$h_{pG}\,(T_{pi}-T_G) + \left(\frac{\rho_p\,C_{pp}\,r_p}{3}\right)\frac{d\,T_{pi}}{dt} = k'_{pG}\,L_M\,(P_G-p_{pi}) \qquad (7\text{-}5)$$

where:

$$h_{pG} = \frac{2k}{d_p} = \text{particle to gas heat transfer coefficient, cal/cm}^2\text{-s-°K} \qquad (7\text{-}6)$$

where C_{pp} = heat capacity of particle, cal/g-°K
k = thermal conductivity of gas, cal/cm^2-s-°K/cm
L_M = latent heat of vaporization for water, cal/gmol
t = time, s
T_{pi} = temperature at particle interface, °K
ρ_p = particle density, g/cm

The overall energy balance for the gas-liquid interface is given by:

$$k'_G\,a_t\,L_M\,(p_G - p_{Li})\,A_p\,dZ =$$

$$h_L\,a_t\,(T_{Li} - T_L)\,A_p\,dZ + h_G\,a_t\,(T_{Li} - T_G)\,A_p\,dZ \qquad (7\text{-}7)$$

where k'_G = mass transfer coefficient, gas to liquid, gmol/cm^2-s-atm

a_t = interfacial area for transfer volume of scrubber, cm^2/cm^3

A_p = cross-sectional area of scrubber, cm^2

h_G = heat transfer coefficient, gas to liquid, cal/cm^2-s-°K

T_L = temperature of liquid bulk, °K

P_{Li} = water vapor partial pressure at vapor-liquid interface. atm

dz = height of bubble rise, cm. in time "Δt", s

T_{Li} = temperature at liquid-gas interface, °K

h_L = liquid phase heat transfer coefficient, cal/s-cm^2-°K

The equations given above are used along with enthalpy and material balances for the total system of gas, liquid, and suspended particles to form a mathematical model for condensation and growth. The model was solved through a finite difference method on an electronic computer for several situations which are discussed below.

PREDICTION OF CONDENSATION

The condensation model was used to predict the fraction of the total condensate which goes to the particles (this fraction defined as "f_p") as a function of several parameters. The conditions investigated are as follows:

1. Scrubber type - one sieve plate
2. Inlet gas - saturated from 310°K to 350°K
3. Water - uniform bulk temperature from 310°K to 325°K
4. Particle number concentration - 10^7 to 10^9 /cm^3
5. Particle diameter - 0.1 to 1.0 μm
6. Liquid phase heat transfer coefficient - 0.01 to 0.1 cal/cm^2-s-°K
7. Condensation can occur when the gas is saturated

The computed values are plotted on Figures 7-3 through 7-7. As can be seen, the figures show the following:

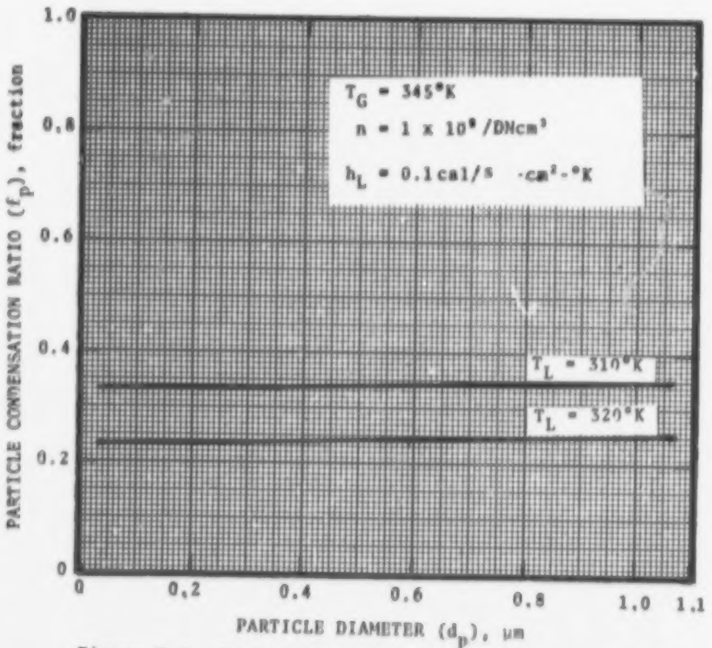

Figure 7-3. Predicted particle condensation ratio (f_p) as a function of particle diameter.

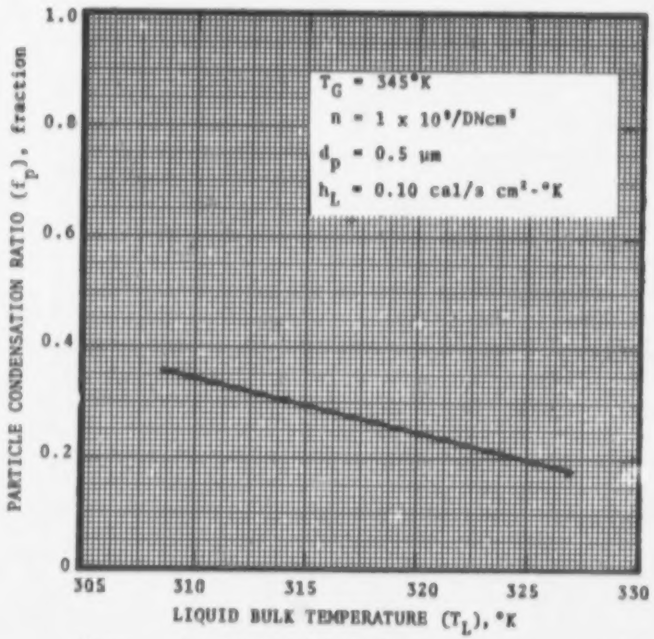

Figure 7-4. Predicted particle condensation ratio (f_p) as a function of liquid bulk temperature.

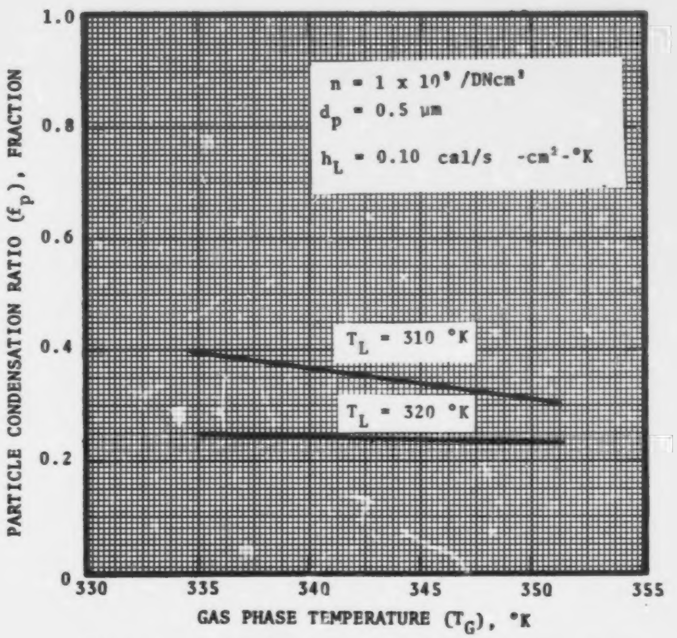

Figure 7-5. Predicted particle condensation ratio (f_p) as a function of gas phase (saturated) temperature.

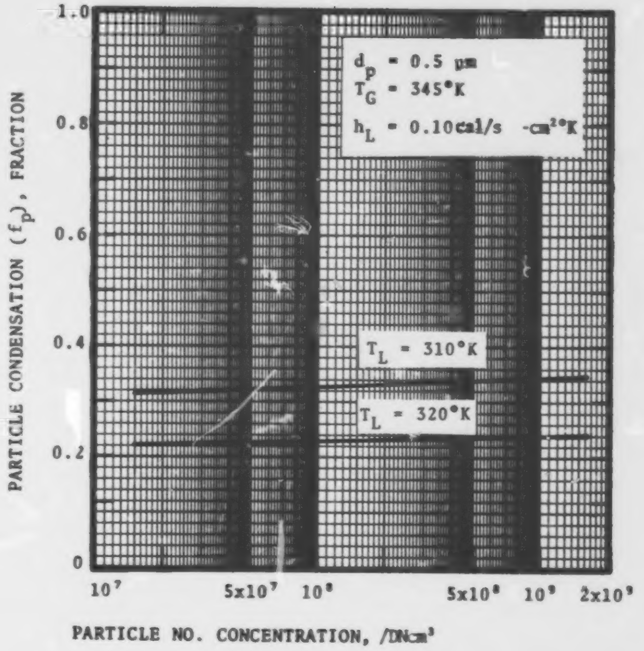

Figure 7-6. Predicted particle condensation ratio (f_p) as a function of particle number concentration.

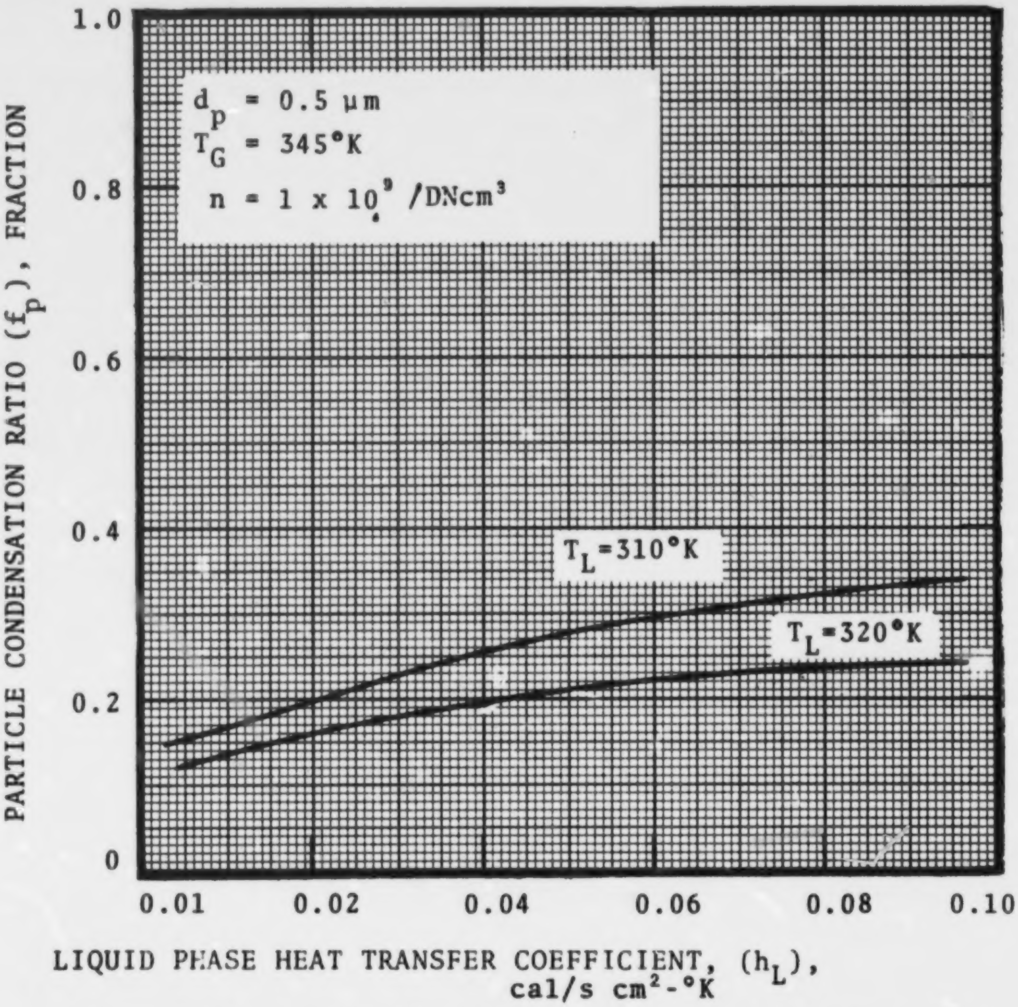

Figure 7-7. Predicted particle condensation ratio (f_p) as a function of liquid phase heat transfer coefficient.

Figure 7-3. "f_p" does not depend much on "d_p"
7-4. "f_p" decreases significantly with "T_L"
7-5. "f_p" decreases with "T_G" to an extent which depends on "T_L"
7-6. "f_p" increases slightly with "n_p" above $10^7/cm^3$
7-7. "f_p" increases with "h_L" up to "h_L" ≈ 0.1 cal/s-cm²-°K

It was found in other computations that "f_p" decreases significantly with "n_p" below about 10^6 particles/cm³. Since industrial emissions generally have particle number concentrations on the order of 10^7 and greater "n_p" has no significant effect on "f_p" in practice. The liquid phase heat transfer coefficient is an important parameter but, unfortunately, predictions of its magnitude vary considerably depending on which correlation is used. The value of 0.1 appears to be the best supported by the literature for mass transfer on perforated plates.

For a combination of parameters such as might be encountered in a practical situation a value of "f_p" ≈ 0.25 appears to be reasonable. Given this one can compute the amount of particle growth that will result from a given condensation ratio (i.e., g water condensed/g dry gas = q' = condensation ratio). If the particle size distribution and the scrubber characteristics are known one can predict the overall penetration that will be achieved in the scrubber.

INTERIAL IMPACTION DURING BUBBLE FORMATION

During the formation of bubbles on a sieve plate the jets of gas emerging from the perforations impact on the liquid. Particles are thus deposited on the liquid surface by inertial impaction. Particle collection can be determined from:

$$Pt_i = \exp\left(-\frac{40\, F^2 d_p^2\, \rho_p\, C'\, u_h}{9\, \mu_G\, d_h}\right) \qquad (7\text{-}8)$$

where F = foam density, volume fraction liquid
d_p = particle diameter, cm
ρ_p = particle density, g/cm³
C' = Cunningham slip correction factor, dimensionless
u_h = gas velocity in the perforation, cm/s
μ_G = gas viscosity, poise
d_h = diameter of perforation, cm
Pt_i = penetration of particles of diameter, d_p, fraction

PERFORMANCE PREDICTION METHOD

The sequence of steps to be followed in predicting the performance of a F/C scrubber system involving a sieve plate column is as follow:

1. Determine the initial particle size distribution.

2. Compute particle penetration from the saturator (Pt_a) based on the saturator collection efficiency characteristics and the initial particle size distribution. No growth occurs in the saturator.

3. Compute particle penetration due to inertial impaction during bubble formation on the first plate (Pt_b). Use the particle size distribution leaving the saturator and the collection efficiency relationship for sieve plate given in equation (7-8).

4. Calculate the condensation ratio corresponding to the scrubber operating conditions, from this compute "f_v", the volume fraction of gas condensing, and then calculate the penetration due to diffsiophoresis (Pt_c) according to equation (7-9) for a conservative estimate or equation (7-10) for an optimistic estimate

$$Pt_c = 1 - 0.85\,(f_v)\,(1 - f_p) \tag{7-9}$$

$$Pt_c = 1 - 0.85\,f_v \tag{7-10}$$

where:

$$f_v = \frac{\text{moles } H_2O \text{ condensed}}{\text{total moles originally in vapor}} = \frac{q'}{H_1 + \frac{18}{29}}$$

where:

H_1 = original humidity ratio, g/g

The diffusiophoretic penetration applies equally to all particle sizes so it will not change the size distribution but will decrease the particle concentration.

5. Determine the particle size distribution leaving the condenser from the values of "q'" and "f_p".

6. Compute the particle penetration function for the remaining stages of the scrubber, based on the penetration for one stage given by equation (7-8). The penetration for a given particle diameter on one stage is "Pt_i". For "N" stages of equal efficiency the penetration for a given particle diameter is "Pt_i^N".

7. Use the relationship between "Pt_i^N" and "d_p" from step 5 and the grown size distribution from step 5 to compute the overall penetration due to inertial impaction after growth (Pt_d).

8. To summarize, the total overall fractional penetration for the F/C scrubber Pt_t will be the product of the following:

a. "Pt_a" due impaction in the saturator

b. "Pt_b" due to impaction in the condenser

c. "Pt_c" due to diffusiophoresis in the condenser

d. "Pt_d" due to impaction in stages after the condenser.

Thus,

$$Pt_t = Pt_a \times Pt_b \times Pt_c \times Pt_d \qquad (7\text{-}11)$$

In order to determine the overall penetration of the system $\overline{Pt}$, the penetration curve has to be integrated over the entire range of the initial size distribution curve. This can be accomplished either mathematically on a programmable calculator or graphically by plotting penetration versus percent mass undersize over the initial size range. Then the area under the curve represents the total penetration, $\overline{Pt}$, of the system. The total efficiency of the system can then be determined as:

$$E = 1 - \overline{Pt} \qquad (7\text{-}12)$$

where $\overline{Pt}$ = overall penetration of the system, fraction
E = overall efficiency of the system, fraction

This value represents the predicted efficiency of the F/C scrubbing system.

Limitations of The Design Model

The revised model is much simpler to use than our previous version and it appears to give very good predictions. It also offers the opportunity for easy modification to suit specific situations. The limitations of the design model are given below:

1. The quencher unit is considered as a humidification chamber but particle collection in this unit of the F/C scrubbing system is neglected. The quencher would have an effect on the collection efficiency of the larger particles but the collection efficiency of the submicron particles would be very low. Since the main area of difficulty is the removal of submicron particles, the effect of particle collection across the quencher is not amended to the design model.

2. The collection mechanisms of inertial impaction and diffusiophoresis are the only ones considered. The flux force theoretical equations for collection by thermophoresis and centrifugation were previously presented in earlier studies (Calvert, et al. 1973 and 1975) but the effect of inertial impaction and diffusiophoresis would overshadow the effect of these other mechanisms.

3. A constant value is used for foam density of the froth over the sieve plates in the scrubber. In actuality, there would be some variation due to different plate hydrodynamics.

4. Particles are assumed to be wettable, but insoluble. If the emitted particles are soluble in water, as was the case at the demonstration plant, the expected performance for the system would be better. The solubility of the particles in water would depress the vapor pressure at the particle-gas interface, resulting in nucleation at a lower saturation ratio and more growth at a given saturation ratio.

5. A constant, average value was used for the fraction of water vapor condensing on the particles. This approximation of "f_p" is based on computer modeling runs using the unit mechanisms of heat and mass balance at conditions comparable to F/C scrubbing at the demonstration plant. This value is affected by different process conditions, among which the important ones are the liquid bulk temperature and the actual value of liquid phase heat transfer coefficient.

6. The liquid phase heat transfer coefficient, h_L, was evaluated from literature correlations for heat and mass transfer to spheres and liquid phase controlled mass transfer on sieve plates.

7. The design model also assumes that all condensation and particle growth occurs at the first plate of the scrubber unit. The following plates then see the fully grown particles which are larger and easier to collect. This is close to what has been observed experimentally.

Example Calculation

An example calculation of particle penetration as predicted from the new design model is given in Appendix "F".

CHAPTER 8

ENGINEERING ANALYSIS

As a framework for the engineering analysis of an F/C scrubbing system applied to a secondary metal recovery furnace, a near optimum design has been prepared and is discussed in this chapter. Design refinements of the demonstration plant are both possible and necessary because of several factors including:

1. The demonstration plant was over-designed in order to provide the apparatus and operational variations and the extensive instrumentation necessary for a quantitative investigation. A commercially practical prototype can be smaller, simpler, and less expensive so a realistic view of F/C scrubbing should be based on this latter approach.

2. Knowledge of the complexities and characteristics of the source operation increased during the demonstration program. Because of the great variability of the source and the consequent demands on the control system, the design must be made appropriate for the range of parameters as now known.

3. In the course of analyzing the demonstration plant performance data and interpreting the complexities of operational behavior, our basic understanding of F/C scrubbing in practice has grown. Part of the increased engineering capability was the development of a greatly simplified method for performance prediction. An F/C system design can be optimized much more readily now than was previously possible.

The following chapter presents a refined F/C design for a secondary metal recovery furnace control system. Capital and operating costs have been estimated for the F/C system and are discussed in relation to a conventional scrubbing system.

Source Characteristics

The first matter to be resolved before proceeding with the engineering design is the definition of the source operation which is to be controlled. While the incinerator furnace design and operation are important in determining the quantity and nature of the emissions, their optimization is beyond the scope of this study. For the present design we will assume that the furnace and afterburner system will be such as to produce emissions comparable to those encountered in the demonstration program.

The type of wire or scrap being fed is the main factor determining the severity of the emissions problem. Economics and scrap supply enter into the picture and dictate what kind of scrap is available and profitable to treat. Although one cannot predict the market, the operator's preferences can be considered. It was not possible for the source operator to "burn" any grade of copper wire scrap, not even no. 1 premium wire, and comply with the air pollution codes.

It would be adequate if the operator could burn all types of no. 1 wire scrap although he would like to be able to burn no. 2 and no. 3. It would not be sufficient to burn only no. 1 premium under present market conditions. Most of the operation during the demonstration plant program was with no. 1 regular and no. 1 premium wire so most of the data are on these.

We can set forth the criteria for burning no. 1 regular wire (which will exceed the requirements for no. 1 premium) and design an F/C system to satisfy them. The limited data available on no. 2 and no. 3 wire indicate that a system adequate for no. 1 regular wire would probably suffice for them too. This is because the emissions from no. 2 and 3 wire are higher than from no. 1 regular wire mainly because of increased acid gases (impinger catch). The acid gases can be absorbed with very high efficiency and it is relatively simple and inexpensive to provide this in the system for no. 1 wire.

The plot plan of the demonstration plant was dictated by the operator's need for access routes and by the arrangement of equipment and scrap piles. While this is a special case, it is likely that any commercial operation will have similar problems. Consequently, the F/C system should be designed to fit the plant encountered in the demonstration.

Liquid waste disposal requirements were obtained from the local authorities and the demonstration plant was operated in compliance. The major requirements are that the liquid discharge to the sewer be neutral and not interfere with the sewage treatment plant process. The small quantity and the composition of the liquid waste from this F/C system are such that compliance can be accomplished by neutralization and daily discharge of the scrubber liquor.

Performance Criteria

The levels of particulate emissions are first established in order to complete the overall efficiency necessary to attain the desired outlet loading for compliance with the legal pollutant limit from the furnace.

The inlet mass particuate loading measured during the operation of the demonstration unit was 1.6 g/DNm^3 plus an approximate average of impinger loading of 0.15 g/DNm^3. The total value of 1.75 g/DNm^3 was computed from the loading data presented in Table 6-3 for modes A to F, which exclude peak-to-peak data and premium wire data. The value of 0.15 g/DNm^3 was approximated from all the impinger data (presented in Table "D" of the appendix) taken during the operation of the demonstration unit.

The design outlet mass particulate loading was set at 0.08 g/DNm^3. This was based on the legal limit of 0.10 g/DNm^3 (corresponding under average conditions to 0.1 gr/SCF corrected to 12% CO_2) minus the expected entrainment from the scrubber and cooling tower units as designed. From the inlet and outlet design criteria, the overall fractional penetration required was calculated to be 0.05. Thus, the system is designed to give an overall efficiency of 95%.

The particulate characteristics were based on both the demonstration unit data and the 1.4 m^3/min pilot plant data.

The size was approximated conservatively for the design of the optimum F/C unit as follows:

$$d_{pg} = 0.75\ \mu mA$$
$$\sigma_g = 2.5$$

In addition, the system must be designed to neutralize and efficiently remove the acid gas by mass transfer in order to both reduce the emission level and prevent excessive corrosion of the system. The design criteria are summarized in Table 8-1.

Process Description

The general characteristics of a refined F/C scrubbing system suited to the design criteria are shown in Figure 8-1, a schematic flow diagram. Major equipment items are also identified in Figure 8-1, while stream quantities and conditions are given in Table 8-2. The discussion which follows will describe the design logic and the most important features of the equipment and the operating conditions.

Flue gas, stream 1, will be drawn from a branch on the afterburner stack into a saturator which serves to quench and saturate the gas before it enters the cross-over duct. The afterburner stack is fitted with a lid which can be opened when the scrubber system is not operating or in case the saturator liquid supply fails. The saturated gas flows through the cross-over duct into a perforated plate condenser unit. There moisture condensation will cause particle growth, removal of particulate matter by diffusiophoresis, and removal of acidic gas by absorption. Next the gas will pass through a venturi scrubber and be vented to the atmosphere through a stack.

Water from the saturator drains to a holding tank and is recirculated to the saturator unit. Liquor from the condenser will be pumped to a cooling tower for evaporative cooling and recycling. The liquor from the venturi scrubber will be recycled through the cooling tower tank.

The liquor used to quench and scrub the gas will be treated periodically with sodium carbonate to adjust the pH

TABLE 8-1. DESIGN CRITERIA SUMMARY

Source	
Charging rate (assumed)	1,800 kg/hr
Type of scrap	No.1 regular wire
Plant layout	As in demonstration
Operation schedule	300 day/yr, 8 hr/day
Gas Flow	
Gas emission rate	200 Am^3/min
Gas temperature	700°C
Gas humidity	0.06 g H_2O/g D.G.
Contaminant Emissions to F/C	
Acid gases	0.85 kg mole equivalents/day
Particle concentration (without impinger catch)	1.6 g/DNm^3
Particle mass median diameter	0.75 μmA
Particle geometric standard deviation	2.5
Particle impinger catch	0.15 g/DNm^3
Emissions from F/C	
Scrubber (without entrainment)	0.08 g/DNm^3
Entrainment (scrubber and cooler)	0.02 g/DNm^3
Total particulates	0.1 g/DNm^3
Liquid discharge	once/day, neutralized

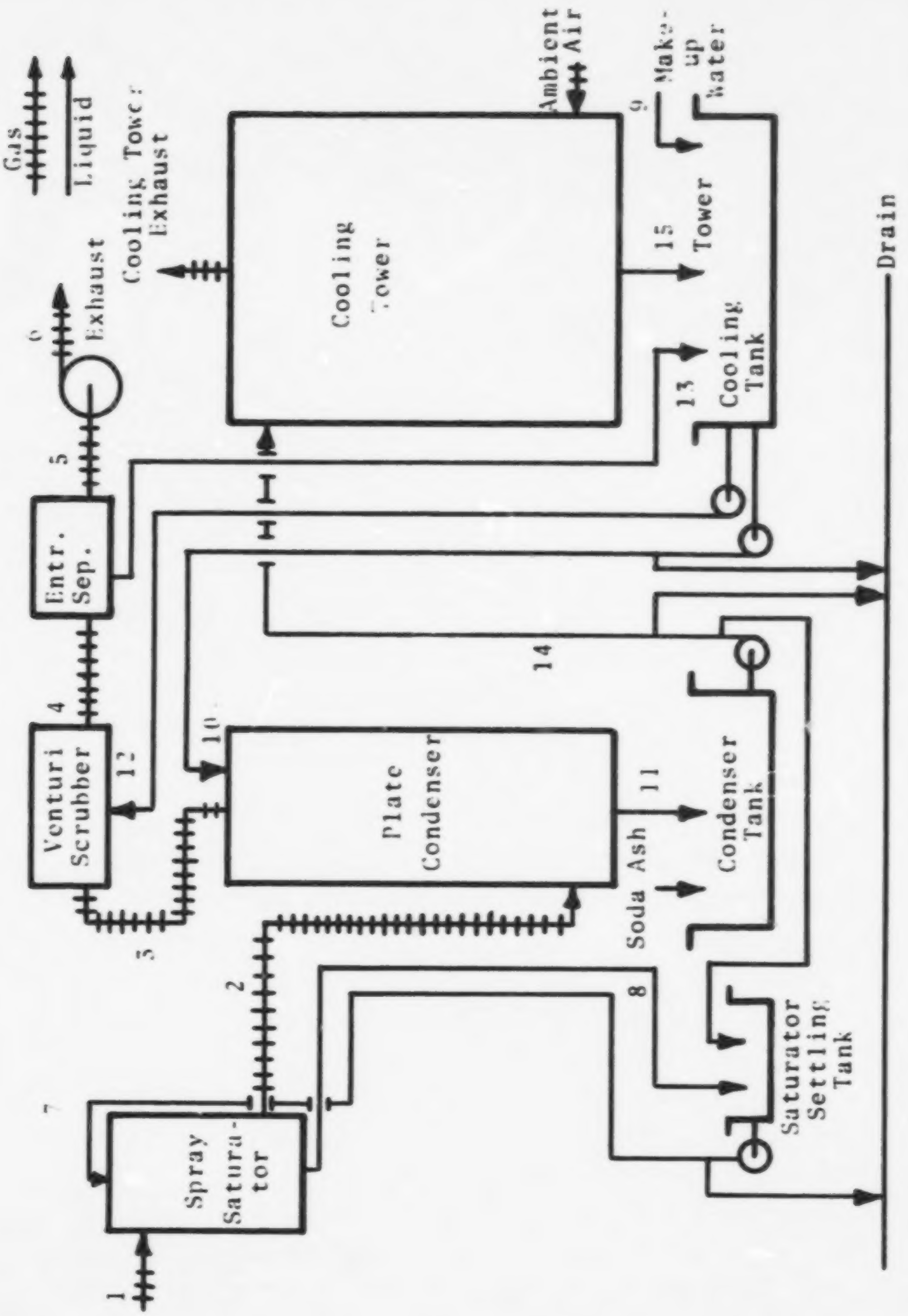
Gas
Liquid
Cooling Tower Exhaust
Exhaust
6
5
Entr. Sep.
4
Venturi Scrubber
12
10
3
Cooling Tower
Ambient Air
9
Make-up Water
15
Tower
13
Cooling Tank
14
Plate Condenser
11
Soda Ash
Condenser Tank
2
8
7
Spray Saturator
1
Saturator Settling Tank
Drain

Figure 8-1. Flowsheet for F/C scrubber optimum design at metals recovery furnace. (See Table 8-2 for description of process streams)

TABLE 8-2. PROCESS STREAMS FOR F/C SCRUBBER OPTIMUM DESIGN AT METALS RECOVERY FURNACE. (See Figure 8-1)

Stream Number	Composition	Temperature	Volume Flow	Mass Flow	Enthalpy	Humidity	Gage Pressure
		°C	*m³/min ℓ /min	kg/min	kgcal/kg	gH₂O/gD.A.	cm W.C.
1	Flue Gas	700	200.0	70.3	225	0.06	0
2	Sat. Gas	73	100.0	88.7	225	0.34	-5
3	Cool Gas	36	61.5	68.8	32.7	0.04	-35
4	Scrubbed Gas	36	69.1	68.8	32.7	0.04	-114
5	Clean Gas	36	69.1	68.8	32.7	0.04	-115
6	Exhaust	36	61.5	68.8	32.7	0.04	0
7	Hot Water	49	56.7	56.7	49.0		
8	Hot Water	73	38.1	38.1	73.0		
9	Make up Water	21	--	--	21.0		
10	Cold Water	32	736.0	736.0	32.2		
11	Hot Water	49	755.9	755.9	49.0		
12	Cold Water	32	123.0	123.0	32.2		
13	Cold Water	32	123.0	123.0	32.2		
14	Hot Water	49	737.3	737.3	49.0		
15	Cold Water	32	714.9	714.9	32.2		

* Gas flow rates in m³/min, liquor flow rates in ℓ/min

of the liquor to 7.0. The saturator tank with a total retention time of 30 minutes also serves a a clarifier by settling out some of the suspended solids. A batch discharge of 8,316 liters at pH = 7.0 from all the tanks to the sewer is provided daily, limiting the solids concentration to 1% maximum.

As indicated in Figure 8-1, the optimum design consists of four major vessels which included the saturator, condenser, venturi scrubber, and the cooling tower. The general design considerations and brief mechanical description of each major vessel are given below.

Saturator

The saturator cools and saturates 200 Am^3/min (3,533 ACFM) initially at 700°C to 73°C (163°F) by evaporating hot water adiabatically. Acid gas absorption and neutralization also occur to some degree in the saturator.

The saturator (see Figure 8-2) consists of a horizontal cyclindrical spray chamber (0.91 m diameter x 1.52 m length). The shell material selected is Hastelloy for protection against high temperature and corrosion. The unit is located adjacent to the stack and has a safety pressure switch to cause city water injection into the unit in case of saturator pump failure. This and the interlocked stack cap opening mechanism will prevent hot, unquenched gas from entering other sections of the F/C system.

The saturator spray requirement is 56.7 ℓ/min (≈ 3 times evaporation rate) of recirculated liquor which is pumped at 2.8 kg/cm^2 (40 psig) to 10 spray nozzles. A holding tank measuring 1.8m x 1.2m x 0.61m is specified for the saturator and a self-priming centrifugal pump is used for pumping the liquor to the unit. The external piping is chlorinated polyvinyl chloride (CPVC) while the internal piping is stainless steel.

From the saturator the gas flows a distance of about 9.2 m (30 ft) through 0.46 m diameter fiberglass reinforced plastic (FRP) duct to the condenser. The long distance between the two units was necessary at the demonstration plant

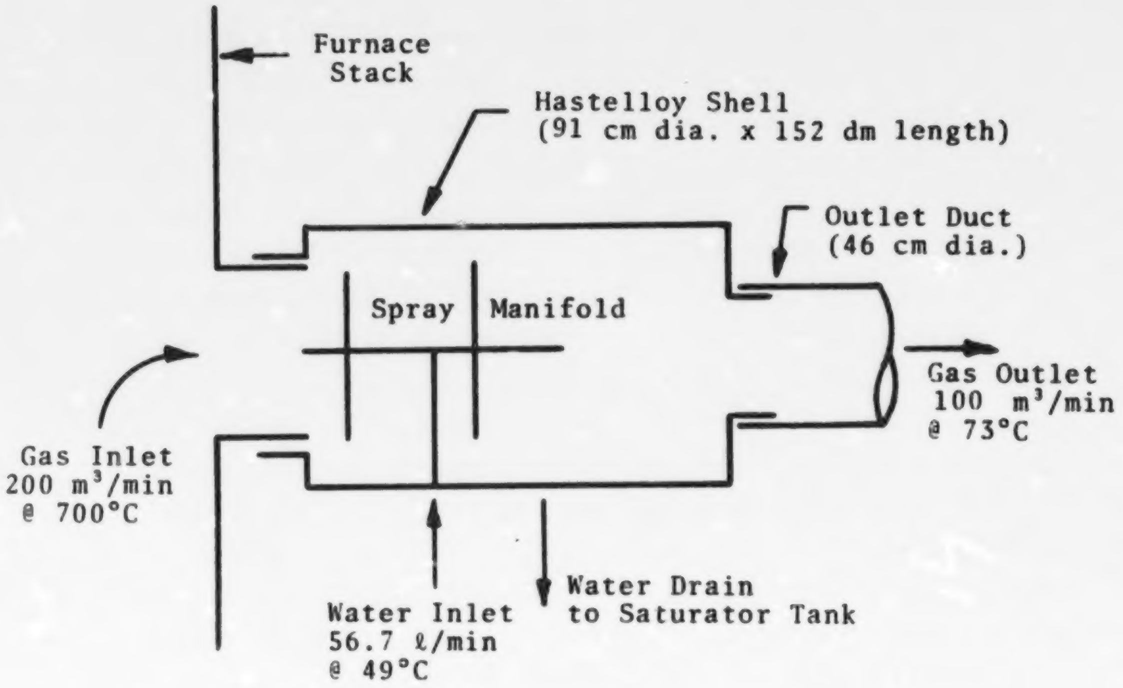
Furnace
Stack
Hastelloy Shell
(91 cm dia. x 152 dm length)
Outlet Duct
(46 cm dia.)
Spray
Manifold
Gas Outlet
100 m³/min
@ 73°C
Gas Inlet
200 m³/min
@ 700°C
Water Drain
to Saturator Tank
Water Inlet
56.7 ℓ/min
@ 49°C

ELEVATION VIEW OF SATURATOR

Figure 8-2. Saturator for F/C optimum design.

site in order to give clear access to the incinerator furnace and is provided for in the refined design. While there is some risk of burning the FRP duct in case of a failure of the pump and the safety interlocks, the cost is much less than corrsion resistant metal ducting and a heavier support structure.

Condenser

One purpose of the condenser unit is to cool the saturated gas at 73°C down to 36°C and a flow rate of 61.5 Am^3/min (2,171 ACFM). Another major function of the condenser is to provide sufficient mass transfer capacity to absorb substantilly all of the acid gases which do not condense. This cooling and absorption is accomplished by bringing the gas in countercurrent contact with cold water at 32°C. The condenser is designed for a condensation ratio of 0.30 g H_2O dry which causes sufficient growth to occur. The amount of particle growth was predicted by means of the design methods described in Chapter 7 to satisfy the design criteria for this refined system. Figure 8-3 is a log probability plot of the original particle size distribution and the size distribution after condensation and growth. The use of these data for the prediction of scrubber system performance is discussed later.

The condenser (see Figure 8-4) is a vertical counter-current tower with three 1.1 m diameter plates and 2.4 m height. The shell is constructed of FRP and the sieve trays are made out of stainless steel.

The water requirement of the condenser is 736 ℓ/min at 32°C. The water is introduced at the top and cascades down to the bottom plates, maintaining cross flow on the sieve plantes. A self-priming centrifugal-type pump at 750 ℓ/min and 2.5 kg/cm^2 head and a polypropylene holding tank, measuring 1.8m x 1.8m x 0.9m are specified.

Venturi Scrubber

Particle growth, particle deposition by diffusiophoresis and thermophoresis, absorption of acid gases, and removal of particles larger than a few microns aerodynamic diameter

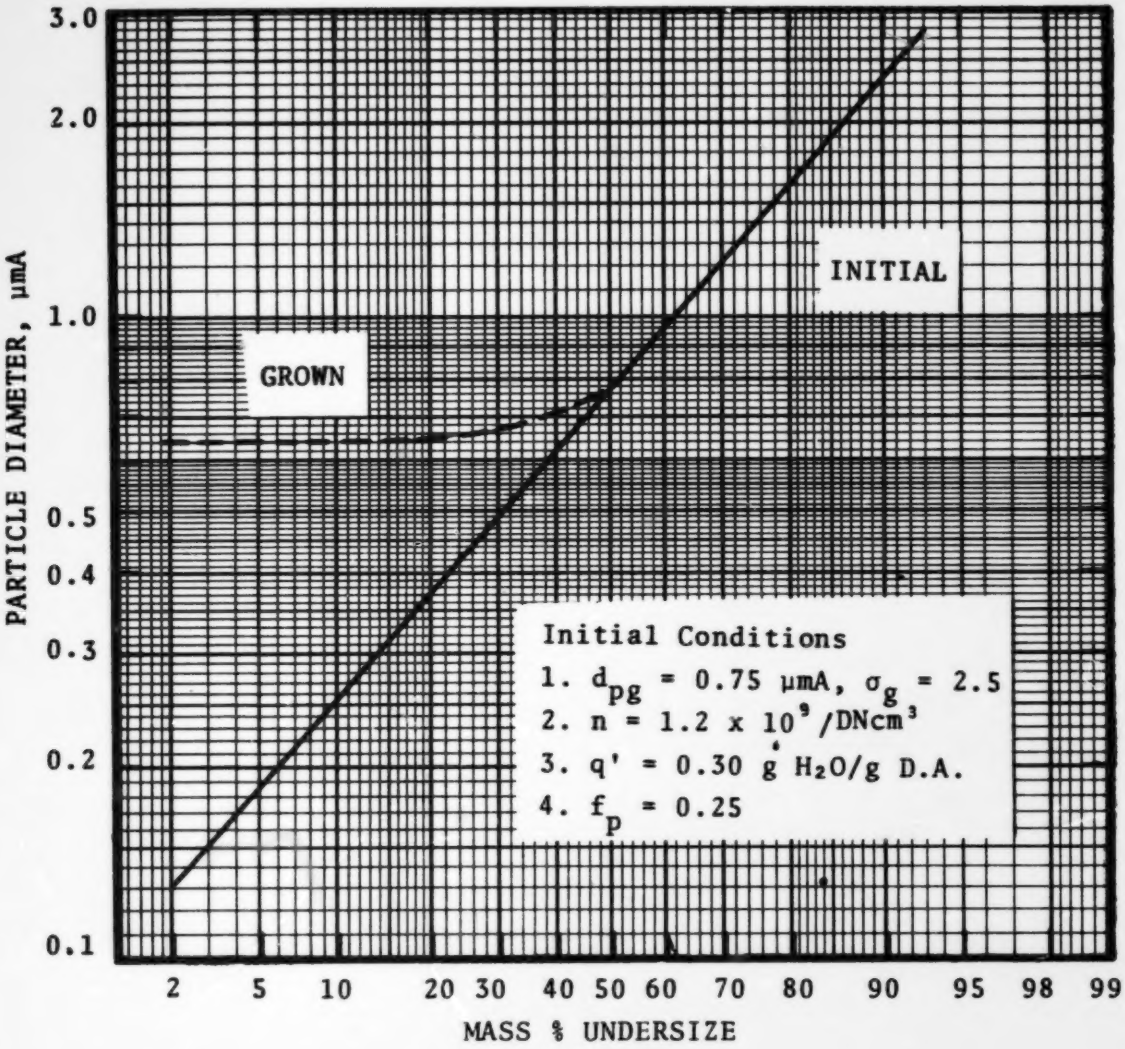

Figure 8-3. Predicted grown particle size distribution for F/C scrubber optimum design.

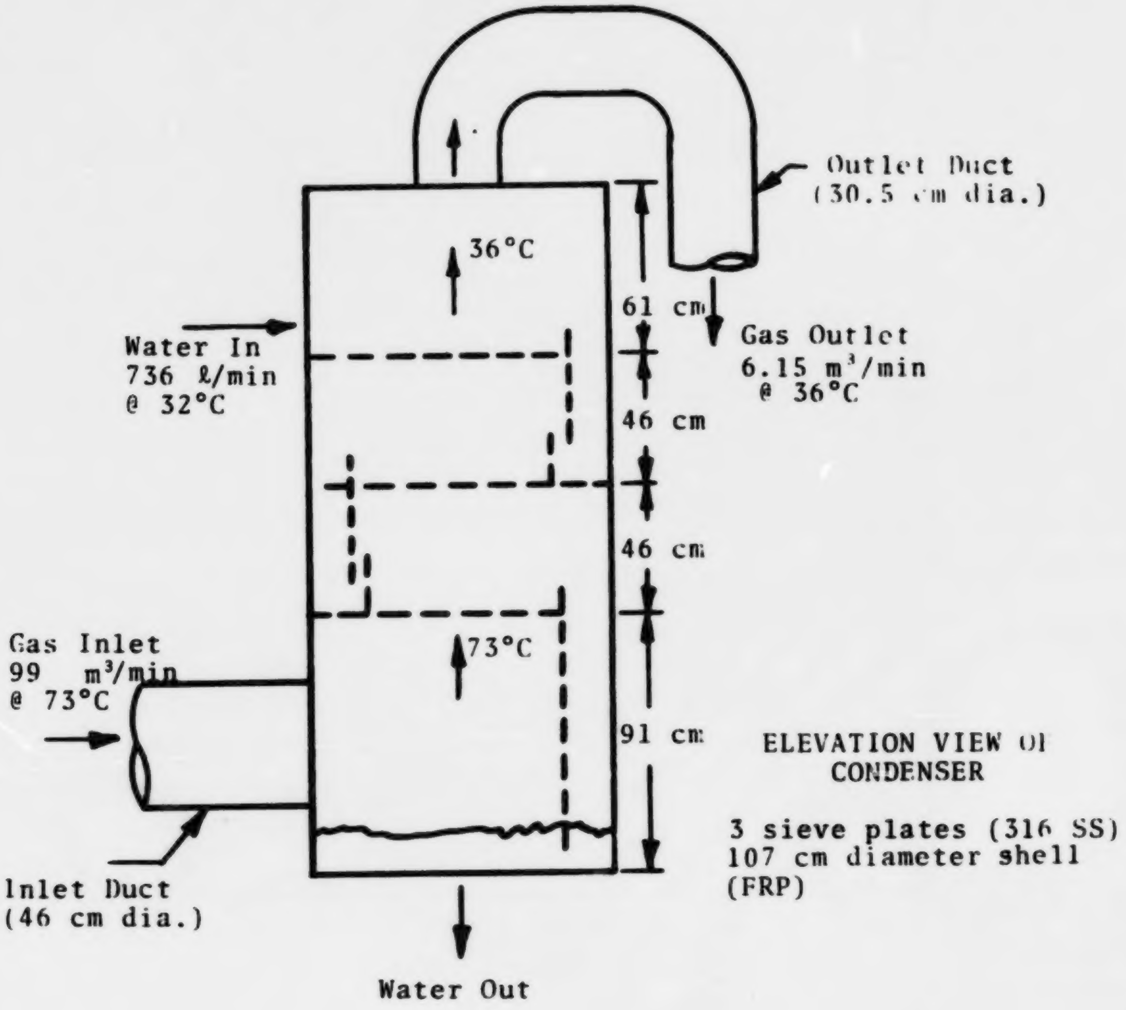
Outlet Duct
(30.5 cm dia.)
36°C
61 cm
Gas Outlet
6.15 m³/min
@ 36°C
Water In
736 ℓ/min
@ 32°C
46 cm
46 cm
Gas Inlet
99 m³/min
@ 73°C
73°C
91 cm
ELEVATION VIEW OF
CONDENSER
3 sieve plates (316 SS)
107 cm diameter shell
(FRP)
Inlet Duct
(46 cm dia.)
Water Out

Figure 8-4. Condenser for F/C optimum design.

will occur in the condenser. The purpose of the venturi scrubber is to provide the capability for collecting submicron particles, which it can do more efficiently than a sieve plate scrubber. On the other hand, the seive plate scrubber is much more efficient than the venturi for mass and heat transfer. Consequently, while it would be appealing to use either one or the other type of scrubber from the standpoint of simplicity the design criteria are such as to make it best to use both.

The venturi scrubber will be followed by a tube-bank-type entrainment separator. This type of separator was selected on the basis of the small cut diameter required to control the predicted entrainment rate and size distribution. Some additional mass transfer capability is provided by the combination of the scrubber and entrainment separator.

The venturi section is designed with a pressure drop of 79 cm W.C. and a Q_L/Q_G ratio of 2 ℓ/m^3. The required penetration across the system was established at 0.05. Accounting for collection by diffusiophoresis in the scrubber, the required penetration through the venturi was calculated as:

$$\overline{Pt} = \frac{0.050}{0.74} = 0.068$$

The grown particle size which enters the venturi unit is given in Figure 8-4. A penetration-particle diameter relationship was calculated for different pressure drops and integrated over the entire size distribution. By trial and error, a pressure drop of 79 cm W.C. was calculated as necessary to obtain a penetration of 0.068 when integrated over the size distribution range. The penetration grade curve for the venturi at this pressure and an overall penetration of 0.068 is given in Figure 8-5.

Physically, the venturi is represented in Figure 8-6. The venturi is built from 1.3 cm wall thickness FRP with a

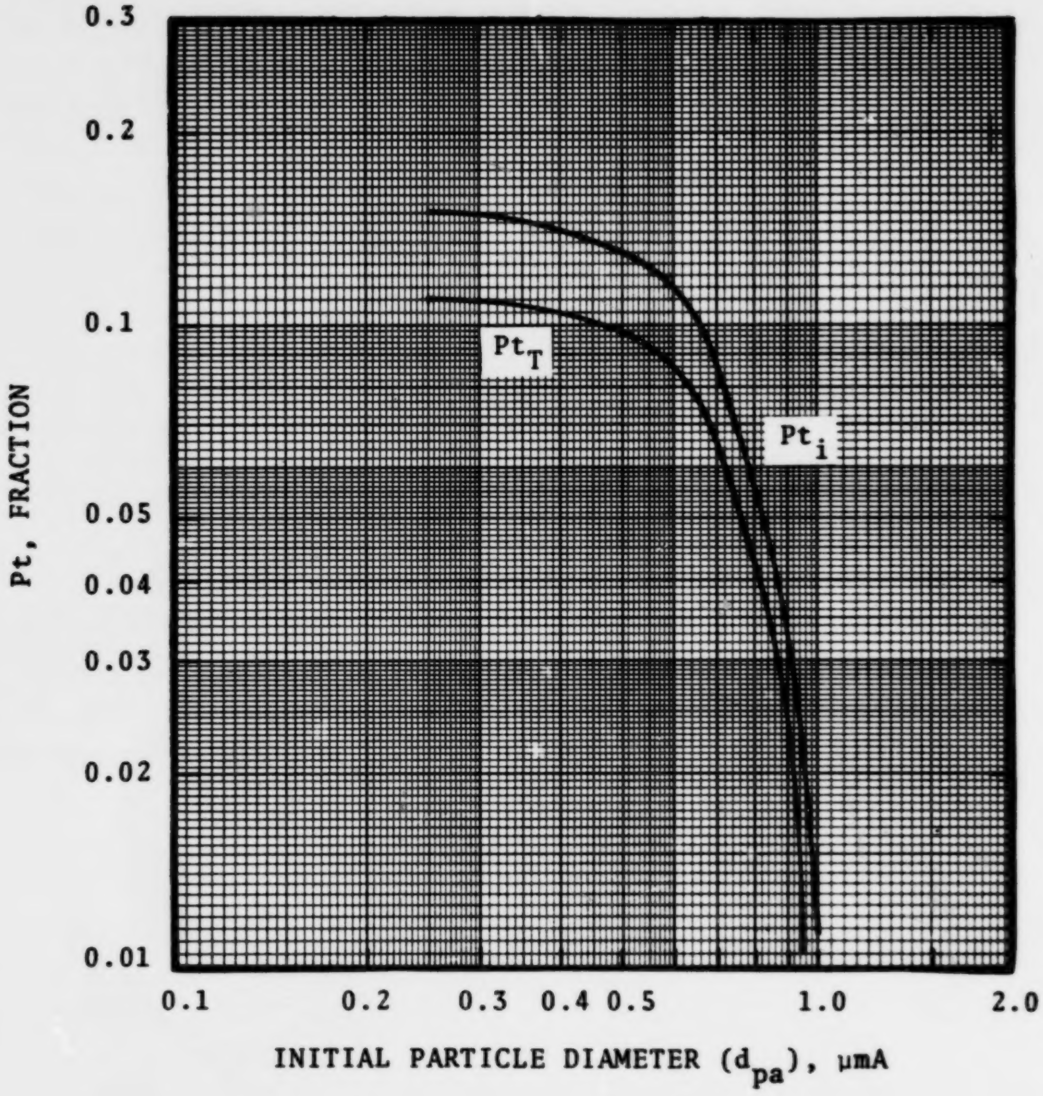

Figure 8-5. Predicted penetration for venturi scrubber as designed for optimum system.

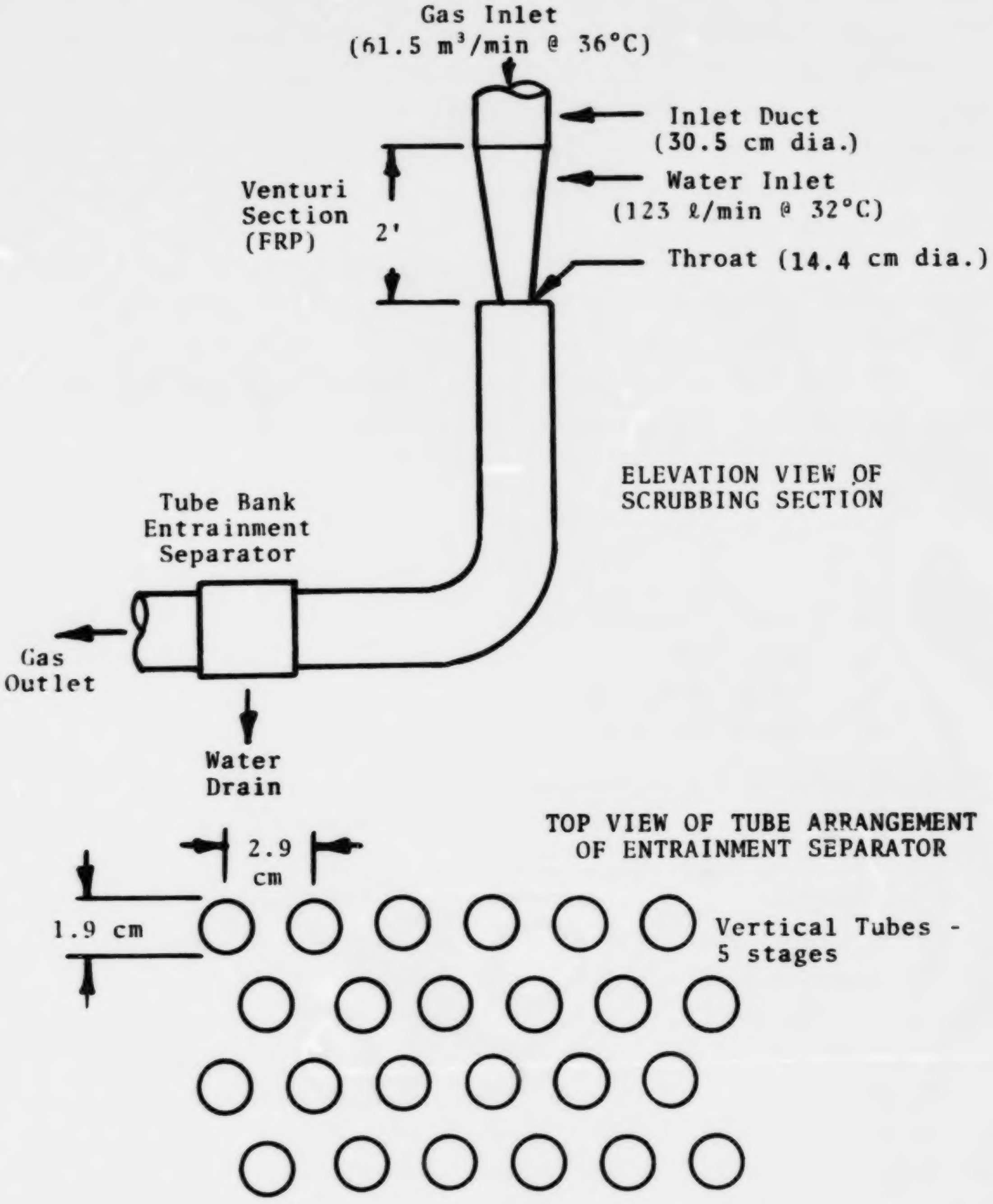
Gas Inlet
(61.5 m^3/min @ 36°C)
Inlet Duct
(30.5 cm dia.)
Water Inlet
(123 ℓ/min @ 32°C)
Venturi
Section
(FRP)
2'
Throat (14.4 cm dia.)
ELEVATION VIEW OF
SCRUBBING SECTION
Tube Bank
Entrainment
Separator
Gas
Outlet
Water
Drain
TOP VIEW OF TUBE ARRANGEMENT
OF ENTRAINMENT SEPARATOR
2.9
cm
1.9 cm
Vertical Tubes -
5 stages

Figure 8-6. Venturi scrubber for F/C optimum design.

gas inlet of 30.5 cm ID and a throat diameter of 12.7 cm ID. The liquor requirements are 123 ℓ/min, which corresponds to a liquid-to-gas ratio f 2 ℓ/m³. A self-priming centrifugal pump giving an operating flow of 132 ℓ/min at 2.5 kg/cm² pressure is provided for this purpose. The pump inlet is fed from the cooling tower sump and PVC piping is specified for both suction and pressure sides of the piping.

The second section of the scrubbing unit is a tube bank entrainment separator with a cut diameter of 13 μm and a designed pressure drop across the unit of 0.8 cm W.C.

The inlet size distribution of the drops to the entrainment separator was approximated using the Nukiyama and Tanasawa correlation:

$$d_s = \frac{50}{u_G \text{ (cm/sec)}} + 92 \left(\frac{Q_L}{Q_G}\right)^{1.5} \qquad (8\text{-}1)$$

where d_s = Sauter mean diameter of drops, cm
u_G = air velocity relative to drops, cm/sec
Q_L = water flow rate m³/sec
Q_G = air flow rate m³/sec

Using equation 8-1 the mean Sauter diameter of the drops was estimated to 163 μm. As discussed by Calvert et al. (1975), the Sauter mean diameter is typically 70% to 90% of the mass median diameter. The conservative value of 70% of the mass median diameter was used. Thus, the mass median diameter was calculated to be 233 μm with a corresponding "σ_g" calculated to be 2.3.

The design of the entrainment separator was based on an inlet entrainment of 2,200 cm³/DNm³, calculated from a L/G ratio of 2 ℓ/m³ and specific gravity of 1.1 g/cm³. The minimum outlet from the entrainment separator was set at 0.01 g/DNm³ with a corresponding entrainment of 0.90 cm³/DNm³. The cumulative entrainment was plotted versus drop diameter, and the cut diameter was approximated to be 13 μm. Figure 8-7 gives the cumulative entrainment as a function of drop diameter.

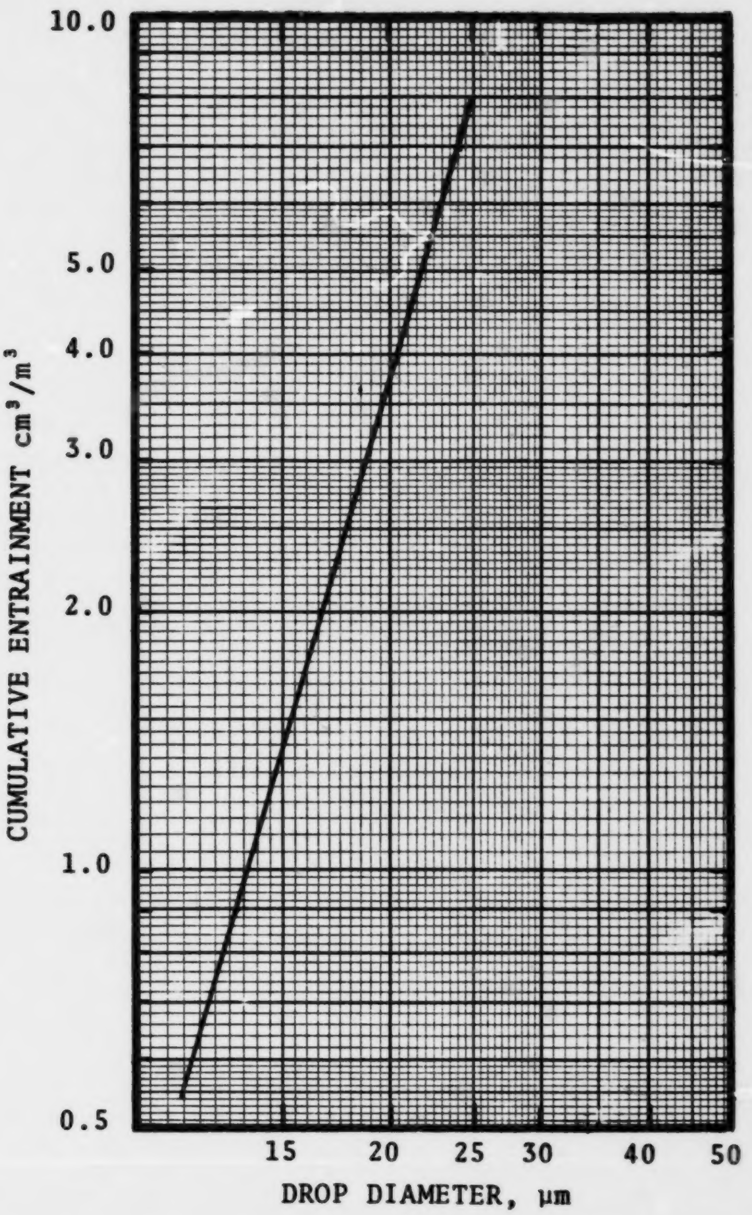

Figure 8-7. Assumed cumulative scrubber entrainment versus drop diameter for optimum system.

Physically, the entrainment separator (see Figure 8-6) consists of 6 rows of 1.9 cm diameter PVC tubing with a center-to-center spacing of 2.9 cm. The expected velocity through the rectangular orifice is about 13 m/sec with a corresponding pressure drop of 0.8 cm W.C.

The entrainment separator is oriented with the tubes running in the vertical direction and enclosed in a 35cm x 35cm x 35cm housing. The unit is provided with a drain which flows to the cooling tower sump for recirculation to the scrubber.

Cooling Tower

The purpose of the cooling tower is to reduce the temperature of the liquor from the condenser at a flow rate of 736 ℓ/min from about 49°C to 32°C. This is accomplished in a mechanical induced draft cooling tower by means of evaporative cooling. An induced draft of ambient air is moved through the unit by a fan located at the top. The liquor flow is introduced at the top and flows down the fill area (see Figure 8-8).

A spray-type cooling tower was used in the demonstration plant because of concern for the fouling of a filled cooling tower if it were used. Experience showed that solids deposition in tanks and wall surfaces of the cooling tower was no problem. Any deposits could be easily washed off. The spray-type tower does have the disadvantages of requiring a higher pressure pump and a more efficient "drift" entrainment separator than a filled tower.

The total cooling requirements of the cooling tower is approximately 880 kJ/s (50,000 BTU/min). The liquor flow rate is 736 ℓ/min, for which a self-priming centrifugal pump with 2.5 kg/cm^2 head is specified.

The cooling tower is so designed to limit the entrainment to 0.006% of the circulating liquor rate. This is approximately 0.010 gram of emission per DNm^3 of flue gas through the scrubber, with the result that the total emission from the system is kept below 0.1 g/DNm^3.

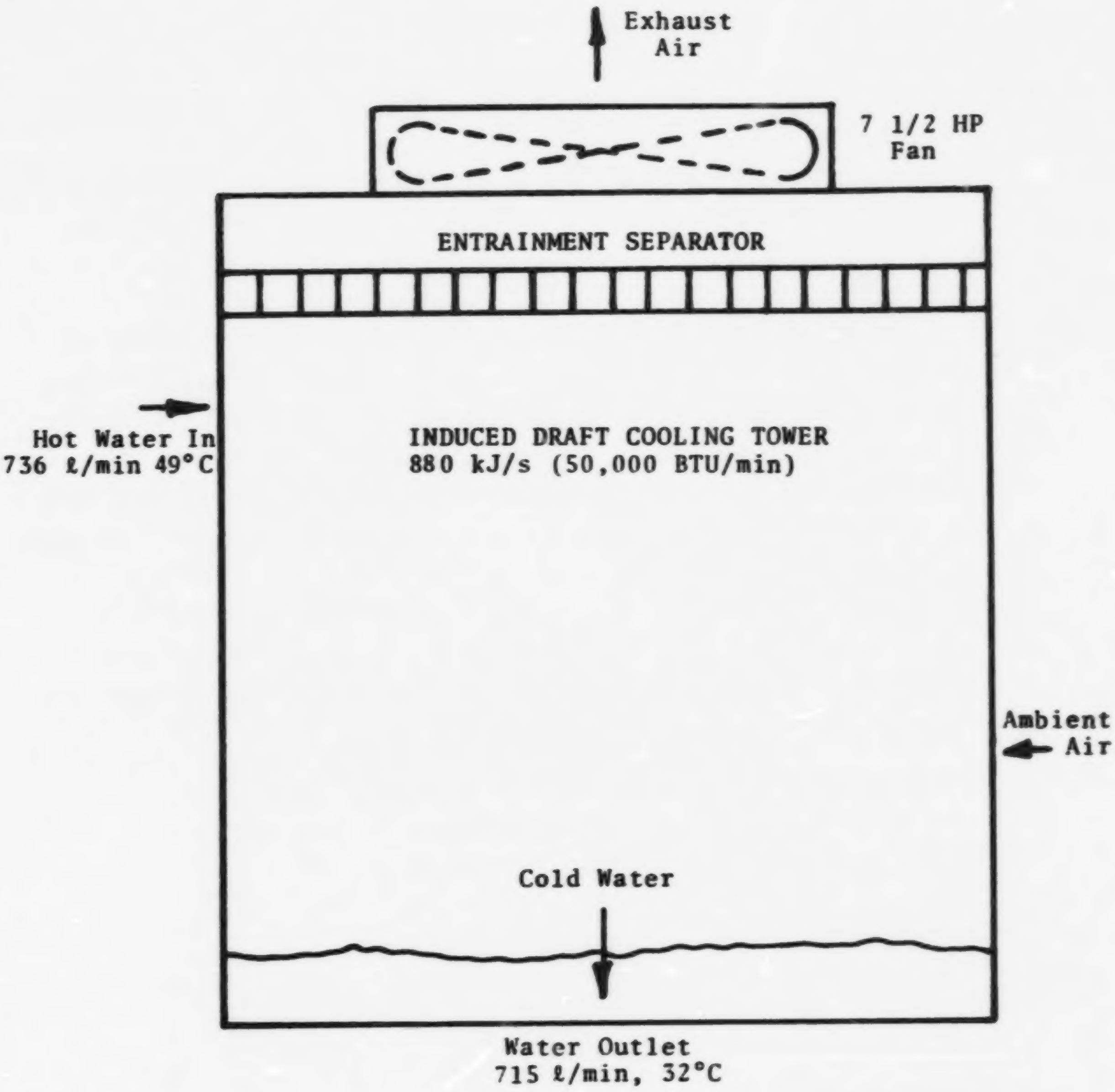
Exhaust Air
7 1/2 HP Fan
ENTRAINMENT SEPARATOR
Hot Water In
736 ℓ/min 49°C
INDUCED DRAFT COOLING TOWER
880 kJ/s (50,000 BTU/min)
Ambient Air
Cold Water
Water Outlet
715 ℓ/min, 32°C

Figure 8-8. Cooling tower of F/C optimum design at metals recovery furnace.

COST OF OPTIMUM SYSTEM

This section discusses the economic aspects of F/C scrubbing by estimating the capital and operating cost of an F/C scrubbing unit at the metals recovery furnace. The economic data are based on the optimum design as presented in the previous section and assumes an overall efficiency of 95% over quite unfavorable particulate conditions ($d_{pg} = 0.75$ μmA and $\sigma_g = 2.5$).

Capital Cost

The capital cost of an F/C scrubber unit would consist of total equipment cost and other direct cost such as installation, piping, electrical, etc. along with indirect costs such as engineering, construction overhead, contingencies, etc. The total equipment costs are based on quoted prices while the other direct and indirect costs have been estimated using ratio factors based on delivered-equipment cost. (Peters et al., 1968)

The detailed equipment costs are presented in Table 8-3 and the other direct and indirect costs are given in Table 8-4. In summary the following costs are estimated for the optimum F/C scrubber at the metals recovery furnace:

Direct Costs		
Equipment	$ 25,290	
Piping, Instruments, etc.	51,084	
		$ 76,374
Indirect Costs		
Engineering, contingencies, etc.	34,647	
		34,647
Total capital investment		$111,021

Operating Costs

The operating cost for the optimum design consists of the annual cost of utilities (power and water), raw materials, and maintenance. The computed costs are summarized in Table 8-5.

The utilities cost is based on both power and water usage. Power usage was estimated to be 42 kw-hr, 8 hours

TABLE 8-3. TOTAL EQUIPMENT COST ESTIMATE FOR F/C OPTIMUM DESIGN

EQUIPMENT	UNIT COST, $*	TOTAL COST, $
Venturi Scrubber		
Venturi Section	325	
Entrainment Separator	600	
Pump, Motor	770	
Total		1,695
Cooling Tower		
Cooling Tower, Fan, Motor, Sump	7,300	
Pump, Motor	1,590	
Total		8,890
Condenser		
Shell (fiberglass)	1,000	
Trays	950	
Tank	500	
Pump, Motor	1,590	
Total		4,040
Saturator		
Shell (Hastelloy)	2,500	
Tank	500	
Pump, Motor	1,065	
Safety Switches, etc.	1,000	
Total		5,065
Blower & Motor		
Blower	4,515	
Motor	1,085	
Total		5,600
TOTAL EQUIPMENT COST		25,290

*Cost based on 4th quarter, 1976.

TABLE 8-4. DIRECT AND INDIRECT COST ESTIMATE FOR F/C OPTIMUM DESIGN

TYPE OF COST	RATIO	COST, $
Direct		
Equipment	1.00	25,290
Installation	0.47	11,886
Instruments	0.18	4,552
Piping, Ducting	0.66	16,690
Electrical	0.11	2,782
Site Preparation	0.10	2,529
Structural	0.50	12,645
TOTAL DIRECT COST	3.02	76,374
Indirect		
Engineering	0.33	8,346
Construction Overhead	0.41	10,369
Contractor Fee	0.21	5,310
Contingency	0.42	10,622
TOTAL INDIRECT COST	1.37	34,647
TOTAL CAPITAL INVESTMENT	4.39	111,021

TABLE 8-5. OPERATING COST OF OPTIMUM F/C DESIGN

TYPE OF COST	UNIT COST	COST
Maintenance	0.06 of total capital investment	6,660
Water Usage	$0.034/1,000 liters	180
Power	$0.045/kw-hr	4,520
Raw Materials	$12.25/100 kg	1,650
TOTAL ANNUAL OPERATING COST		$13,010

operation, 300 operating days per year. The water usage is approximately 17,780 ℓ/day, mainly due to evaporation and blowdown losses, and unit cost of water was based on $0.034/1,000 liters.

Raw material cost is mainly the use of sodium carbonate as the neutralizing agent. Based on the demonstration plant operation, approximately 45 kg/day is necessary at a cost of $12.25/ 100 kg. The maintenance cost was estimated as a ratio of 0.06 of the fixed capital investment.

The total annual cost of the F/C scrubber at the metal recovery furnace was calculated as the sum of the annual capital cost and the annual operating cost. The annual capital cost is based on a 10-year life and straight-line depreciation and calculated as $11,102. The annual operating cost as shown in Table 8-4 is estimated at $13,010. Thus, the total estimated annual cost of a F/C scrubber adds up to $24,112.

CONVENTIONAL SCRUBBER

For comparison with the F/C scrubbing system a conventional high energy system is considered below. It will be seen that conventional scrubbing would be impractical for no. 1 regular wire because of the excessively high pressure drop required. Thus, a comparison could not be made within the bounds of the design criteria but in order to illustrate the potential advantage of an F/C system the data are given for no. 1 regular and no. 1 premium wire burning control.

Any pollution control system on this source would have to reduce the acid gas emission rate as well as control the condensable particulates. Consequently, the high energy scrubber would have to include the same mass transfer capacity as the F/C system. The arguments in favor of using a saturator right at the stack in order to reduce the actual gas volumetric flow rate and temperature and to enable the use of FRP also apply to the conventional scrubber case.

The conventional scrubber system would have the same components as the F/C system except for the cooling tower and associated apparatus. The scrubber and sieve plate column tanks can be combined into one large tank. Thus, the flow sheet for the conventional scrubber will be similar to that for the F/C system.

In order to achieve the penetration of 0.05 on an inlet $d_{pg} = 0.75$ μmA and $\sigma_g = 2.5$, a pressure drop of 535 cm W.C. (210 in. W.C.) would be required. This would be an impractically high pressure drop for a fan and would involve operating at a suction pressure of 368 mm Hg absolute if an induced draft compressor were used.

Beside the high pressure drop, the fan for a conventional scrubber would have to treat a larger gas volume than the F/C scrubber fan. For example in this case, even if the fan had the same pressure drop the F/C fan would only require 61.5% as much power as the conventional. For comparison, the F/C system handles 69 Am^3/min at 36°C and a pressure drop of -138 cm W.C. The gas leaving a conventional scrubber would be at the adiabatic saturation condition corresponding to the inlet gas enthalpy so the fan would have to handle 112 Am^3/min at 73°C for a similar pressure drop of -138 cm W.C.

Equipment costs for a conventional high energy scrubber to control no. 1 regular wire emissions are estimated to be as shown in Table 8-6.

The estimated total annual cost for the F/C system to control no. 1 regular wire burning was given previously as $24,112. It is obvious that even if a conventional high energy scrubber could be made to operate at $\Delta P = 535$ cm W.C., it would not be worth doing.

Conventional Scrubber for No. 1 Premium Wire

A conventional scrubber could be operated to control the emissions from burning no. 1 premium wire at a high but practical pressure drop. The penetration required for no. 1 premium wire recovery is 0.12, based on an inlet particle loading of 0.68 g/DNm^3 and an outlet requirement of 0.08 g/DNm^3.

TABLE 8-6

HIGH ENERGY SCRUBBER COSTS FOR REGULAR NO. 1 WIRE

Venturi Scrubber (ΔP = 535 cm W.C., Q_L/Q_G = 2 ℓ/m^3)

Venturi Section (FRP)	$ 325
Entrainment separator (PVC and FRP)	600
Pump and motor	860
Sub-total	$ 1,785
Condenser (same as F/C)	4,038
Sieve plate column (same as F/C)	5,065
Blower (ficticious)	30,703
Motor (ficticious)	10,840
Total Equipment	52,431
Total Capital Investment	$230,172

Total annual costs of operating the 535 cm W.C. scrubber system would be as follows:

Capital cost, 10 years straight line depreciation	$23,020
Maintenance	13,810
Water	180
Raw Material	1,650
Power	39,400
Total Annual Cost	$78,060

The particle size distribution was taken as the same as for no. 1 regular wire recovery, i.e., $d_{pg} = 0.75\ \mu mA$ and $\sigma_g = 2.5$. An F/C scrubber system would need an overall pressure drop of 70 cm W.C. while a conventional scrubber would require 238 cm W.C. to give 12% penetration.

The main costs for the two systems are given in Table 8-7. It can be seen that F/C scrubbing to control no. 1 premium wire recovery would have an annual cost about 66% of that for conventional high energy scrubbing. As previously discussed, however, the system would have to be capable of controlling emissions from no. 1 regular wire in order to be commercially useful.

TABLE 8-7. COST COMPARISON FOR PREMIUM WIRE RECOVERY

Cost Item	Cost for F/C	Cost for Conventional
Venturi	$ 1,700	$ 1,790
Cooling Tower	8,900	0
Condenser	4,040	4,040
Saturator	5,060	5,060
Blower & Motor	3,790	14,450
Total Equipment	23,490	25,340
Total Capital Investment	$103,121	$111,242
Depreciation	$10,310	$11,125
Maintenance	6,185	6,675
Water	180	180
Raw Materials	1,650	1,650
Power	2,370	11,530
Total Annual Cost	$20,695	$31,160

CHAPTER 9

FUTURE RESEARCH RECOMMENDATIONS

In the course of this demonstration plant program there has been a considerable gain in our understanding of F/C scrubbing in addition to the general validation of the system in a practical setting. Some of the lessons learned have changed previous notions and point up the need for new information, while others reinforced our former perceptions of research needs.

Our concept of F/C scrubbing has been sharpened since this demonstration began. We now see the bare essentials of F/C scrubbing as follow:

1. The fine particle collection efficiency (fractional) due to diffusiophoresis will be about equal to 85% of the volume fraction of gas condensed, regardless of particle size and equipment type.

2. Thermophoretic deposition will add only a few percent to the particle collection efficiency by diffusiophoresis.

3. High efficiency fine particle collection must be accomplished by some mechanism other than flux force deposition. If the high efficiency is to be achieved at lower pressure drop (or energy input) than a conventional (no F/C) scrubber, there must be particle growth by water condensation. The condensation must occur before the gas enters the high efficiency section of the scrubber system.

Some of the future research needs discussed below are for the purpose of providing information related to the points above. Others of the needs are concerned with commercial operating systems and their accessory components. Progressing from the basic through the applied, our recommendations for future research are as discussed below.

Particle Growth

Laboratory research on particle growth is necessary to provide data which can be used in validating and/or revising the mathematical model. The experiments should be done with wettable and non-wettable particles in several types of bench-scale apparatus which incorporate contacting mechanisms typifying large scale equipment.

This experimental and analytical work is needed to clear up the present uncertainties about several interacting phenomena as represented in the mathematical model for particle growth. The points needing clarification are as follow:

1. The nucleation of condensation on the surface of insoluble particles may require some supersaturation of the gas, depending on the wettability of the surface. As presently set, the model accounts for condensation and growth when the saturation ratio is 1.0 or greater. It has been assumed that the supersaturation which occurs in the gas phase boundary layer close to the cold liquid surface when the bulk of the gas is just saturated (i.e., $s = 1.0$) might be sufficient to nucleate condensation on slightly wettable particles.

Because the degree and extent of the boundary layer supersaturation effect depends on the conditions of the gas and liquid, the geometry, and the hydrodynamics, there is no simple relationship defining the "effective" saturation ratio. As will be seen, it is also impossible to distinguish between the effects of the several phenomena which occur simultaneously during condensation scrubbing.

2. Liquid phase heat transfer coefficient has a pronounced effect on liquid surface temperature and, thereby, on heat and mass transfer and gas phase saturation ratio. There are large differences among heat transfer coefficients computed from various correlations given in the literature

for sieve plates and even larger differences between them and some experimental data from earlier studies of F/C scrubbing.

3. Gas phase heat and mass transfer coefficients are somewhat better defined than for the liquid phase in sieve plates but there is still appreciable uncertainty as to the gas flow patterns and the size and shape of the gas-liquid interface. These factors all have a bearing on the state of saturation and mixing of the gas and particles.

4. The rate of condensation from the gas depends on the temperature and vapor pressure differences between the phases and on the transfer coefficients. It also affects the fraction of total condensation which goes to the particles (i.e., "f_p") as predicted by the mathematical model.

5. The particle number concentration also influences "f_p", as computed from the model. The experimental data taken previously have not enabled very precise computation of number concentration, so the influence of this parameter has not been distinguishable from those of other parameters.

6. Soluble particles can cause condensation at saturation ratios less than 1.0 because the vapor pressure of water is lowered by the solute. The present demonstration plant source particles contained a large fraction of soluble material but the beneficial effect of this was neglected in predictions computed with the model.

Field Measurements

Field measurements of particle number concentration and growth characteristics for a number of important air pollution sources would provide the key information needed to assess the suitability of F/C scrubbing for the specific source. Apparatus of the same general size and nature as that used for making performance tests could be taken anywhere in the U.S. and operated by a 3-man crew.

By sampling the source plant effluent and measuring the particle size after condensation and growth, one has evaluated the combined effects of particle number concentration, solubility, wettability, and size distribution. Gas temperature and humidity effects will also be properly accounted for. Liquid temperature and cooling apparatus design will be the controllable parameters.

Once the measurements have been made and the aerodynamic diameter of the grown particles determined, it will be a routine matter to design a scrubber to give the appropriate particle collection efficiency. As mentioned early in this chapter, the diffusiophoretic deposition can be accounted for with a simple computation. Thus, the main outlines of an F/C scrubber system for a specific source could be established with a good degree of confidence on the basis of particle growth data.

The scale of the experiment should be based on a gas flow rate on the order of 0.1 m^3/min (3 CFM). This will give a balance between being large enough to minimize wall losses and small enough to require convenient sized accessories. The sampling system would be very similar in nature to the systems used for particle sampling and sizing in the plant.

A two or three-man crew could go to a plant site, set up the equipment, and make the measurements in about one week, exclusive of travel time. Special test conditions, measurements in a number of system variations, or the aquisition of other kinds of data could increase the time requirement.

By making the particle growth measurements in a number of plants representing the major sources which are apparently amenable to F/C scrubbing, one would obtain the essential data for making reliable process designs and cost estimates for controlling these sources by F/C scrubbing. Without this experimental measurement one can only speculate on the basis of several assumptions about the particles from a specific source and the resulting design and cost estimate will be very approximate.

Table 9-1, from Calvert et al. (1975), lists the major fine particle sources for the U.S.A. with the features that

Table 9-1. MAJOR INDUSTRIAL PARTICULATE SOURCES FOR WHICH F/C SCRUBBING IS ATTRACTIVE

NOTE: The following information was taken from the Midwest Research Institute Report (1970). The source number (Roman numeral) refers to its rank in the U.S. as an industrial particulate pollution source.

SOURCE	ANNUAL PRODUCTION	NET CONTROL FRACTION	EMISSIONS MKg/yr
IV. IRON AND STEEL			
A. Sinter Plants (Sintering process)	46,300,000 MKg of Sinter	0.90	46,300
B. Coke Manufacture			
1. By-Product	81,600,000 MKg of Coal	0	81,600
2. Pushing & Quenching	82,800,000 MKg of Coal	---	19,000
C. Blast Furnace	80,600,000 MKg of Iron	.99	52,600
D. Steel Furnaces			
1. Open Hearth	59,700,000 MKg of Steel	.40	306,000
2. Basic Oxygen	43,500,000 MKg of Steel	.99	9,000
3. Electric Arc	15,200,000 MKg of Steel	.78	16,300
E. Scarfing	118,800,000 MKg of Steel	.68	57,200
VI. FOREST PRODUCTS			
A. Wigwam Burners	24,900,000 MKg of Waste	0	120,000
B. Pulp Mills			
1. Kraft Process	22,000,000 MKg of Pulp		
a. Recovery Furnace		.91	149,000
b. Lime Kilns		.94	29,900
c. Dissolving Tanks		.30	38,100
2. Sulfite Process	2,300,000 MKg of Pulp		
(Recovery Furnace)	756,000 MKg of Pulp	.91	9,000
3. NSSC Process	3,200,000 MKg of Pulp		
a. Recovery Furnace	1,100,000 MKg of Pulp	.91	900
b. Fluid-Bed Reactor	470,000 MKg of Pulp	.70	38,100
4. Bark Boilers	---	---	74,400

TABLE 9-1 (Continued)

SOURCE		ANNUAL PRODUCTION	NET CONTROL FRACTION	EMISSIONS MKg/yr
VII.	LIME			
	A. Rotary Kilns	14,700,000 MKg of Lime	0.81	267,000
	B. Vertical Kilns	1,600,000 MKg of Lime	.39	3,600
VIII.	PRIMARY NONFERROUS METALS			
	A. Aluminum			
	1. Calcining of Hydroxide	5,300,000 MKg of Aluminum	.90	52,600
	2. Reduction Cells			
	a. H. S. Soderberg	730,000 MKg of Aluminum	.40	31,700
	b. V. S. Soderberg	640,000 MKg of Aluminum	.64	9,000
	c. Prebake	1,600,000 MKg of Aluminum	.64	18,100
	B. Copper			
	1. Roasting	520,000 MKg of Copper	.85	6,000
	2. Reverb. Furnace	1,300,000 MKg of Copper	.81	25,400
	3. Converters	1,300,000 MKg of Copper	.81	29,900
	C. Zinc			
	1. Roasting			
	a. Fluid-Bed	690,000 MKg of Zinc	.98	13,600
	b. Ropp, multi-hearth	138,000 MKg of Zinc	.85	3,600
	2. Sintering	560,000 MKg of Zinc	.95	2,700
	3. Distillation	560,000 MKg of Zinc	---	13,600
	D. Lead			
	1. Sintering	420,000 MKg of Lead	.86	15,400
	2. Blast Furnace	420,000 MKg of Lead	.83	9,000
	3. Dross Reverb. Furnace	420,000 MKg of Lead	.50	1,800
XI.	ASPHALT			
	A. Paving Material	228,000,000 MKg of Material		
	1. Dryers		.96	150,000
	2. Secondary Sources		.96	36,300

would be generally suited to F/C scrubbing. Given the particle growth data, one could prepare another table showing the costs of conventional and F/C scrubbing for attaining given levels of emission rate. The engineering design and analysis involved would be straightforward and based on existing knowledge and methodology.

Cooling Towers

Field studies of solids deposition on surfaces of various materials which could be used for cooling tower construction would give the most important piece of information needed in selecting the type of cooler to use. These tests would be done at the same sites as described in the previous section and could most efficiently be done concurrently with the particle characterization tests.

Prior concern over the possibility that solids deposition on cooling tower surfaces would lead to the heavy buildup of adherent scale led to studies of spray-type coolers. The spray coolers have their own drawbacks which are sufficiently serious that packed or filled cooling towers look attractive again. Experience with the demonstration plant cooling tower and observations of other systems in the field leads us to believe that in some systems solids deposition on plastic surfaces may cause no problems.

The cooling tower is an important part of F/C scrubbing and represents the major cost difference between F/C and conventional scrubbing for many applications. Therefore, the use of a standard commercial cooling tower would give the best combination of cost, reliability, and proven design features. Purchase and installation of a standard cooling tower are also routine matters which can be accomplished through many vendors.

The solids deposition test involves the simple process of pumping a scrubber liquor over pieces of various packing materials to simulate their exposure in a cooling tower. If scrubber liquor is not available some collected particulate material can be mixed with water in the proper concentration and used in a recirculating system.

The length of the test period will depend on the severity of the deposition problem, if any. Observation over a few days of continuous operation should enable a rough evaluation of the deposition characteristics. The experimental apparatus can be left running for days or weeks with only occasional attention. Thus, it could be set up at a plant and left in the care of plant personnel for an extended test. Alternatively, in some cases the particulate material can be shipped to the contractors laboratory and the tests performed there.

It would be most economical and convenient to carry out the solids deposition tests at the same time as particle growth measurements at a given plant. A three-man crew could set up the solids deposition experiment with no more than an additional day's time if they were already at the plant site.

Steam Injection

The use of steam injection into saturated gas is an attractive but insufficiently explored ramification of F/C scrubbing. A bench-scale laboratory study could yield the information needed to determine the optimum balance between the quantity of steam to inject and the amount of condensation by cooling. Engineering design studies followed by pilot tests should be done to identify the best way of generating steam inexpensively.

Data from previous studies indicated that fine particle collection efficiency was greater when a given amount of steam was introduced into the gas than when an equivalent quantity was condensed from the gas. (See Calvert, et al., 1975). The steam injection experiments were not made under the same conditions so the comparisons between them and F/C scrubbing with condensation only are not conclusive. However, the apparent benefit of steam injection is so large that further study is warranted.

The reason(s) for performance improvement by steam injection is (are) not known but can be hypothesized. If steam is mixed with saturated gas only a small fraction will condense, depending on gas temperature. Thus, a given quantity of steam (say, 0.05 g/g dry gas) will give less condensate than 0.05 g/g, yet the particle collection efficiency is higher than for just condensation of 0.05 g/g. The most persuasive explanation is that steam injection causes an extremely high saturation ratio in the vicinity of the injection nozzle and this enhances the nucleation of condensation. This mechanism should be more significant for insoluble particles than for soluble ones.

If it is possible to obtain a substantial benefit from injection without subsequent cooling of the gas, there will be a reduction of the liquor cooling cost. On the other side, there will be some cost for steam generation. It would be valuable to know what benefits could be obtained by using various proportions of steam injection and condensation and what the costs would be.

An experimental program of determining particle growth under a range of parameters would provide the information needed to predict scrubber performance. The experiments could be done on bench scale with gas flow rates on the order of 0.1 to 0.5 m^3/min. Soluble and insoluble particles should be studied at number concentrations ranging from $10^6/cm^3$ to $10^9/cm^3$.

Costs for steam generation should be determined by engineering analysis and design studies. Conventional and non-conventional waste heat boilers should be evaluated. Cooling costs can be based on existing technology.

Demonstration Plant

F/C scrubbing is highly suited to the control of fine particles from basic oxygen furnace (B.O.F.) emissions and a demonstration plant would be valuable. The B.O.F. emits gas at temperatures up to around 2,000°C, which is unusually high for a large volume source. The high gas enthalpy gives the opportunity to evaporate a lot of water and to obtain a high condensation ratio even with relatively hot scrubber water.

It is generally necessary to have a water-cooled hood over the B.O.F. vessel mouth in order to protect the ductwork and to reduce the gas temperature before quenching. There is great concern that the gas temperature be less than about 1,700°C when it is first contacted with water so that dissociation of water will not cause explosive mixtures of hydrogen and oxygen to form. Since steam can be generated in the water-cooled hood, which must be provided in any case, there is an opportunity to obtain steam at very low cost.

B.O.F. emissions contain a large percentage of fine particles, often running over 50 mass percent smaller than 1.0 μmA diameter. These emissions must be collected at fairly high efficiency. Thus, the criteria for amenability to F/C scrubbing are all satisfied by B.O.F. emissions.

Following the presently reported demonstration plant, a second F/C demonstration program has been initiated on a foundry cupola. The B.O.F. demonstration plant would make a reasonable extension of F/C scrubbing technology into extremes of temperature and magnitude.

REFERENCES

1. Calvert, S., J. Goldshmid, D. Leith, and D. Mehta. Scrubber Handbook. A.P.T., Inc., EPA Contract No CPA-70-95. NTIS No. PB 213-016. August, 1972.

2. Calvert, S., J. Goldshmid, D. Leith, and N. Jhaveri. Feasibility of Flux Force/Condensation Scrubbing for Fine Particulate Collection. A.P.T., Inc., EPA Contract No. 68-02-0256. NTIS No. PB 227-307. October, 1973.

3. Calvert, S., and N. Jhaveri. Flux Force/Condensation Scrubbing. J. Air Pollution Control Association. 24 (10): 947-951. October, 1974.

4. Calvert, S., N. Jhaveri, and T. Huisking. Study of Flux Force/Condensation Scrubbing of Fine Particles. A.P.T., Inc., EPA Contract No. 68-02-1082. August, 1975.

5. Calvert, S., and S. Yung. Study of Horizontal Spray Flux Force/Condensation Scrubber. A.P.T., Inc., EPA Contract No. 68-02-1328, Task No. 10. July, 1976.

6. Calvert. S., S. Yung, and J. Leung. Entrainment Separators for Scrubbers, Final Report, A.P.T., Inc. EPA Contract No. 68-02-0637. August, 1975.

7. Calvert, S., H.F. Barbarika, and S. Yung. Development of Superior Entrainment Separators. A.P.T., Inc., EPA Contract No. 68-02-2184. First Quarterly Progress Report. December, 1976. (Unpublished).

8. Handbook of Emissions, Effluents and Control Practices for Stationary Particulate Pollution Source. Midwest Research Institute. Report to NAPCA. Contract No. CPA 22-69-104. 1970

9. Peters, M.S., and K.D. Timmerhaus. Plant Design and Economics for Chemical Engineers. New York. McGraw Hill. 1968.

10. Taheri, M., and S. Calvert. Removal of Small Particles from Air by Foam in a Sieve-Plate Column. J. Air Pollution Control Association. 18: 240-245, 1968.

11. Whitmore, P.J.. Diffusiophoretic Under Turbulent Conditions, Ph.D. Thesis, University of British Columbia, 1976.

APPENDIX A

PROCESS DATA

TABLE A-1. PROCESS DATA
F/C SCRUBBER DEMONSTRATION *

Run No.	q'	Gas Flow	Gas Temperature			Liquid Flow Rate					Liquid Temp.	
	g/g	Am³/sec	°C			ℓ/sec					°C	
		G_2	T_2	T_3	T_4	L_1	L_2	L_3	L_4	L_5	T_{27}	T_{28}
1	0.15	0.76	600	65	31	1.1	8.7	8.6	8.6	1.1	34	26
2	0.14	0.80	592	65	27	1.2	8.8	8.8	8.8	1.1	25	22
3	0.13	0.91	548	58	22	1.2	8.8	8.8	8.8	1.1	26	20
4	0.12	0.80	592	61	28	1.1	8.8	8.8	8.8	1.1	29	23
5	0.10	0.80	598	58	28	1.1	8.8	8.8	8.8	1.1	29	23
6	0.12	0.78	493	60	26	1.1	8.8	8.8	8.8	0.57	27	23
7	0.14	0.80	573	62	23	0.95	8.8	8.8	8.8	0.57	29	22
8	0.19	0.55	570	66	18	0.82	8.8	8.8	8.8	0.57	24	18
9	0.24	0.57	600	69	20	0.82	8.8	8.8	8.8	0.57	27	20
10	0.11	0.87	600	81	25	0.70	8.2	8.2	8.2	0.57	35	23
11	0.24	0.87	715	95	25	0.67	8.8	8.1	8.8		35	35
12	0.13	0.87	725	83	31	1.0	8.8	7.8	8.8	1.1	44	30
13	0.16	0.87	680	79	31	0.95	8.8	7.8	8.8	1.1	44	30
14	0.22	0.90	727	87	32	0.90	8.8	7.4	8.8	1.1	47	31
15	0.18	0.82	725	85	27	0.85	8.8	7.1	7.9	1.1	39	26
16	0.13	0.80	760	88	31	0.85	8.8	7.1	7.9	1.1	46	30
17	0.18	0.80	780	93	33	0.83	8.8	7.2	7.7	1.1	47	29
18	0.28	0.82	792	86	32	0.83	8.8	7.0	7.7	1.1	47	33
19	0.29	0.87	743	85	33	0.83		6.9	7.1	1.1	46	28
20	0.28	0.88	770	87	36	0.83		6.9	7.1	1.1	47	30

* See Figure 5-1 for explanation of symbols.

Continued

TABLE A-1 (continued)

Run No.	q'	Gas Flow	Gas Temperature			Liquid Flow Rate					Liquid Temp.	
	g/g	Am³/sec	°C			ℓ/sec					°C	
		G_2	T_2	T_3	T_4	L_1	L_2	L_3	L_4	L_5	T_{27}	T_{28}
21	0.28	0.82	725	89	39	0.82	8.8	6.6	7.2	1.0	36	25
22	0.28	0.82	732	83	40	0.82	8.8	6.6	7.0	1.1	36	28
23	0.26	0.75	717	83	40	0.67	8.8	6.3	7.1	1.0	40	26
24	0.20	0.75	730	83	41	0.67	8.8	6.3	7.1	1.0	40	28
25	0.32	0.75	780	77	43	1.07	8.8	6.7	7.6	1.1	42	30
26	0.32	0.75	802	79	36	1.0	8.8	6.2	6.7	1.1	47	32
27	0.38	0.75	825	79	35	1.0	8.8	6.2	6.7	1.1	59	34
28	0.35	0.73	795	77	34	1.1	8.8	5.8	6.3	1.1	51	33
29	0.38	0.73	820	79	33	1.0	8.8	5.8	6.3	1.1	52	32
30	0.30	0.73	696	75	34	1.0	8.8	5.8	7.0	1.1	43	30
31	0.28	0.80	710	74	33	0.98	8.8	5.9	7.0	1.1	42	28
32	0.40	0.75	775	80	36	1.1	8.8	5.9	6.4	1.1	49	33
33	0.35	0.75	760	78	33	1.0	8.8	5.6	6.4	1.1	48	34
34	0.27	0.74	443	71	37		8.4	7.1	7.2	1.1	45	33
35	0.13	0.75	466	65	34	1.3	9.3	7.8	8.2	1.1	46	34
36	0.29	0.74	417	70	37	1.7	8.8	7.6	7.8	1.1	44	34
37	0.31	0.74	417	65	35	2.1	8.8	7.3	7.7	1.1	46	38
38	0.24	0.74	340	61	36	1.9	8.9	7.6	8.0	1.1	44	35
39	0.30	0.75	510	75	38	1.9	9.2	7.6	7.8	1.1	47	38
40	0.24	0.74	450	71	35	1.6	9.2	8.2	8.6	1.1	42	34

Continued

TABLE A-1 (continued)

Run No.	q' g/g	Gas Flow Am³/sec	Gas Temperature °C			Liquid Flow Rate ℓ/sec					Liquid Temp. °C	
		G_2	T_2/T_1*	T_3	T_4	L_1	L_2	L_3	L_4	L_5	T_{27}	T_{28}
41						1.6	9.1	8.2	8.3	1.1	45	36
42	0.21	0.74	328	68	33	1.7	8.8	8.1	7.8	1.3	40	32
43	0.22	0.73	360	66	27	1.7	8.9	8.1	7.9	1.3	39	30
44*	0.18	0.81	590	67	32	2.5	9.1	9.8	10.7	1.3	37	33
45	0.25	0.81	665	73	35	1.7	9.3	9.1	9.3	1.3	40	32
46	0.24	0.81	670	72	35	1.7	9.2	8.6	9.1	1.3	45	35
47	0.23	0.81	670	71	37	1.7	9.2	8.4	8.6	1.3	45	35
48	0.22	0.81	675	70	33	1.7	9.2	9.1	9.8	1.3	40	33
49	0.21	0.77	650	69	34	1.7	9.1	9.9	10.1	1.3	41	31
50	0.20	0.81	682	68	32	1.7	9.1		9.9	1.3	36	31
51	0.21	0.93	620	70	37	1.6	8.9	9.4	9.8	1.3	48	36
52	0.30	0.92	730	76	39	1.7	8.7	9.6	9.9	1.3	52	37
53	0.22	0.96	690	71	37	1.7	8.6	9.6	9.3	1.3	49	36
54	0.22	0.93	665	69	36	1.6	8.8	9.1	9.3	1.3	48	36
55	0.25	0.73	698	71	33	1.6	8.8	8.6	9.1	1.3	48	33
56	0.31	0.70	698	75	36	1.6	8.8	9.5	9.6	1.3	46	37
57	0.21	0.82	715	70	39	1.5	8.9	9.3	9.5	1.3	45	40
58	0.22	0.87	710	70	36	1.5	8.8	9.3	9.5	1.3	38	30
59	0.28	0.73	790	74	40	1.6	8.8	9.2	9.5	1.3	52	39
60	0.22	0.82	680	70	36	1.6	8.9	9.2	9.5	1.3	43	38

*T_1 value given instead of T_2 from run 44 on.

Continued

TABLE A-1 (continued)

Run No.	q' g/g	Gas Flow Am³/sec	Gas Temperature °C			Liquid Flow Rate ℓ/sec					Liquid Temp. °C	
		G_2	T_1	T_3	T_4	L_1	L_2	L_3	L_4	L_5	T_{27}	T_{28}
61	0.18	0.82	685	67	34	1.6	8.8	9.2	9.5	1.3	43	38
62	0.24	0.82	710	72	39	1.6	8.8	9.2	9.1	1.3	47	38
63	0.28	0.82	725	74	36	1.6	8.8	9.2	9.1	1.3	47	35
64	0.24	0.80	710	72	38	1.5	9.1	9.2	9.3	1.3	45	35
65	0.31	0.82	770	76	42	1.5	8.8	9.2	9.3	1.3	52	41
66	0.32	0.80	750	76	39	1.5	8.8	0.2	9.3	1.3	50	39
67	0.28	0.82	730	74	38	1.5	8.8	9.1	9.3	1.3	46	34
68	0.24	0.82	690	72	38	1.5	8.8	9.1	9.3	1.3	46	37
69	0.29	0.82	735	75	41	1.5	8.9	9.1	9.3	1.3	51	39
70	0.28	0.75	700	76	50	1.5	9.1	9.1	9.2	1.3	52	29
71	0.24	0.82	725	75	38	1.5	9.1	9.1	9.2	1.3	50	38
72	0.28	0.82	725	75	38	1.5	9.1	9.1	9.2	1.3		35
73	0.29	0.88	740	75	38	1.5	9.1	9.0	9.1	1.3	50	37
74	0.24	0.88	661	73	36	1.5	9.1	8.9	9.1	1.3	45	34
75	0.19	0.88	565	69	38	1.5	8.9	9.0	9.1	1.3	48	37
76	0.22	0.82	635	71	37	1.5	8.9	8.9	9.2	1.3	48	36
77	0.19	0.88	520	68	36	1.5	9.1	9.0	9.1	1.3	46	35
78	0.24	0.88	600	72	38	1.5	8.9	8.9	9.1	1.3	48	36

APPENDIX B

PARTICLE SIZE DATA

Table B-1. INLET & OUTLET SAMPLE PARTICLE DATA FOR RUN #3

IMPACTOR STAGE NUMBER	INLET		OUTLET	
	M_{cum} (mg/DNm³)	d_{pc} (µmA)	M_{cum} (mg/DNm³)	d_{pc} (µmA)
Precutter	89.0	6.4	23.9	6.0
1	89.0	15.8	22.3	17.2
2	74.9	11.7	20.8	12.7
3	72.6	7.23	20.8	7.83
4	70.3	2.94	20.8	2.83
5	65.6	1.47	20.8	1.47
6	60.9	1.04	20.0	0.77
7	53.9	0.66	18.5	0.49
Filter	37.5		11.5	
Sample Volume (DNm³)	0.080		0.131	

Table B-2. INLET & OUTLET SAMPLE PARTICLE DATA FOR RUN #4 (SCRUBBER ONLY)

IMPACTOR STAGE NUMBER	INLET		OUTLET	
	M_{cum} (mg/DNm^3)	d_{pc} (μmA)	M_{cum} (mg/DNm^3)	d_{pc} (μmA)
Precutter	1910.0	6.4	338.0	6.0
1	1770.0	15.9	323.0	17.0
2	1760.0	11.7	323.0	12.5
3	1750.0	7.25	321.0	7.74
4	1740.0	2.62	320.0	2.80
5	1670.0	1.36	318.0	1.46
6	1130.0	0.71	301.0	0.76
7	498.0	0.46	161.0	0.49
Filter	257.0		57.9	
Sample Volume (DNm^3)	0.082		0.129	

Table B-3. INLET & OUTLET SAMPLE PARTICLE DATA FOR RUN #7 (SCRUBBER ONLY)

IMPACTOR STAGE NUMBER	INLET		OUTLET	
	M_{cum} (mg/DNm^3)	d_{pc} (μmA)	M_{cum} (mg/DNm^3)	d_{pc} (μmA)
Precutter	116.0	6.4	33.7	6.0
1	34.9	15.4	32.9	15.3
2	34.9	11.4	32.9	11.3
3	33.2	7.04	32.2	7.00
4	33.2	2.54	31.4	2.53
5	29.9	1.32	29.2	1.32
6	28.3	0.69	27.7	0.69
7	16.6	0.44	18.0	0.44
Filter				
Sample Volume (DNm^3)	0.059		0.108	

Table B-4. INLET & OUTLET SAMPLE PARTICLE DATA FOR RUN #42 (SCRUBBER ONLY)

IMPACTOR STAGE NUMBER	INLET		OUTLET	
	M_{cum} (mg/DNm^3)	d_{pc} (μmA)	M_{cum} (mg/DNm^3)	d_{pc} (μmA)
Precutter	395.0	5.8	121.0	6.0
1	393.0	14.3	120.0	14.9
2	341.0	10.6	120.0	11.0
3	340.0	6.52	116.0	6.82
4	336.0	2.36	113.0	2.47
5	328.0	1.23	112.0	1.28
6	309.0	0.64	107.0	0.67
7	224.0	0.41	72.4	0.43
Filter	94.0		27.4	
Sample Volume (DNm^3)	0.088		0.160	

Table B-5. INLET & OUTLET SAMPLE PARTICLE DATA FOR RUN #43 (SCRUBBER ONLY)

IMPACTOR STAGE NUMBER	INLET		OUTLET	
	M_{cum} (mg/DNm^3)	d_{pc} (μmA)	M_{cum} (mg/DNm^3)	d_{pc} (μmA)
Precutter	274.0	5.8	106.0	6.0
1	273.0	14.1	105.0	15.0
2	240.0	10.4	101.0	11.1
3	235.0	6.44	97.0	6.86
4	229.0	2.33	93.3	2.48
5	221.0	1.21	89.5	1.29
6	203.0	0.63	82.6	0.67
7	153.0	0.41	57.6	0.43
Filter	51.0		19.4	
Sample Volume (DNm^3)	0.086		0.160	

Table B-6. INLET & OUTLET SAMPLE PARTICLE DATA FOR RUN #56

IMPACTOR STAGE NUMBER	INLET		OUTLET	
	M_{cum} (mg/DNm^3)	d_{pc} (μmA)	M_{cum} (mg/DNm^3)	d_{pc} (μmA)
Precutter	1170.0	5.3	48.4	6.0
1	647.0	12.9	40.1	15.0
2	618.0	9.53	40.1	11.1
3	577.0	5.88	39.5	6.86
4	515.0	2.39	38.8	2.48
5	368.0	1.20	36.3	1.29
6	294.0	0.85	33.7	0.67
7	274.0	0.53	28.6	0.43
Filter	141.0		15.3	
Sample Volume (DNm^3)	0.066		0.157	

Table B-7. INLET & OUTLET SAMPLE PARTICLE DATA FOR RUN #58

IMPACTOR STAGE NUMBER	INLET		OUTLET	
	M_{cum} (mg/DNm^3)	d_{pc} (μmA)	M_{cum} (mg/DNm^3)	d_{pc} (μmA)
Precutter	829.0	6.7	30.2	6.2
1	802.0	16.5	30.2	15.5
2	688.0	12.2	30.2	11.4
3	529.0	7.54	30.2	7.06
4	472.0	3.06	30.2	2.55
5	263.0	1.54	30.2	1.33
6	192.0	1.09	29.8	0.69
7	157.0	0.68	27.0	0.44
Filter	124.0		16.5	
Sample Volume (DNm^3)	0.085		0.249	

Table B-8. INLET & OUTLET SAMPLE PARTICLE DATA FOR RUN #59

IMPACTOR STAGE NUMBER	INLET		OUTLET	
	M_{cum} (mg/DNm^3)	d_{pc} (μmA)	M_{cum} (mg/DNm^3)	d_{pc} (μmA)
Precutter	1250.0	6.1	31.2	6.0
1	390.0	15.4	30.8	15.5
2	375.0	11.4	30.0	11.5
3	369.0	7.02	30.0	7.08
4	342.0	2.85	29.6	2.56
5	211.0	1.43	29.2	1.33
6	145.0	1.01	28.0	0.69
7	122.0	0.64	25.7	0.45
Filter	98.6		20.1	
Sample Volume (DNm^3)	0.052		0.253	

Table B-9. INLET & OUTLET SAMPLE PARTICLE DATA FOR RUN #61

IMPACTOR STAGE NUMBER	INLET		OUTLET	
	M_{cum} (mg/DNm^3)	d_{pc} (μmA)	M_{cum} (mg/DNm^3)	d_{pc} (μmA)
Precutter	886.0	5.1	53.3	6.0
1	306.0	12.9	53.3	15.5
2	277.0	9.57	53.3	11.5
3	273.0	5.91	53.3	7.10
4	252.0	2.40	53.3	2.56
5	122.0	1.20	53.0	1.34
6	79.1	0.85	52.6	0.69
7	58.2	0.54	48.0	0.45
Filter	38.8		31.2	
Sample Volume (DNm^3)	0.067		0.262	

Table B-10. INLET & OUTLET SAMPLE PARTICLE DATA FOR RUN #62

IMPACTOR STAGE NUMBER	INLET		OUTLET	
	M_{cum} (mg/DNm^3)	d_{pc} (µmA)	M_{cum} (mg/DNm^3)	d_{pc} (µmA)
Precutter 1 2 3 4 5 6 7 Filter	1150.0 505.0 463.0 446.0 395.0 217.0 137.0 103.0 69.2	5.3 13.0 9.62 5.94 2.15 1.12 0.58 0.37	51.7 32.4 32.0 32.0 31.6 30.8 29.2 25.3 16.2	6.0 15.4 11.4 7.04 2.54 1.32 0.69 0.44
Sample Volume (DNm^3)	0.065		0.253	

Table B-11. INLET & OUTLET SAMPLE PARTICLE DATA FOR RUN #64

IMPACTOR STAGE NUMBER	INLET		OUTLET	
	M_{cum} (mg/DNm^3)	d_{pc} (µmA)	M_{cum} (mg/DNm^3)	d_{pc} (µmA)
Precutter 1 2 3 4 5 6 7 Filter	2490.0 953.0 918.0 900.0 872.0 770.0 684.0 429.0 106.0	5.2 12.9 9.51 5.87 2.12 1.10 0.57 0.37	140.0 129.0 129.0 128.0 128.0 128.0 121.0 88.2 41.5	6.1 15.6 11.5 7.11 2.57 1.34 0.70 0.45
Sample Volume (DNm^3)	0.064		0.250	

Table B-12. INLET & OUTLET SAMPLE PARTICLE DATA FOR RUN #66

IMPACTOR STAGE NUMBER	INLET		OUTLET	
	M_{cum} (mg/DNm^3)	d_{pc} (µmA)	M_{cum} (mg/DNm^3)	d_{pc} (µmA)
Precutter 1 2 3 4 5 6 7 Filter	1250.0 588.0 561.0 545.0 473.0 337.0 212.0 129.0 65.0	5.2 12.9 9.51 5.87 2.12 1.10 0.57 0.37	48.2 48.2 46.6 43.8 41.0 38.6 35.0 30.1 22.1	6.1 15.5 11.4 7.06 2.55 1.33 0.69 0.45
Sample Volume (DNm^3)	0.063		0.249	

Table B-13. INLET & OUTLET SAMPLE PARTICLE DATA FOR RUN #69

IMPACTOR STAGE NUMBER	INLET		OUTLET	
	M_{cum} (mg/DNm^3)	d_{pc} (µmA)	M_{cum} (mg/DNm^3)	d_{pc} (µmA)
Precutter 1 2 3 4 5 6 7 Filter	701.0 399.0 386.0 380.0 354.0 260.0 181.0 157.0 52.0	5.3 13.1 9.66 5.96 2.15 1.12 0.58 0.38	77.1 75.1 74.7 74.7 74.2 73.4 71.8 61.7 35.3	6.1 15.4 11.4 7.04 2.5 1.3 0.69 0.44
Sample Volume (DNm^3)	0.062		0.246	

Table B-14. INLET & OUTLET SAMPLE PARTICLE DATA FOR RUN #71

IMPACTOR STAGE NUMBER	INLET		OUTLET	
	M_{cum} (mg/DNm³)	d_{pc} (μmA)	M_{cum} (mg/DNm³)	d_{pc} (μmA)
Precutter	1230.0	5.3		
1	784.0	12.9		
2	607.0	9.57		
3	528.0	5.91		
4	458.0	2.13		
5	268.0	1.11		
6	168.0	0.58		
7	73.4	0.37		
Filter	14.4			
Sample Volume (DNm³)	.063			

Table B-15. INLET & OUTLET SAMPLE PARTICLE DATA FOR RUN #72

IMPACTOR STAGE NUMBER	INLET		OUTLET	
	M_{cum} (mg/DNm³)	d_{pc} (μmA)	M_{cum} (mg/DNm³)	d_{pc} (μmA)
Precutter	969.0	5.2	80.7	6.0
1	786.0	12.9	64.2	15.3
2	698.0	9.51	63.4	11.3
3	569.0	5.87	63.4	7.00
4	549.0	2.12	63.4	2.53
5	440.0	1.10	63.4	1.32
6	354.0	0.57	63.4	0.69
7	237.0	0.37	58.3	0.44
Filter	124.0		33.5	
Sample Volume (DNm³)	0.064		0.254	

Table B-16. INLET & OUTLET SAMPLE PARTICLE DATA FOR RUN #73

IMPACTOR STAGE NUMBER	INLET		OUTLET	
	M_{cum} (mg/DNm³)	d_{pc} (μmA)	M_{cum} (mg/DNm³)	d_{pc} (μmA)
Precutter	1100.0	5.4	36.7	6.2
1	270.0	13.4	36.7	15.5
2	232.0	9.93	35.9	11.4
3	214.0	6.13	34.7	7.05
4	198.0	2.21	32.8	2.55
5	123.0	1.15	31.2	1.33
6	89.6	0.60	29.2	0.69
7	64.0	0.39	26.4	0.44
Filter	25.6		21.3	
Sample Volume (DNm³)	0.063		0.253	

Table B-17. INLET & OUTLET SAMPLE PARTICLE DATA FOR RUN #74

IMPACTOR STAGE NUMBER	INLET		OUTLET	
	M_{cum} (mg/DNm³)	d_{pc} (μmA)	M_{cum} (mg/DNm³)	d_{pc} (μmA)
Precutter	1140.0	5.4	49.0	6.1
1	405.0	13.2	48.6	15.5
2	359.0	9.75	48.2	11.5
3	339.0	6.02	47.4	7.09
4	311.0	2.17	45.8	2.56
5	257.0	1.13	45.8	1.33
6	216.0	0.59	44.7	0.69
7	150.0	0.38	40.0	0.45
Filter	57.2		24.5	
Sample Volume (DNm³)	0.065		0.253	

Table B-18. INLET & OUTLET SAMPLE PARTICLE DATA FOR RUN #75

IMPACTOR STAGE NUMBER	INLET		OUTLET	
	M_{cum} (mg/DNm³)	d_{pc} (µmA)	M_{cum} (mg/DNm³)	d_{pc} (µmA)
Precutter	1200.0	5.4	48.3	6.1
1	434.0	13.5	33.4	15.4
2	398.0	10.0	32.6	11.4
3	375.0	6.17	32.6	7.03
4	345.0	2.23	32.2	2.54
5	246.0	1.16	31.4	1.32
6	169.0	0.60	30.6	0.69
7	112.0	0.39	24.3	0.44
Filter	68.4		14.9	
Sample Volume (DNm³)	0.064		0.255	

Table B-19. INLET & OUTLET SAMPLE PARTICLE DATA FOR RUN #76

IMPACTOR STAGE NUMBER	INLET		OUTLET	
	M_{cum} (mg/DNm³)	d_{pc} (µmA)	M_{cum} (mg/DNm³)	d_{pc} (µmA)
Precutter	2240.0	5.5	36.0	6.0
1	575.0	13.5	31.7	15.4
2	413.0	9.95	31.3	11.4
3	378.0	6.14	30.9	7.05
4	334.0	2.22	30.5	2.55
5	198.0	1.16	30.1	1.32
6	143.0	0.60	29.3	0.69
7	97.3	0.39	25.7	0.44
Filter	70.6		18.6	
Sample Volume (DNm³)	0.064		0.253	

Table B-20. INLET & OUTLET SAMPLE PARTICLE DATA FOR RUN #77

IMPACTOR STAGE NUMBER	INLET		OUTLET	
	M_{cum} (mg/DNm³)	d_{pc} (µmA)	M_{cum} (mg/DNm³)	d_{pc} (µmA)
Precutter	763.0	5.4	50.5	6.0
1	276.0	13.4	33.1	15.4
2	265.0	9.91	30.8	11.4
3	253.0	6.12	30.0	7.04
4	237.0	2.21	29.6	2.54
5	173.0	1.15	28.8	1.32
6	126.0	0.60	28.4	0.69
7	92.1	0.30	24.9	0.44
Filter	68.7		15.4	
Sample Volume (DNm³)	0.064		0.253	

Table B-21. INLET & OUTLET SAMPLE PARTICLE DATA FOR RUN #78

IMPACTOR STAGE NUMBER	INLET		OUTLET	
	M_{cum} (mg/DNm³)	d_{pc} (µmA)	M_{cum} (mg/DNm³)	d_{pc} (µmA)
Precutter	1220.0	5.8	13.6	6.1
1	459.0	14.3	7.6	15.4
2	407.0	10.6	6.8	11.4
3	382.0	6.52	6.4	7.05
4	331.0	2.36	6.0	2.55
5	144.0	1.23	6.0	1.33
6	58.0	0.64	6.0	0.69
7	32.9	0.41	5.6	0.44
Filter	18.8		5.2	
Sample Volume (DNm³)	0.064		0.251	

APPENDIX C

PARTICLE SIZE DISTRIBUTION PLOTS

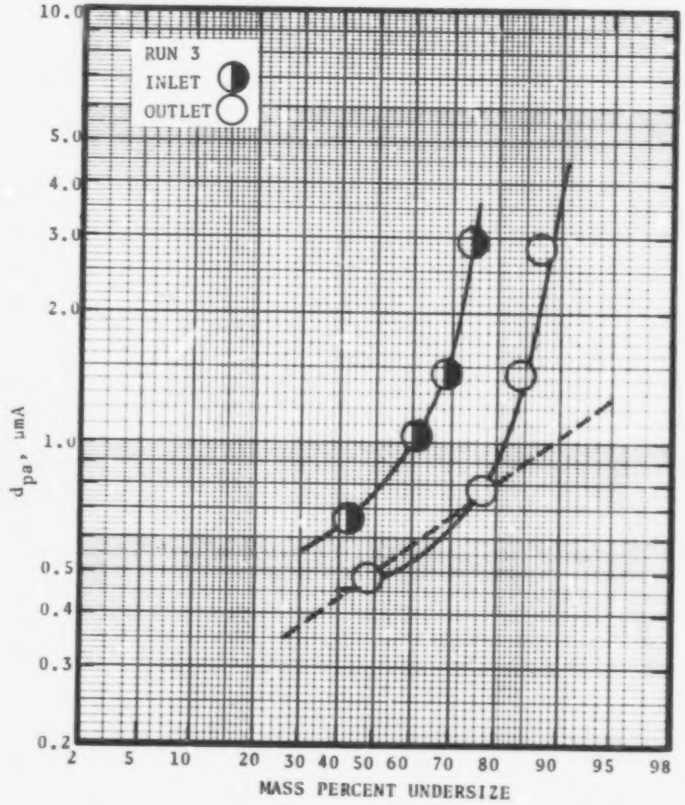

Figure C-1. Inlet and outlet size distributions for run 3.

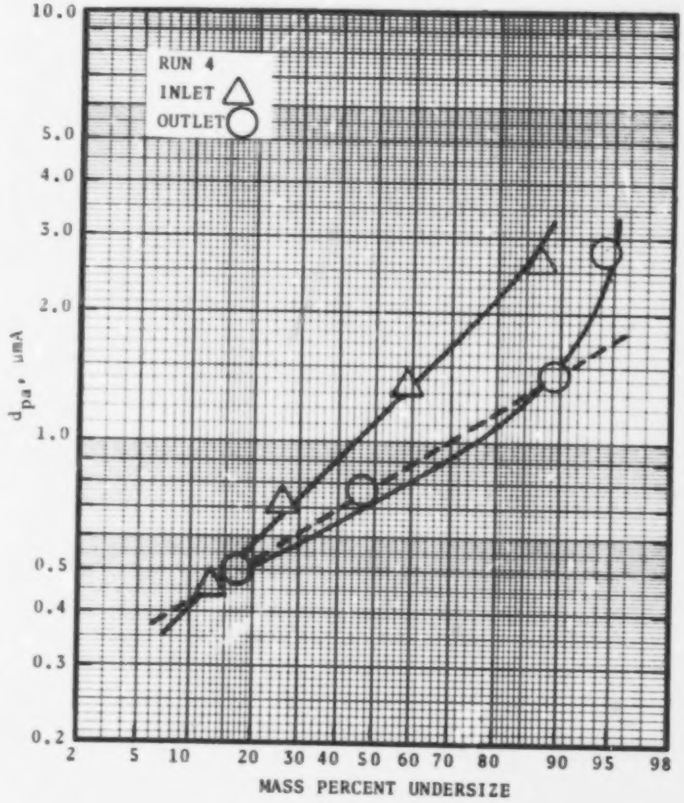

Figure C-2. Inlet and outlet size distribution for run 4 (scrubber only).

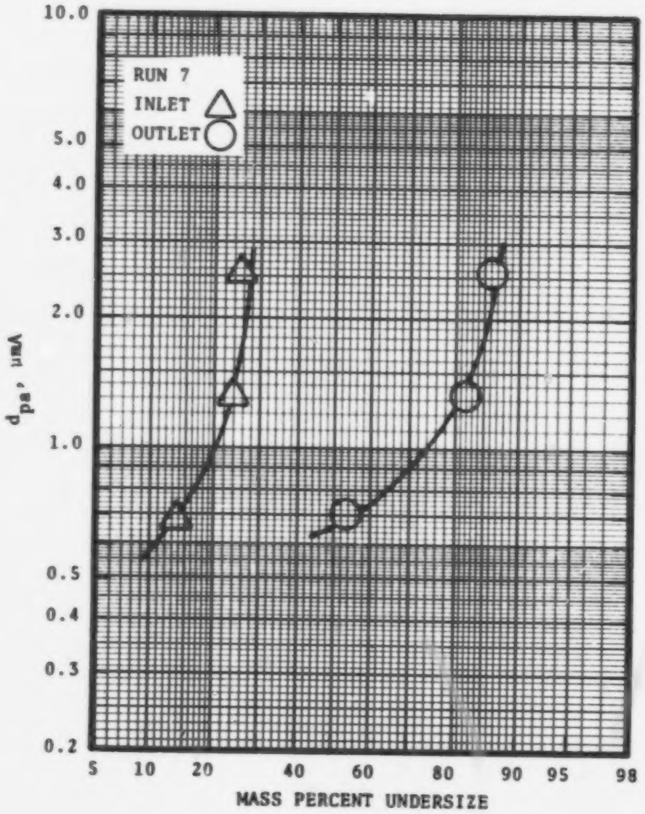

Figure C-3. Inlet and outlet size distributions for run 7.

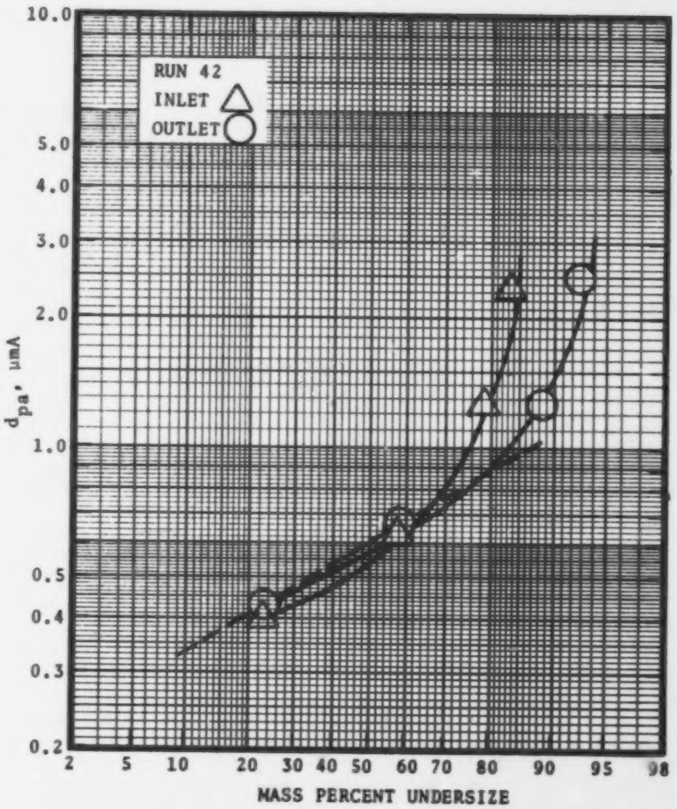

Figure C-4. Inlet and outlet size distribution for run 42 (scrubber only).

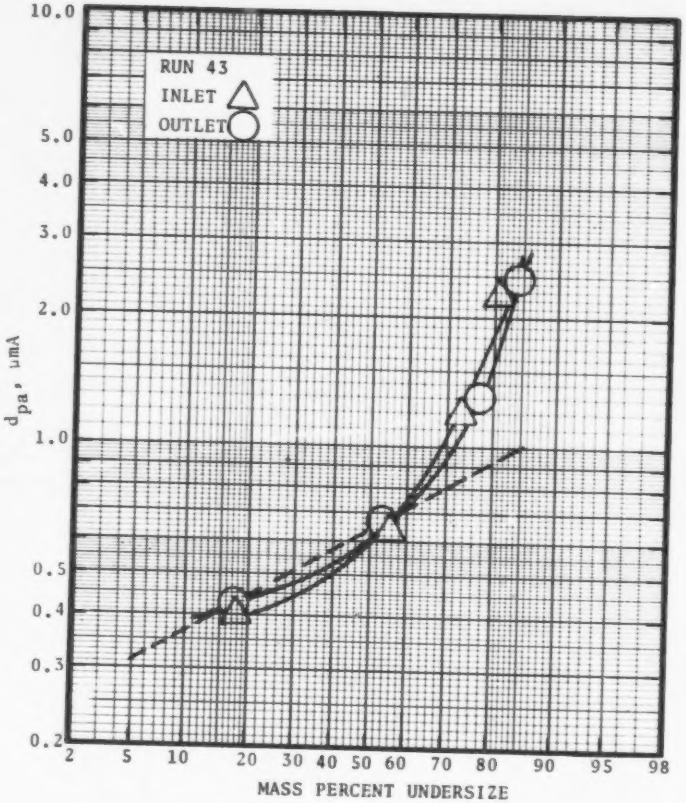

Figure C-5. Inlet and outlet size distributions for run 43 (scrubber only).

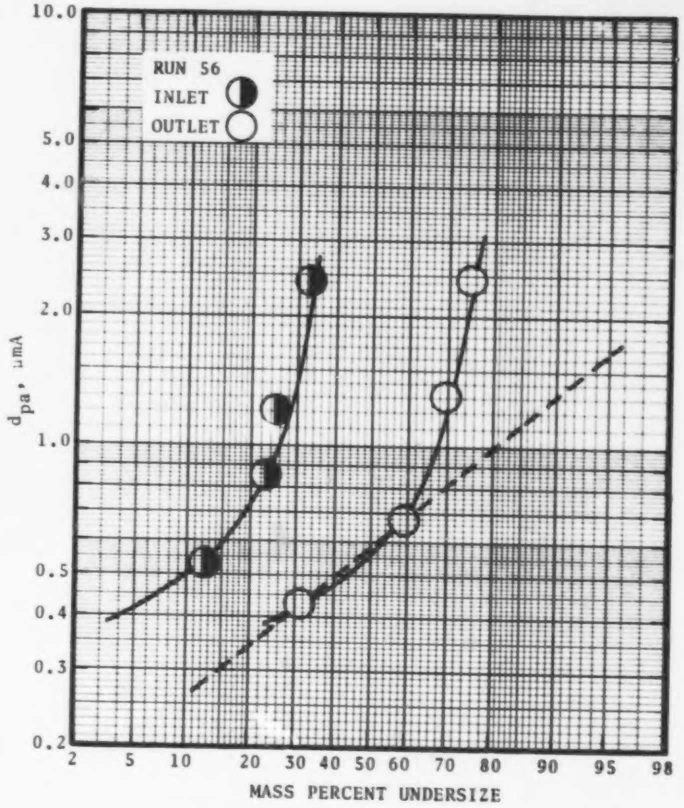

Figure C-6. Inlet and outlet size distributions for run 56.

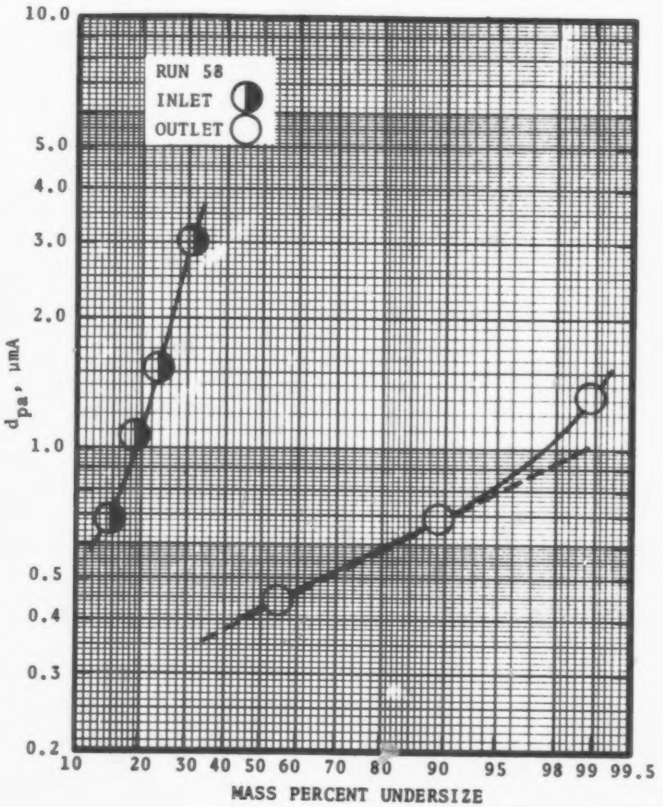

Figure C-7. Inlet and outlet size distributions for run 58.

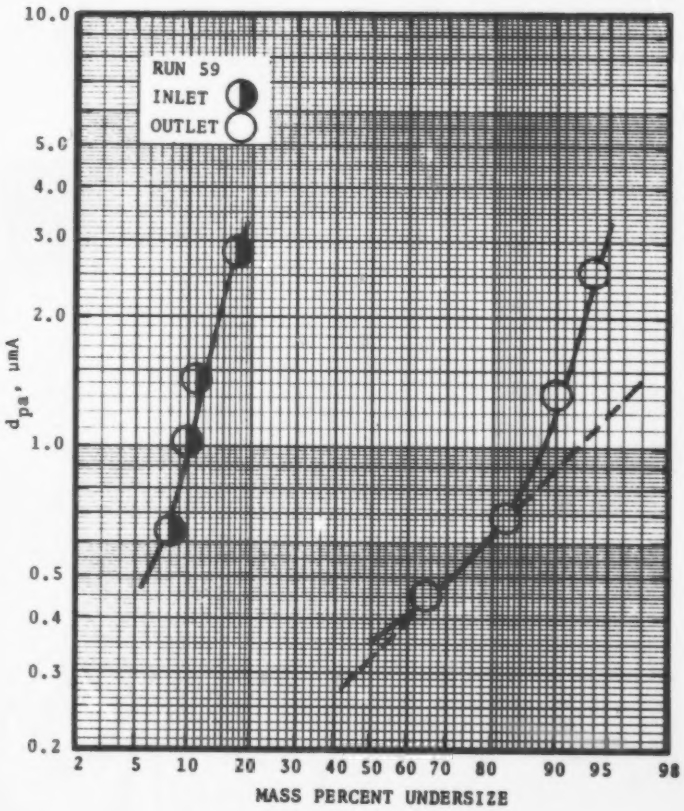

Figure C-8. Inlet and outlet size distributions for run 59.

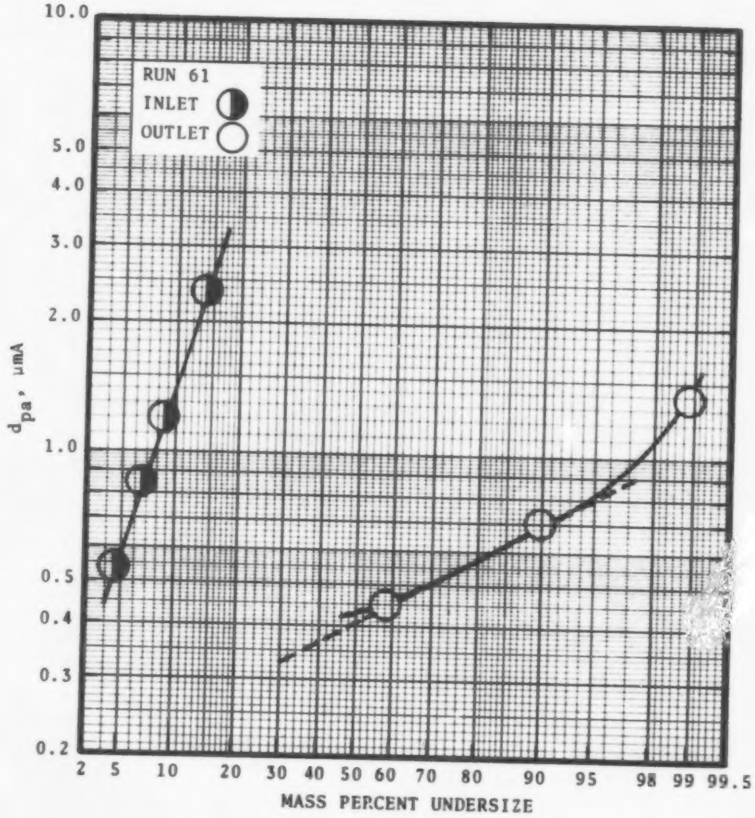

Figure C-9. Inlet and outlet size distribution for run 61.

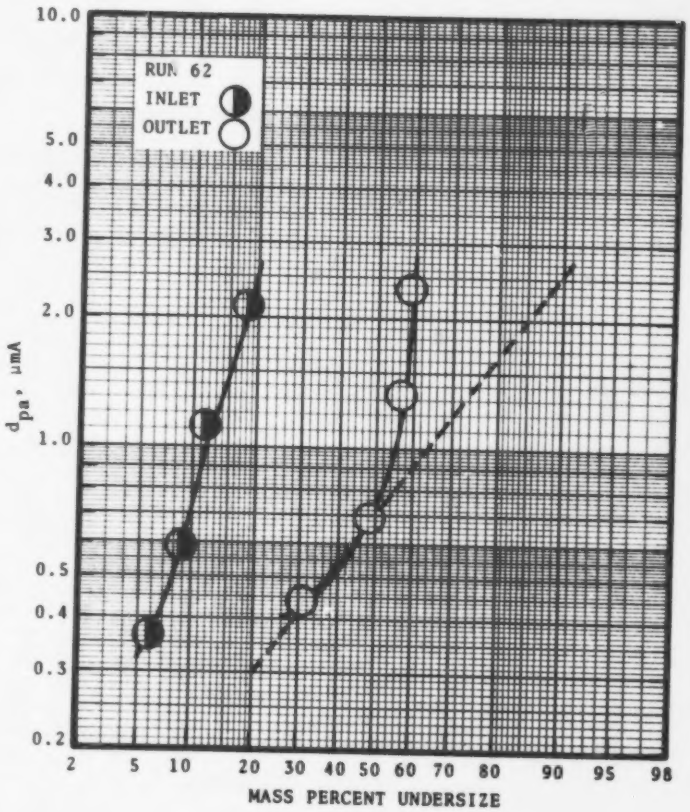

Figure C-10. Inlet and outlet size distributions for run 62.

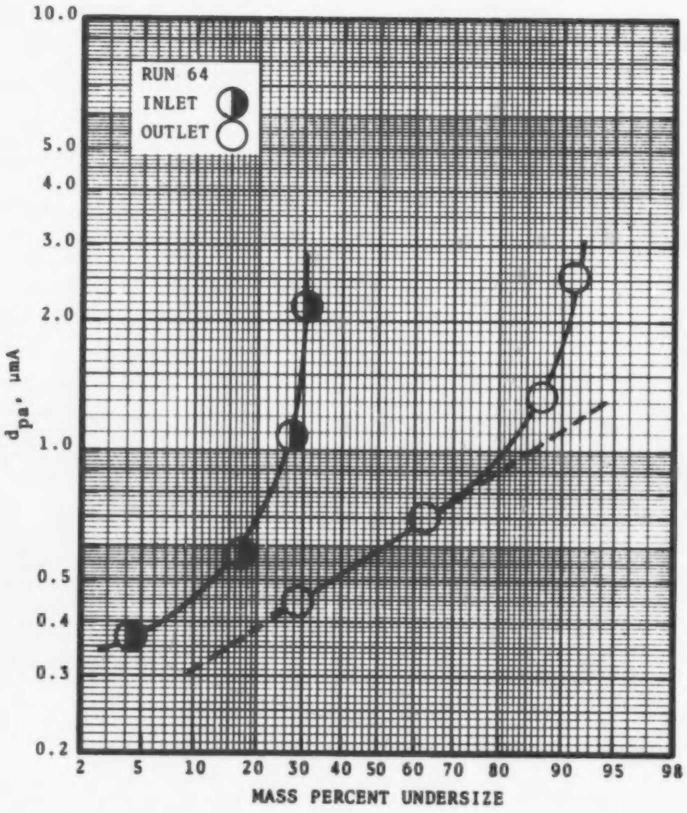

Figure C-11. Inlet and outlet size distributions for run 64.

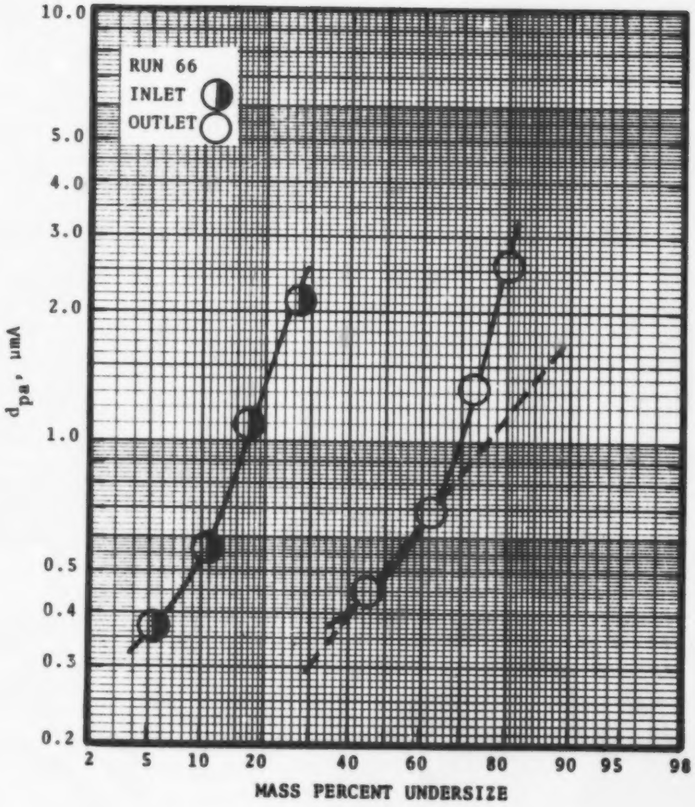

Figure C-12. Inlet and outlet size distribution for run 66.

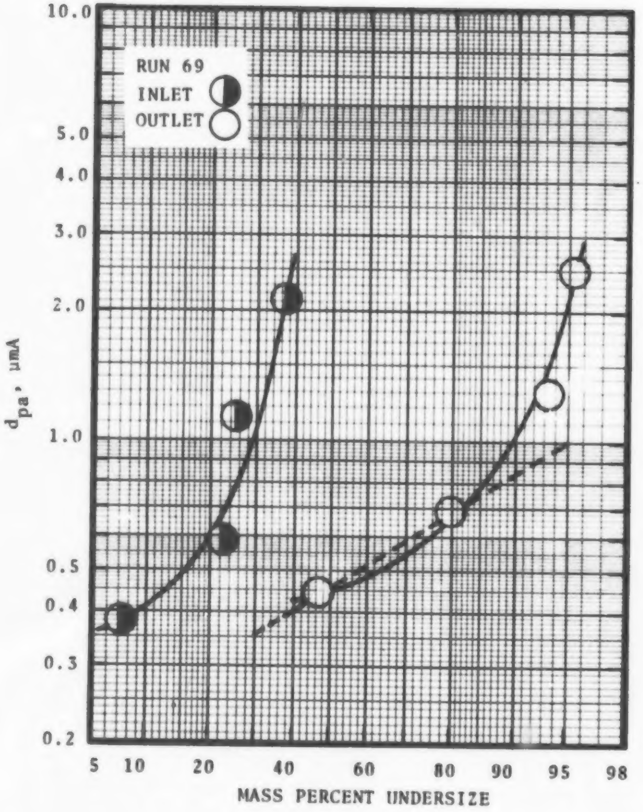

Figure C-13. Inlet and outlet size distribution for run 69.

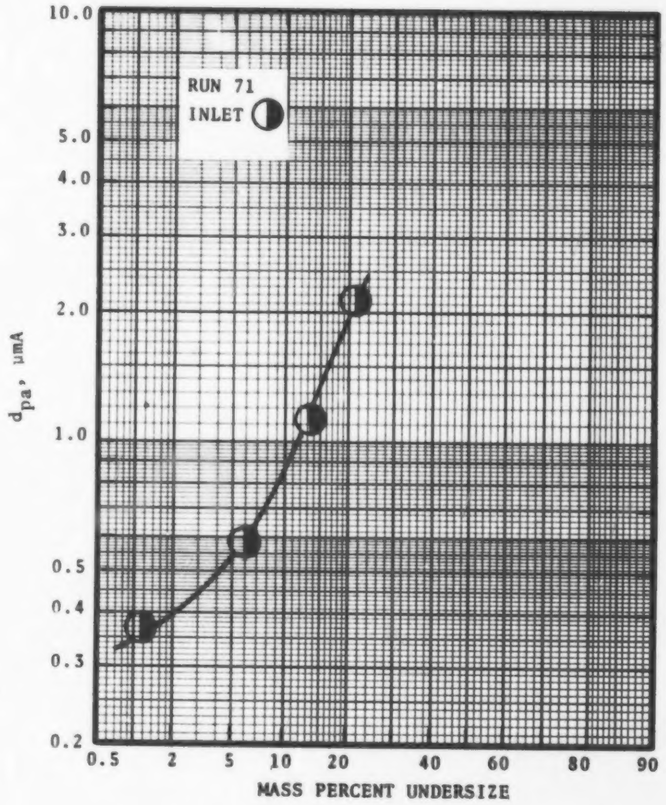

Figure C-14. Inlet size distribution for run 71.

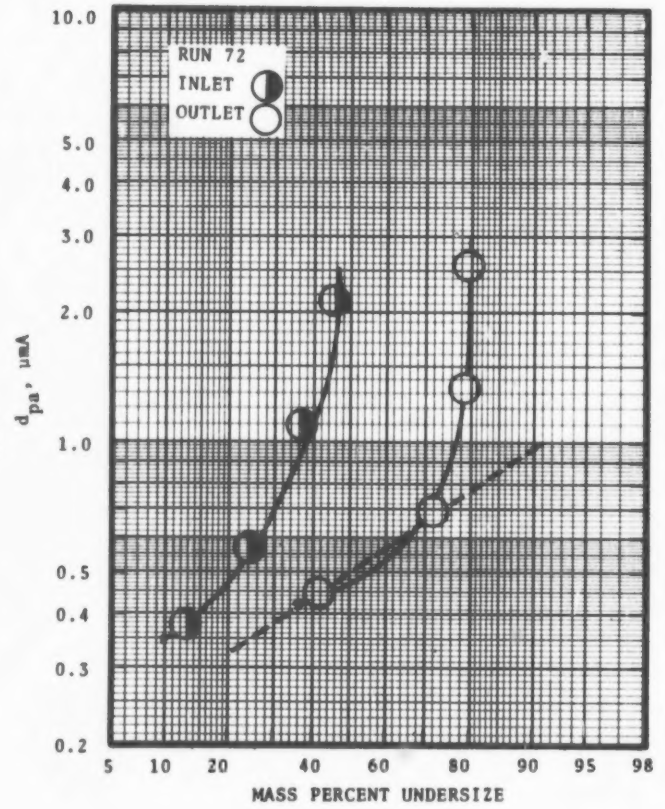

Figure C-15. Inlet and outlet size distribution for run 72.

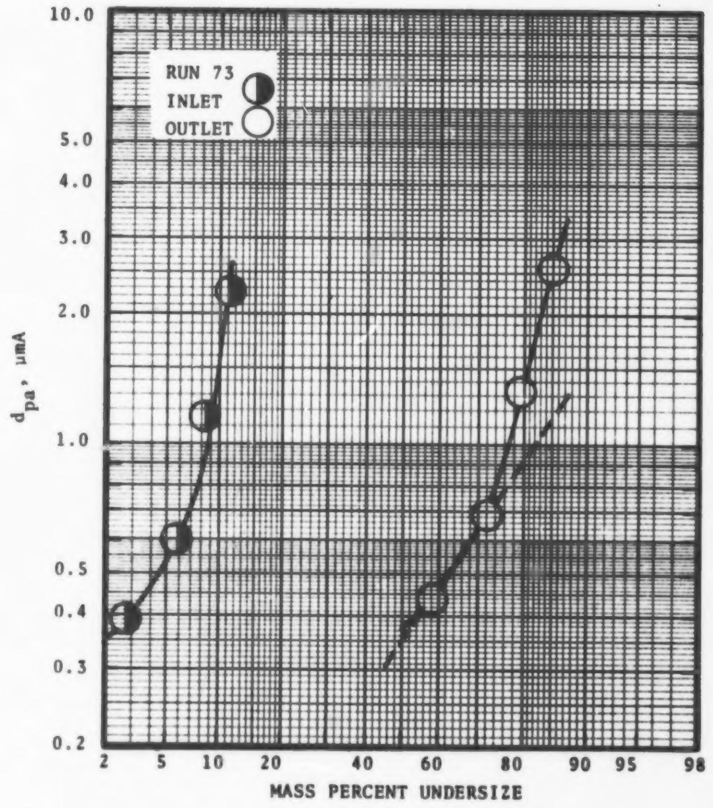

Figure C-16. Inlet and outlet size distribution for run 73.

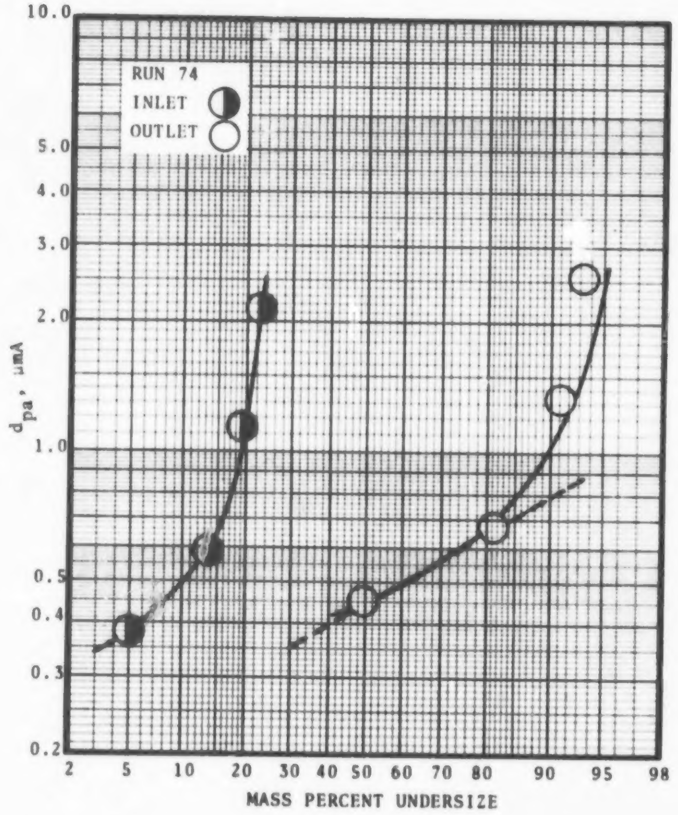

Figure C-17. Inlet and outlet size distribution for run 74.

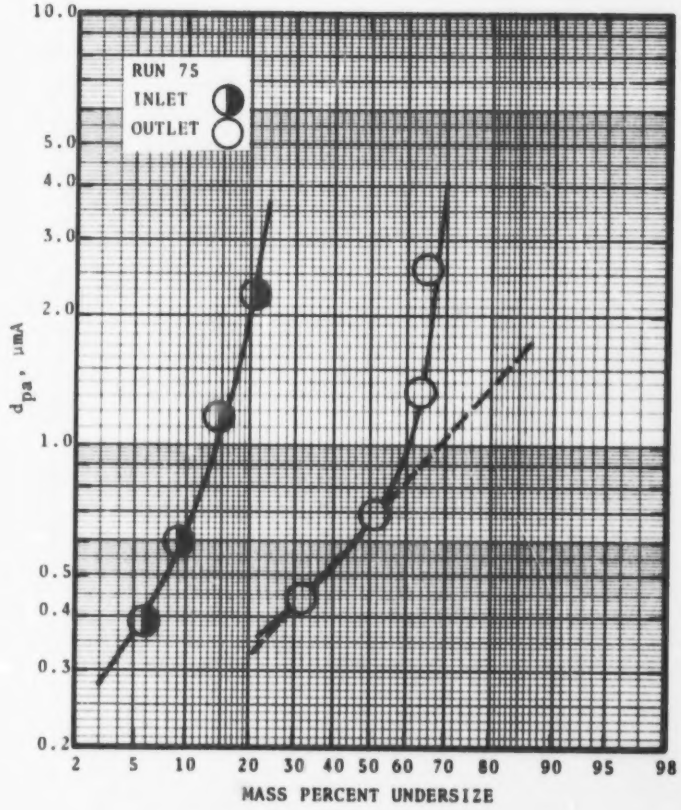

Figure C-18. Inlet and outlet size distributions for run 75.

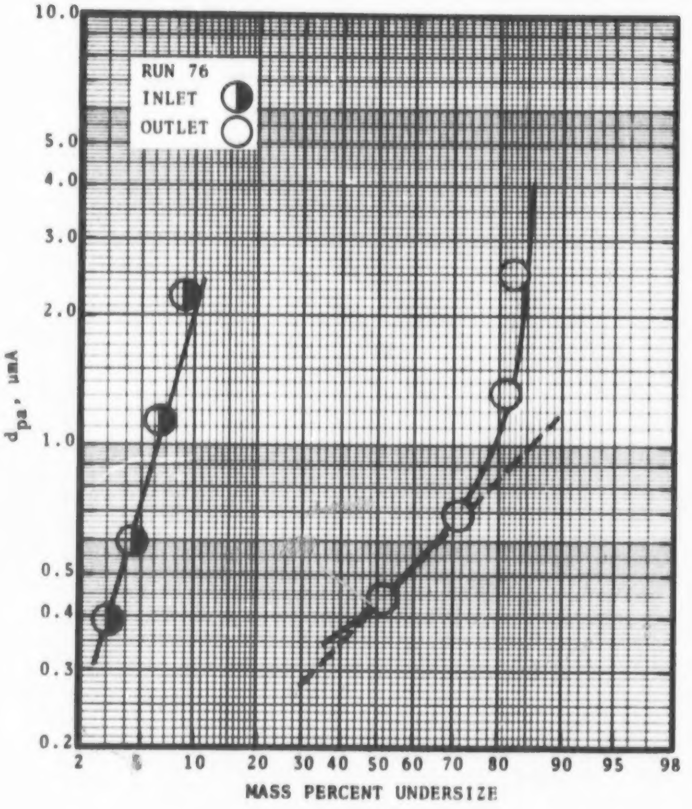

Figure C-19. Inlet and outlet size distributions for run 76.

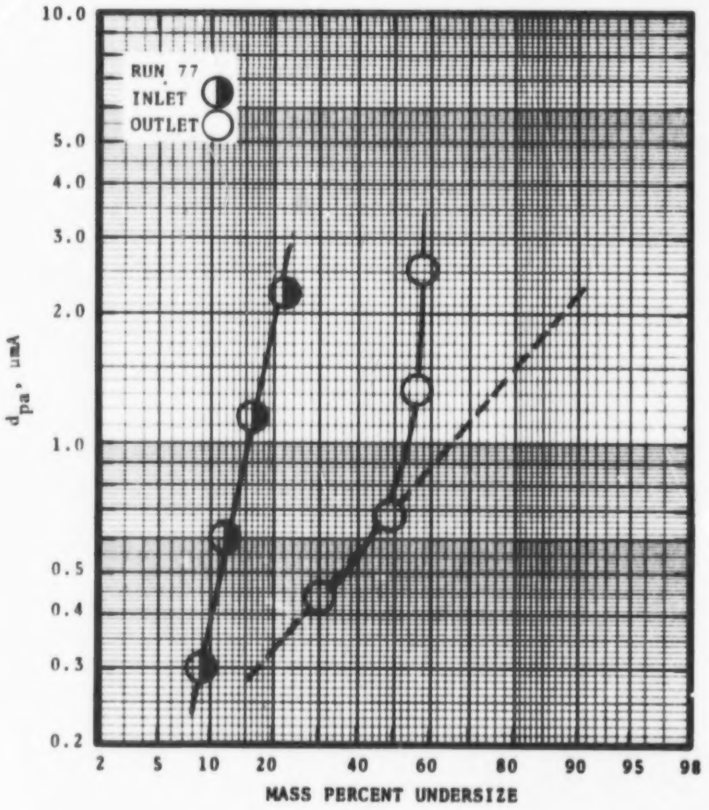

Figure C-20. Inlet and outlet size distribution for run 77.

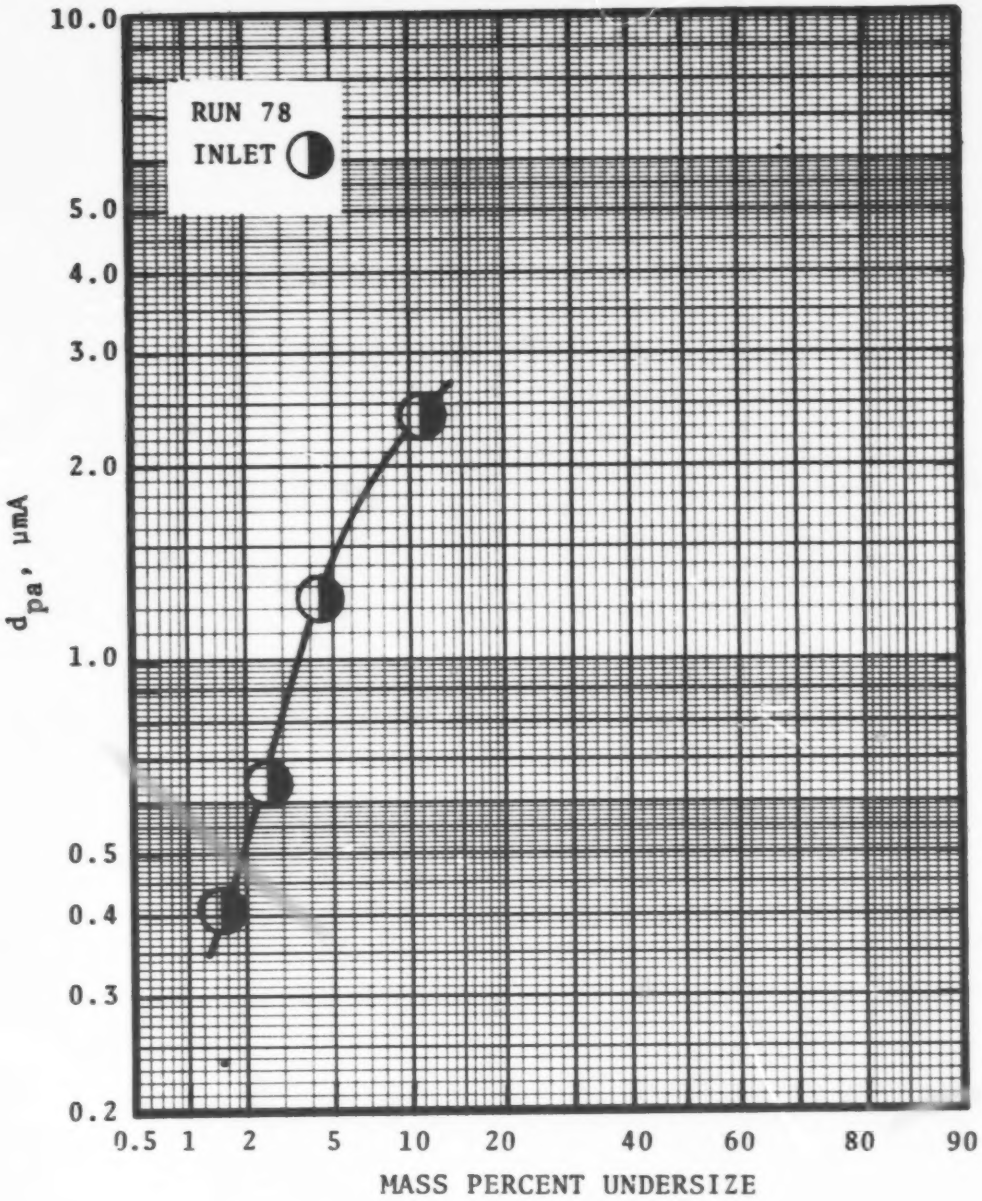

Figure C-21. Inlet size distribution for run 78.

APPENDIX D

IMPINGER DATA

TABLE D-1. IMPINGER DATA AND RESULTS

Run	Quencher Inlet			Scrubber Outlet			Pt
No.	Concentration mg/DNm^3	Cl^-	pH	Concentration mg/DNm^3	Cl^-	pH	%
1	110.0	10,000	1.7	85.2	120	5.6	77.5
2	132.0	10,000	1.3	19.1	300	13.3	14.5
3*	1,580.0	1,100	2.3	267.7	45	6.8	16.9
4*	N.A.			8.0	50	5.7	
5	"			24.1	8,000	2.4	
6	"			14.9	< 1	4.0	
7*	"			17.7	< 1	4.0	
8	"			2.1	< 1	4.2	
9	"			2.9	< 1	4.1	
10	"			0.6	< 1	3.3	
11	"			1.0	< 1	3.3	
12	"			13.8	39	3.2	
13	"			18.8	32	3.3	
14	"			12.7	< 1	4.2	
15	"			11.4	30	3.3	
16	"			18.1	39	3.3	
17	111.0	2,900	1.9	0	80	3.3	0
18	62.1	450	2.5	14.9	170	3.5	24.0
19	45.2	380	2.4	5.1	20	5.5	11.3
20	102.0	120	2.5	12.4	13	4.0	12.1
21	179.0	1,600	2.1	2.1	50	3.7	1.2
22	172.0	2,000	1.9	0.7	78	3.3	0.4

*Cascade impactor runs.

TABLE D-1. (continued)

Run	Quencher Inlet			Scrubber Outlet			Pt
No.	Concentration mg/DNa^3	Cl^-	pH	Concentration mg/DNm^3	Cl^-	pH	%
23	207.0	1,800	1.9	1.3	32	3.2	0.6
24	161.0	10,000	1.3	1.3	20	3.3	0.8
25	199.0	1,100	2.3	0	90	3.3	0
26	103.0	220	2.6	0	< 1	4.4	0
27	125.0	900	2.2	0	4	4.1	0
28	38.0	1,400	2.2	5.6	12	4.9	14.7
29	18.4	20	4.0	7.1	4	4.9	38.6
30	19.6	32	3.1	10.1	8	6.4	51.5
31	15.5	80	3.0	14.0	4	4.2	90.3
32	38.0	78	2.7	7.1	8	4.5	18.7
33	17.8	34	2.8	9.1	8	5.1	51.1
34	0	250	2.6	0	1	4.9	0
35	0	20	3.1	0	4	4.4	0
36	40.0	90	3.1	28.0	1	4.7	70.0
37	12.7	20	3.3	9.2	10	3.8	72.4
38	12.0	400	2.8	11.9	20	4.1	99.0
39	0	200	2.6	0	< 1	4.2	0
40	38.3	33	2.8	0	2	4.4	0
41	11.2	39	2.9	0	4	4.7	0
42*	N.A.			0	< 1	4.8	
43*	"			0.4	< 1	4.6	
44	154.5	500	2.4	38.4	8	3.9	24.8

*Cascade impactor runs.

TABLE D-1. (continued)

Run	Quencher Inlet			Scrubber Outlet			Pt
No.	Concentration mg/DNm³	Cl^-	pH	Concentration mg/DNm³	Cl^-	pH	%
45	** 111.0	20	2.9	53.3	1	4.1	48.2
46	** 98.2	25	2.9	14.9	1	4.2	15.2
47	** 103.0	240	2.5	1.0	< 1	3.8	1.0
48	** 103.0	180	2.8	0	55	4.2	0
49	** 101.0	470	2.3	4.5	14	3.7	4.4
50	** 171.0	280	2.4	4.5	20	4.1	2.6
51	** 76.7	120	2.9	0	13	3.5	0
52	** 26.5	180	2.5	0	8	4.2	0
53	** 4.9	125	2.8	0	18	4.1	0
54	** 66.2	310	2.3	12.0	15	4.2	18.1
55	** 131.0	2,100	1.9	6.9	9	4.0	5.3
56*	86.3	30	3.2	28.1	21	4.4	32.5
57	160.0	< 1	4.8	0	< 1	4.2	0
58*	0	100	2.4	0	9	4.2	0
59*	121.0	20	3.0	0	< 1	4.2	0

* Cascade impactor runs.

** Furnace outlet.

TABLE D-1. (continued)

Run	Quencher Inlet			Scrubber Outlet			Pt
No.	Concentration mg/DNm³	Cl^-	pH	Concentration mg/DNm³	Cl^-	pH	%
60	** 90.7	1,500	1.8	1.0	< 1	4.9	1.1
61*	0	6	3.7	0	< 1	4.4	0
62*	N.A.						
63	** 30.0	120	2.7	45.2	< 1	4.2	
64*	281.0	550	2.2	19.6	4	4.6	7.0
65	** 10.3	250	2.3	3.2	8	4.3	31.1
66*	8.1	500	2.7	0	< 1	4.7	0
67	0	40	3.3	0	< 1	4.6	0
68	** 10.7	200	2.6	8.4	30	3.5	78.5
69*	325.8	500	2.3	0	< 1	4.5	0
70	N.A.	120	2.6		2.5	4.4	
71*	363.4	250	2.4	0	20	5.1	
72*	364.0	260	2.2	0	10	5.2	0
73*	189.0	62	2.6	0	< 1	4.6	0
74*	33.8	200	2.3	0	10	4.2	0
75*	267.0	80	2.3	9.6	< 1	4.3	3.6
76*	269.0	70	2.4	3.2	< 1	4.5	1.2
77*	436.0	80	2.4	8.8	< 1	4.2	2.0
78*	20.3	40	2.8	38.4	< 1	4.7	

* Cascade impactor runs.

** Furnace outlet.

APPENDIX E

CALCULATION OF PARTICLE NUMBER CONCENTRATION FROM CASCADE IMPACTOR DATA

The F/C model for prediction of scrubber performance uses particle number concentration as one of its parameters. Data on particle size distribution by mass as taken with a cascade impactor can be used to compute the particle number concentration. The procedure used in this study to calculate particle count using size distribution data is summarized below.

Particle number concentration is related to mass concentration and the mass mean diameter by equation (E-1).

$$n = \frac{6\ c}{\pi\ \rho_p\ d_m{}^3} \tag{E-1}$$

where n = number concentration, number/DNcm³
c = mass concentration, g/DNcm³
ρ_p = particle density, g/cm³
d_m = mass mean diameter of particle, cm

The mass mean diameter is defined by:

$$d_m = \frac{\Sigma\ n_i\ d_i{}^3}{n} \tag{E-2}$$

where "i" represents an individual particle size. If the distribution of diameter is log normal over the whole range of sizes, the relationships between various mean diameter are simple. The mass mean diameter is related to the mass median (geometric mass mean) diameter by:

$$\ln d_m = \ln d_{pg} - 1.5 \ln \sigma_g^2 \tag{E-3}$$

Preceding page blank

where d_{pg} = mass median diameter, cm
σ_g = geometric standard deviation

In the demonstration program the particle size distributions were measured gravimetrically using the cascade impactor as a device to fractionate particles of different size. Cumulative mass concentrations of particles collected at each stage and all the stages below, including the absolute filter, were calculated. The cut diameters for the impactor stages were calcualted from the sampling rate in conjunction with the calibration data for A.P.T. impactors. These data are presented in Appendix "B" while the size distribution plots are given in Appendix "C".

The particle size data obtained from cascade impactors are reported in terms of aerodynamic diameter. Equation (E-4) shows the relationship between aerodynamic and physical diameters.

$$d_{pa} = d_p \, (\rho_p \, C')^{1/2} \qquad \text{(E-4)}$$

where d_{pa} = aerodynamic diameter, μmA
d_p = particle diameter, μm
ρ_p = particle density, g/cm³
C' = Cunningham correction factor, dimensionless

Bimodal Size Distribution

The demonstration plant inlet data showed that the particles entering the quencher were widely dispersed and possessed a bimodal distribution. The particle population was a mixture of very small condensation aerosol and large size particles from the sodium carbonate spray in the cross-over duct to the quencher unit. As operated the cascade impactor data covered only the range of approximately 0.5 μmA to 6 μmA. The cut point of the last stage of the impactor was about 0.5 μmA, while the cut point of the pre-cutter was around 6 μmA. Since the data over the whole size range of the particles entering the quencher were not log normal, it was not possible to define a true mass median diameter and "σ_g" simply from a straight line plot of size distribution on log probability paper. An alternate rationale for defining particle size distribution in a way useful for computing number concentration had to be devised.

Using equations (E-1) to (E-4) it can be shown that the majority of particles by number are in the submicron range and therefore the size distribution in the larger diameter range is unimportant for determining number concentration. Consequently, one can compute number concentration from hypothetical values of "d_{pg}" and "σ_g" obtained by assuming log normal distribution over only the cumulative mass data below about 1 μmA. This was done in a consistent manner by plotting the distribution line through only the last two data points and taking "d_{pg}" and "σ_g" from that line.

Inlet "n"

The inlet size data deviated more from log normal than the outlet and also the outlet data were more extensive in the small particle size range than the inlet. It was found that more consistent results were obtained by computing inlet number concentration from outlet data than from inlet data. The computation method used the outlet particle number concentration in conjunction with the penetration curve for each run. It was established that the majority of particles by number (over 90%) were below 0.5 μmA and that the penetration curve for the F/C scrubber in the region below this size was constant due to particle growth characteristics, as shown in Figure E-1. Inlet particle number concentration was determined from the following:

$$n_{in} = \frac{n_{out}}{Pt^*} \qquad \text{(E-5)}$$

where n_{out} = calculated number concentration at outlet, no. particles/DNcm³ using equation (E-1)

Pt^* = constant penetration value for particles below about 0.5 μmA size

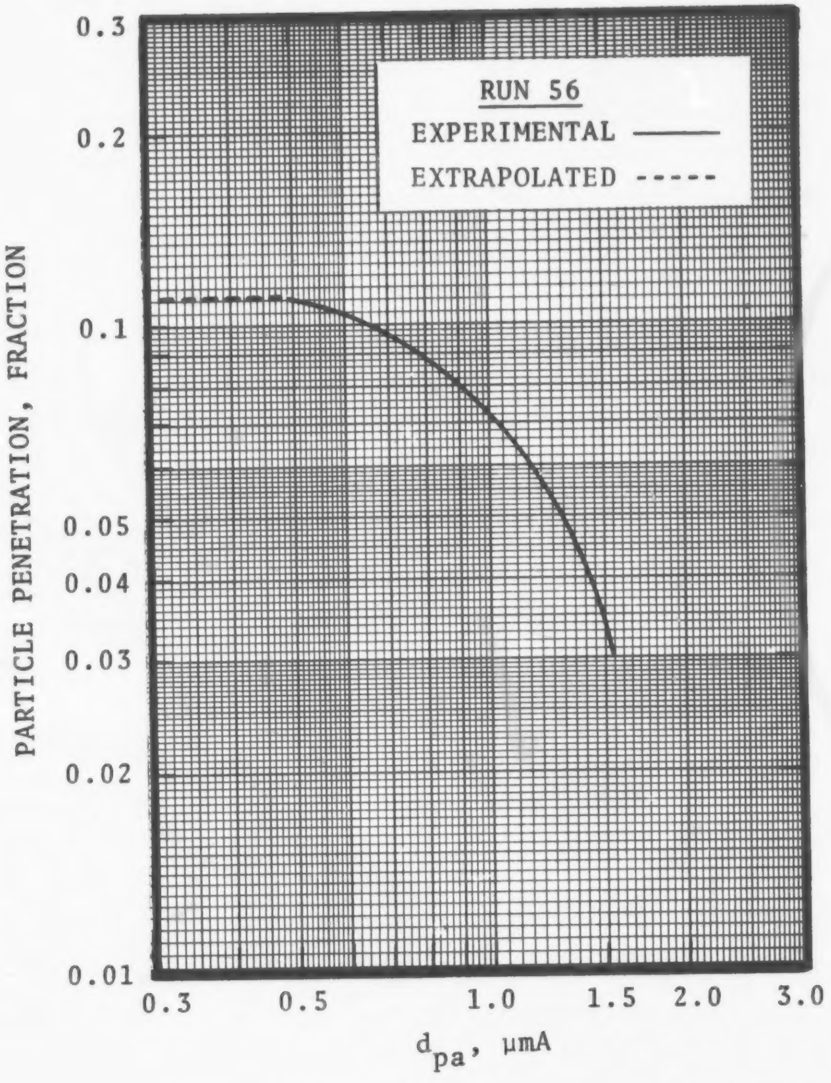

Figure E-1. Particle penetration versus aerodynamic diameter for run 56.

n_{in} = calculated number concentration at inlet, no. particles/DNcm³

The values of "n_{in}" as determined from equation (E-5) were used for predicting the performance of the F/C demonstration system in conjunction with the methods presented in Chapter 7. The validity of the use of a constant value of "Pt" in the procedure was established by comparing number concentrations computed by detailed accounting for "Pt" as a function of particle size and the integration over the entire size distribution with concentrations computed by the simpler procedure. There was little difference between the two methods. These values are given in Table E-1 with the corresponding "d_{pg}" and "σ_g" from hypothetical distribution based on the last two stages.

Summary

In summary, the following procedure is followed for calculation of particle number concentration for each run:

1. Determine cumulative mass loadings for each stage of cascade impactor. This stage data are presented in Appendix "B".
2. Calculate and plot size distribution by plotting percent of mass undersize for each stage versus particle size.
3. Determine hypothetical values of "d_{pg}" and "σ_g" for the outlet size distribution using only the last two data points in the small particle region.
4. Calculate the outlet particle number concentration using equations (E-1) and (E-3).
5. Calculate the inlet particle number concentration using equation (E-5) in conjunction with the experimental penetration curves as presented in Chapter 6 for each run.

TABLE E-1. PARTICULATE DATA F/C SCRUBBER DEMONSTRATION

Run No.	Inlet Particulate*		Outlet Particulate*		
	Pt*,Fr.[(a)]	n x 10^{-7} no./DNcm^3	d_{pg},μmA	σ_g	n x 10^{-7} no./DNcm^3
3	0.22	8.2	0.50	2.0	1.8
4**	0.42	3.6	0.78	1.6	1.5
42**	0.32	4.3	0.60	1.6	1.4
43**	0.55	1.7	0.64	1.6	0.94
56	0.11	19.0	0.58	1.9	1.5
58	0.25	4.4	0.42	1.5	1.1
59	0.30	67.0	0.33	2.1	20.0
61	0.65	3.8	0.40	1.5	2.5
62	0.25	40.0	0.70	2.7	9.9
64	0.19	13.0	0.58	1.7	2.5
66	0.11	380.0	0.48	2.7	42.0
69	0.21	13.0	0.45	1.6	2.8
72	0.19	16.0	0.50	1.7	3.1
73	0.16	30.0	0.35	3.1	356.0
74	0.20	9.0	0.45	1.6	1.8
75	0.21	31.0	0.65	2.5	6.4
76	0.25	52.0	0.43	2.3	13.0
77	0.27	14.0	0.70	2.4	3.7

* Particulate data across quencher inlet and scrubber inlet unless otherwise noted.

** Particulate data across plate scrubber only.

NOTE: (a) Pt* is the experimental penetration over the small particle range (less than about 0.5 μmA).

EXAMPLE CALCULATION

For illustration purposes, an example calculation based on the above procedure is given below. Data from run 56 are used to calculate the particle number concentration.

Step 1: The stage data as collected by the cascade impactor for run 56 are given in Table B-6. The mass percent undersize is calculated for each stage based on the total mass collected by the impactor. These values are presented in Table E-2.

Step 2: The size distribution (d_{pc} versus mass percent undersize) is plotted on log probability paper as shown in Figure E-2.

Step 3: The "d_{pg}" and "σ_g" for the outlet size distribution are approximated using only the data from the last two stages of the impactor. This is represented by a dashed line in Figure E-2. For run 56, the "d_{pg}" and "σ_g" on the outlet were approximated as 0.58 μmA and 1.9.

Step 4: The "d_{pg}" of the outlet size distribution is in terms of aerodynamic diameter. The physical diameter of an equivalent sphere is calculated as 0.22 μm using equation (E-4) and particle density of 4 g/cm³. The "σ_g" is also in terms of aerodynamic distribution and should be changed to actual "σ_g," however, for consistency this conversion is neglected.

Step 5: The outlet particle number concentration is determined using equations (E-1) and (E-3).

$$n_{outlet} = 1.47 \times 10^7 \text{ DNcm}^3$$

Step 6: The fractional penetration over the small particle size is approximated to be 0.11 using the experimental penetration for run 56 presented in Figure E-1.

Step 7: The inlet particle number concentration is calculated using equation (E-5) as:

$$n_{inlet} = 1.3 \times 10^8 \text{ DNcm}^3$$

TABLE E-2. INLET AND OUTLET SAMPLE DATA FOR RUN 56

Impactor Stage Number	Inlet			Outlet		
	M_{cum} Mg/DNm³	% by Mass Under	d_{pc} μmA	M_{cum} Mg/DNm³	% by Mass Under	d_{pc}
Precutter	1,170	100.0	5.3	48.4	100.0	6.0
1	647	55.3	13.0	40.1	82.8	15.0
2	618	52.8	9.5	40.1	82.8	11.0
3	577	49.3	5.9	39.5	81.6	6.9
4	515	44.0	2.4	38.8	80.1	2.5
5	368	31.4	1.2	36.3	75.0	1.3
6	294	25.1	0.85	33.7	69.6	0.67
7	274	23.4	0.53	28.6	59.1	0.43
Filter	141	12.1		15.3	31.6	

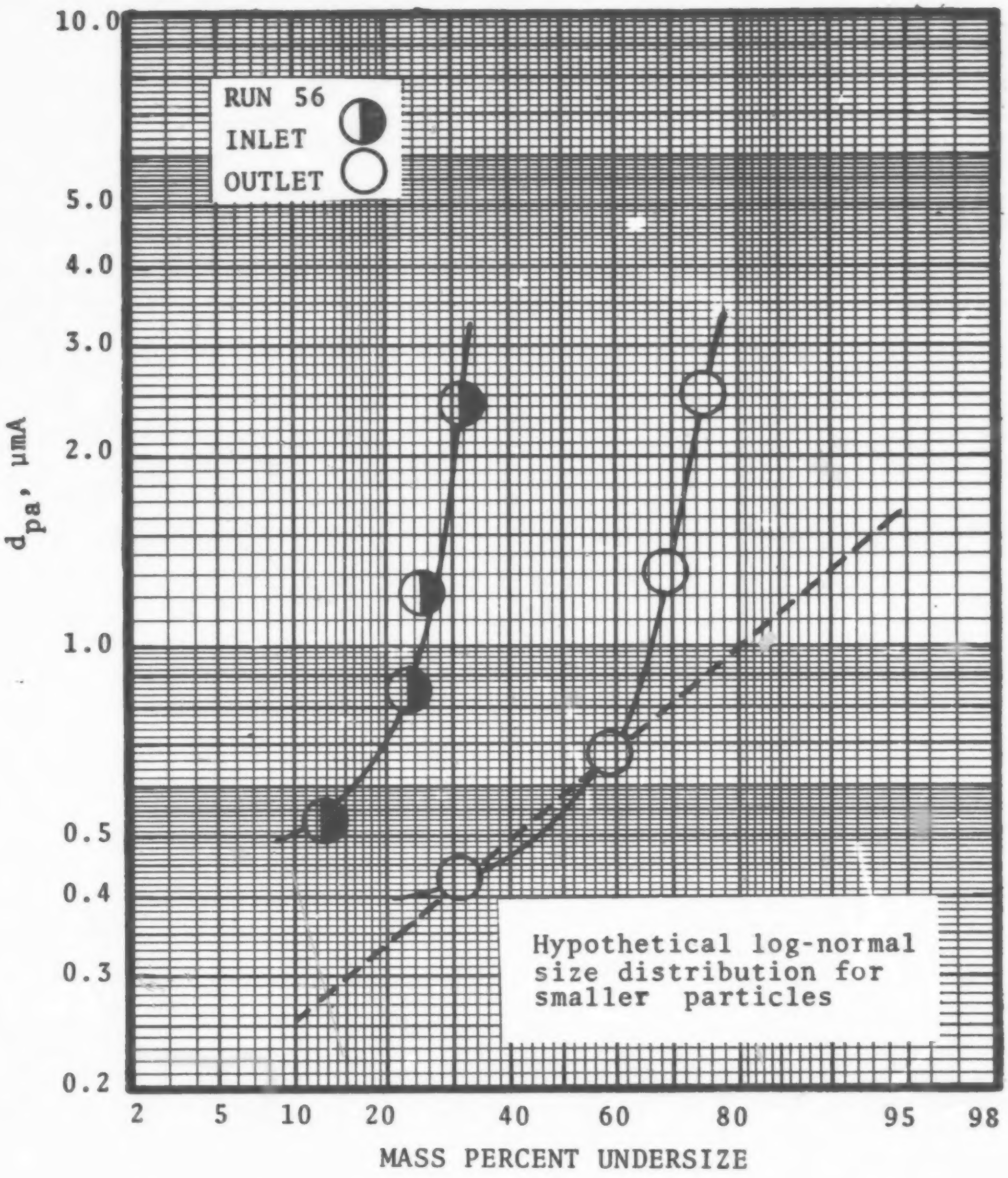

Figure E-2. Inlet and outlet size distribution for run 56.

APPENDIX F

EXAMPLE CALCULATION AND PREDICTION OF FRACTIONAL AND OVERALL PENETRATION

SUMMARY

The sequence of steps to be followed in predicting the performance of an F/C scrubber system involving a sieve plate column are presented in detail in Chapter 7. In outline, the prediction of the fractional and overall penetration of a flux force scrubber is based on the following steps:

1. Determine the initial particle size distribution.
2. Compute particle penetration from the saturator.
3. Compute particle penetration due to inertial impaction on the first plate of the sieve plate column.
4. Calculate the volume fraction of gas condensing, "f_v", and then calculate the penetration due to diffusiophoresis.
5. Determine the grown particle size distribution.
6. Compute the particle penetration function due to inertial impaction for the remaining stages of the sieve plate scrubber.
7. Use the grown particle size distribution and the particle penetration function of step 6 to compute the penetration due to inertial impaction after growth.
8. Compute the penetration of the F/C scrubber as the product of the penetrations due to steps 2, 3, 4 and 7.

DATA (Initial Conditions)

The data for run 56 will be used for illustration purposes.

1. Size distribution of the particulate matter at inlet, see Table B-6.

Preceding page blank

2. Particle number concentration, $n = 1.3 \times 10^8$/DNcm^3 (see Appendix "E" for calculation procedure).
3. Condensation ratio, $q' = 0.31$ g/g (see Appendix "A").
4. Inlet absolute humidity, $H = 0.35$ g/g
5. Particle density, $\rho_{p_1} = 4.0$ g/cm^3
6. Scrubber operating mode, I (see Table 6-3).

CALCULATION PROCEDURE

Step 1: The cumulative mass fraction undersize is tabulated as a function of initial particle aerodynamic size, d_{pa_1}, from the inlet size data given in Table B-6 and plotted in Figure E-2. Column 1 of Table F-1 lists the cumulative mass fraction undersize, while the corresponding particle diameter is given in column 2. The initial aerodynamic diameter, d_{pa_1}, is converted to physical diameter, d_{p_1}, using equation E-4. Column 3 gives the physical particle diameter, d_{p_1}.

Step 2: The next step is to compute the particle penetration from the saturator (Pt_a) based on the saturator collection efficiency characteristics and the initial particle size distribution. Since the saturator is not very efficient over the submicron particle size range of less than 1.5 μmA and the main purpose of this calculation is to determine the penetration curve over this size range, the particle penetration from the saturator was neglected.

Step 3: The collection efficiency relationship for sieve plate as given in equation 7-8 was utilized to compute the particle penetration due to inertial impaction during the bubble formation on the first plate (Pt_b). Figure F-1 presents the penetration curve computed from this relationship. The first plate impaction penetration for each size can be read from curve no. 1 in Figure F-1 and the results are listed in column 5 of Table F-1. Curves 2, 3, and 4 are for the total penetration for the sequence of plates from 2 through 6. A constant gas flow of 50 Am^3/min and foam density of 0.4 is assumed.

At this point it should be noted that data reduction of all the runs in the main text (Chapter 6) were based on the simplifying and optimistic assumption that growth had occurred before the first plate. Therefore, predicted penetrations for the runs in the main text are slightly lower than actually the case using the more conservative performance prediction procedure followed in this appendix, which assumes insoluble particles and no particle growth before the first plate.

Step 4: The next step is to determine the penetration for collection by diffusiophoresis, Pt_c. Equation 7-10 is utilized to calculate "Pt_c". It will assume that the vapor condensing on the particles is completely utilized in causing agglomeration. Since the inertial impaction efficiency is sufficiently high, most of the particles swept to other particles will eventually be collected by impaction. In order to calculate Pt_c, the volume fraction of gas condensing, f_v, is calculated from the condensation ratio, q'. For "q'" equal to 0.31 g/g, the volume fraction of gas condensing is calculated to be 0.32. "Pt " is calculated from equation 7-10:

$$Pt_c = 1-0.85(f_v) = 0.73$$

The diffusiophoretic penetration applies equally to all particle sizes as listed in column 6 of Table F-1.

Step 5: This step determines the grown particle size leaving the condenser (sieve plate column) from the values of "q" and "f_p". Figure F-2 is a size distribution plot showing lines for the particles before and after particle growth. The conditions used for this plot were:

$n = 1.3 \times 10^8/\text{DNcm}^3$ @ 0°C

$q' = 0.31$ g/g

$f_p = 0.25$ (see Chapter 7)

Column 3 lists the grown particle diameter, d_{pa_2}, for each d_{p_1}.

Step 6: The particle penetration (Pt_i^N) due to inertial impaction for the remaining plates 2-6 is calculated. The collection efficiency relationship for sieve plate is given in equation 7-8, and the results for different operating configurations at the demonstration plant are presented in Figure F-1.

Step 7: The relationship between Pt_i^N and d_{pa} (from step 6) and the grown size distribution (from step 5) are used to compute the fractional penetration due to inertial impaction after growth (Pt_d). Column 7 of Table F-1 lists these values for each d_{pa_2}.

Step 8: The total fraction penetration for the F/C scrubber, Pt_t, is calculated as follows and presented in column 8 of Table F-1:

$$Pt_t = Pt_a \times Pt_b \times Pt_c \times Pt_d$$

where "Pt_a" due to impaction in the saturator (neglected)
"Pt_b" due to impaction in the condenser (column 5)
"Pt_c" due to diffusiophoresis in the condenser (column 6)
"Pt_d" due to impaction in stages after the condenser (column 7)

The total fraction penetration, Pt_t, is plotted for each initial particle size, d_{pa_1}, to give the predicted penetration curve (see Figure F-3).

In addition, the overall penetration can be determined by integrating the fractional penetration, Pt_t (column 8), over the entire range of initial size distribution (column 1). This integration can be accomplished graphically (see Figure F-4) or algebraically. Using trapezoidal approximation, the integration is done algebraically using a programmable calculator to give:

$$\overline{Pt} = 0.043 = 4.3\%$$

Thus, the predicted overall penetration of the F/C scrubber at given initial conditions is 4.3%.

TABLE F-1. EXAMPLE CALCULATION FOR PREDICTION OF FRACTIONAL AND OVERALL PENETRATION OF F/C SCRUBBER SYSTEM (RUN 56, configuration I)

Initial Particulate			Grown	Penetration, Fraction			
Mass Fr. 1	d_{pa_1} µmA 2	d_{p_1} µm 3	d_{pa_2} µmA 4	Pt_b 5	Pt_c 6	Pt_d 7	Pt_t 8
0	0	0	1.22	1.0	0.73	0.23	0.17
0.10	0.50	0.18	1.22	0.97	0.73	0.23	0.16
0.21	0.75	0.30	1.25	0.94	0.73	0.22	0.15
0.25	1.0	0.43	1.32	0.89	0.73	0.185	0.12
0.27	1.25	0.55	1.43	0.83	0.73	0.145	0.088
0.29	1.50	0.67	1.59	0.77	0.73	0.076	0.043
0.30	1.75	0.80	1.77	0.68	0.73	0.045	0.022
0.30	2.0	0.92	2.0	0.62	0.73	0.019	0.0089
0.31	2.25	1.05	2.25	0.55	0.73	-	-

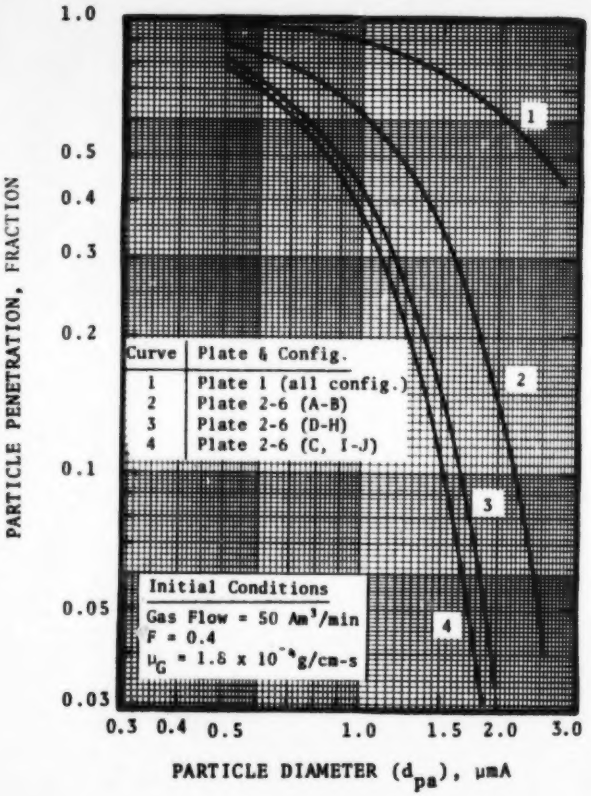

Figure F-1. Scrubber penetrations for collection by inertial impaction as computed from equation 7-8 for different operating configurations (see Table 6-2).

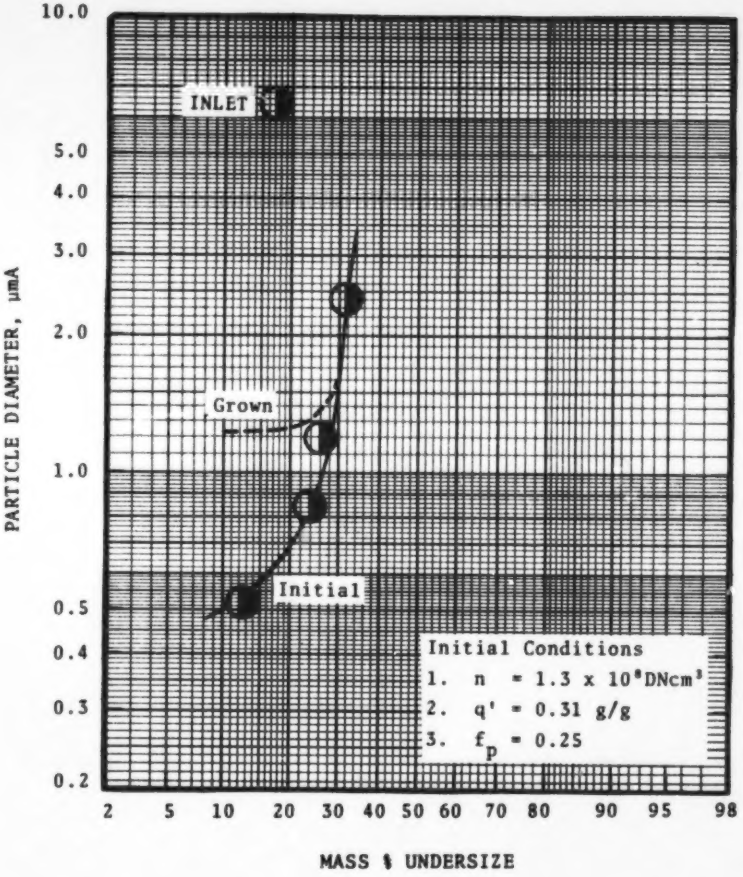

Figure F-2. Predicted grown particle size distribution (Run 56 data).

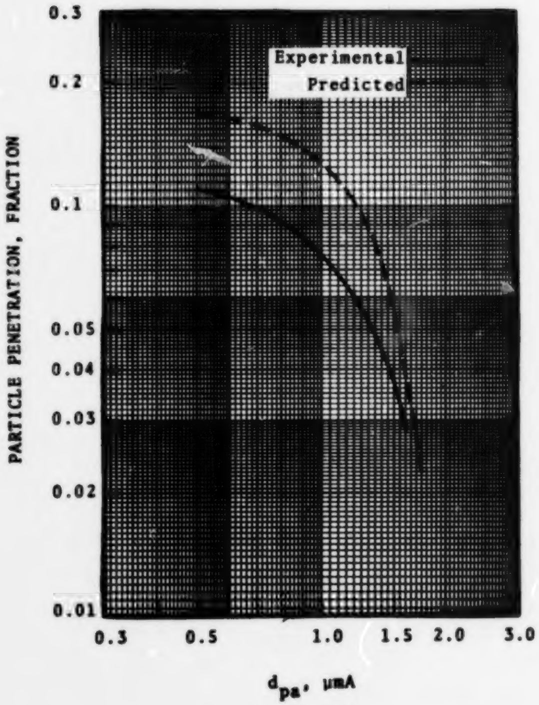

Figure F-3. Particle penetration versus aerodynamic diameter (Run 56 data).

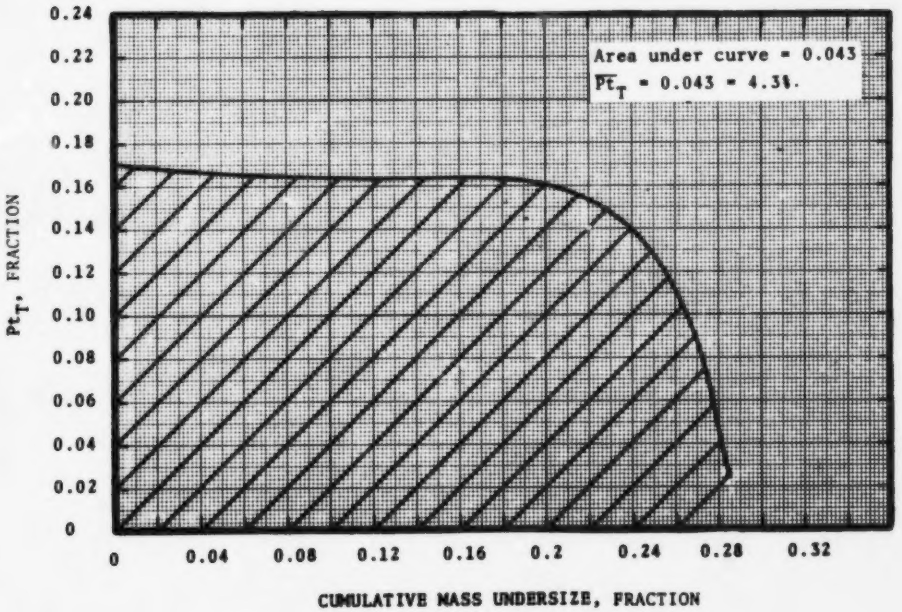

Figure F-4. Prediction of overall penetration for Run 56 using graphical integration (Run 56 data).